Development of biosensors based on Odorant Binding Proteins

A Thesis submitted to the University of Manchester for the Degree of
Doctor of Philosophy
In the Faculty of Engineering and Physical Science

2014

Elena Tuccori

School of Chemical Engineering and Analytical Science

Contents

Abstract

This PhD project aimed to investigate the possibility of using Odorant Binding Proteins (OBPs) as sensing layers of chemical sensors, for the detection of organic compounds in both vapour and liquid phases.

OBPs are small soluble proteins present in high concentrations in the olfactory system of vertebrates and insects. OBPs are attractive in the biosensor field since they can bind odorants and pheromones in a reversible way. They are resistant to high temperatures and protease activity and they can be easily expressed in large amounts.

OBPs belonging to different species of mammals and insects were utilised for developing biosensors relied on different transduction mechanisms.

Recombinant OBPs were grafted on the gold electrode of transducers by using Self-assembled monolayers (SAMs) of alkanethiols. The efficiency of the immobilisation method was proved by using electrochemical techniques.

Quartz crystal microbalances (QCMs), screen-printed electrodes (SPEs) and interdigitated electrodes (IDEs) were employed for developing three types of OBP-based biosensors.

I. QCMs functionalised with OBPs were tested against pheromones (i.e. bombykol and bombykal) and volatile compounds found in foodstuffs (i.e. pyrazine derivatives and geosmin) in vapour phase. The QCM based biosensors showed a good degree of selectivity and a detection limit of the order of parts per billion, in air.

II. In liquid phase, impedimetric biosensors based on SPEs also showed a good selectivity and sensitivity being able to detect analyte concentrations of the order of 10^{-9} M.

III. OBPs immobilised on the gold electrodes of IDEs were instead tested against S-(+) carvone vapour, proving that the binding activity of the proteins was preserved in vapour phase and can be quantified as variation of capacitance.

The developed OBP biosensors showed good selectivity, sensitivity and stability over time in both liquid and vapour phase. The responses of the sensors were reversible, allowing to the device to be used several times. Moreover, the biosensors were label-free, hence the interaction between OBPs and ligand was directly detected without using auxiliary probes/species.

With these findings, we envisage the use of our biosensors in several applications, including monitoring of the quality of food along the transportation and storage, controlling of pests and useful insects in agriculture, or as analytical devices for studying the dynamics in binding processes.

Declaration

No portion of the work referred to in the thesis has been submitted in support of an application of another degree or qualification of this or any other university or other institute of learning.

Copyright Statement

I. The author of this thesis (including any appendices and/or schedules to this thesis) owns certain copyright or related rights in it (the “Copyright”) and she has given The University of Manchester certain rights to use such Copyright, including for administrative purposes.

II. Copies of this thesis, either in full or in extracts and whether in hard or electronic copy, may be made only in accordance with the Copyright, Designs and Patents Act 1988 (as amended) and regulations issued under it or, where appropriate, in accordance with licensing agreements which the University has from time to time. This page must form part of any such copies made.

III. The ownership of certain Copyright, patents, designs, trade marks and other intellectual property (the “Intellectual Property”) and any reproductions of copyright works in the thesis, for example graphs and tables (“Reproductions”), which may be described in this thesis, may not be owned by the author and may be owned by third parties. Such Intellectual Property and Reproductions cannot and must not be made available for use without the prior written permission of the owner(s) of the relevant Intellectual Property and/or Reproductions.

IV. Further information on the conditions under which disclosure, publication and commercialisation of this thesis, the Copyright and any Intellectual Property and/or Reproductions described in it may take place is available in the University IP Policy (see http://documents.manchester.ac.uk/DocuInfo.aspx?DocID=487), in any relevant Thesis restriction declarations deposited in the University

Library, The University Library's regulations (see http://www.manchester.ac.uk/library/aboutus/regulations) and in The University's policy on Presentation of Theses.

Acknowledgements

I owe sincere and earnest thanks to my supervisor Prof. Krishna C. Persaud for giving me the opportunity to work in his group and for his continued support, patience, motivation and knowledge.

I would like to acknowledge the FlexSMELL project for the financial support and the fruitful collaboration with all the partners.

I want to thank my colleagues for their constant support and help through the project, especially Dr. Anna Maria Pisanelli, Dr. Daniela Angione, Dr. Ehsan Danesh, Dr. Mara Bernabei, Dr. Khasim Cali and Dr. Simone Pantalei.

Moreover, I want to thank Prof. Paolo Pelosi for all his precious advice, teaching and for providing the plasmids used for the expression of protein. Thanks to Dr. Imma Iovinella for her friendship and her useful suggestions.

A special thanks to Stefania and Arjan because Manchester will not be the same without them.

I wish also to thank all my friends spread around Europe (too many to list here but you know who you are!) for providing continuous support and friendship.

My warmest gratitude is for my Mum, Dad and Nico who always encouraged and supported me in all my choices.

At last but not least, I would like to express my sincere gratitude to Roberto, the person I am sharing my life with, for being always beside me.

This project was supported by Marie Curie ITN Flexsmell grant number 238454.

List of Abbreviations

1-AMA	1-aminoanthracene
1-NPN	1-N-phenylnaphthylamine
ANOVA	Analysis of variance
ASP	Antennal Specific Protein
B_{max}	Number of maximum binding sites
BET	Brunauer- Emmett- Teller model
CV	Cyclic voltammetry
ddH_2O	Double distilled water (MilliQ water)
dH_2O	Distilled water
DMF	Dimethylformamide
DET	Direct electron transfer
DNA	Deoxyribonucleic acid
DTT	Dithiothreitol
CPE	Constant phase element
GA	Glutaraldehyde
GC-MS	Gas chromatography–mass spectrometry
GFP	Green fluorescence protein
GOBP	General Odorant Binding Protein
GOx	Glucose oxidase
ε	Dielectric constant
EDC	1-Ethyl-3-(3-dimethylaminopropyl)-carbodiimide
EDL	Electrical double-layer
EIS	Electrochemical impedance spectroscopy
ELISA	Enzyme-linked immunosorbent assay
FET	Field-effect-transistor
HEK	Human embryonic kidney
HSA	Human serum albumin
HCl	Hydrogen chloride
IBMP	2-Isobutyl-3-methoxypyrazine
IDE	Interdigitated electrode
IMAC	Immobilized metal affinity chromatography

IPTG	Isopropylthio-D-galactoside
IC50	Half-maximal inhibitory concentration
IUPAC	International Union of Pure and Applied Chemistry
ISE	Ion-selective electrodes
ISFET	Ion-selective field effect transistors
K_D	Dissociation constant
LAPS	Light-addressable potentiometric sensor
MHA	16-Mercaptohexadecanoic
MEA	Microelectrode arrays
mRNA	messenger RNA
MUP	Major Urinary Protein
NHS	N-hydroxysulfosuccinimide
OB	Olfactory bulb
OBPs	Odorant Binding Proteins
OE	Olfactory epithelium
OR	Olfactory receptor
Orco	Olfactory co-receptor
ORN	Olfactory receptor neuron
PB	Phosphate buffer
PBP	Pheromone Binding Protein
ppb	parts per billion
ppbv	parts per billion by volume
ppm	parts per million
QCM	Quartz crystal microbalance
SAMs	Self-assembled monolayers
SAW	Surface acoustic waves
swCNT-FET	Single walled carbon nanotube -field effect transistors
SDS-PAGE	Sodium dodecyl sulphate- polyacrylamide gel electrophoresis
SPE	Screen-printed electrode
SPR	Surface plasmon resonance
R_{ct}	Electron transfer resistance

R_s	Solution resistance
R_t	Retention time
RNA	Ribonucleic acid
TA	Thioctic acid
TEOS	Tetraethyl orthosilicate
TIC	Total ion chromatogram
TMOS	Tetramethyl orthosilicate
Tris-Cl	Tris(hydroxymethyl)aminomethane
VNS	Vomeronasal secretory proteins
VEG	Von Ebner's gland
VOC	Volatile organic compound
Z_w	Warburg impedance

Amino acid nomenclature

Name	1 Letter code	3 Letters code
Alanine	A	Ala
Arginine	R	Arg
Asparagine	N	Asn
Aspartic acid	D	Asp
Cysteine	C	Cys
Glutamic acid	E	Glu
Glutamine	Q	Gln
Glycine	G	Gly
Histidine	H	His
Hydroxyproline	O	Hyp
Isoleucine	I	Ile
Leucine	L	Leu
Lysine	K	Lys
Methionine	M	Met
Phenylalanine	F	Phe
Proline	P	Pro
Serine	S	Ser
Threonine	T	Thr
Tryptophan	W	Trp
Tyrosine	Y	Tyr
Valine	V	Val

1 Introduction

1.1 FlexSMELL project

FlexSMELL was a Marie Curie Initial Training Network (ITN) funded by the European community. The aim of the FlexSMELL project was to develop smart tags, for controlling food freshness and quality through the transport and storage in order to reduce the waste of food. In fact, every year 1.3 billion tonnes of food is lost before it reaches the marketplace (1). The use of detectors, for monitoring parameters as freshness, ripening and deterioration of food in real-time, could considerably reduce their waste. The FlexSMELL tags consisted of chemical sensors based on biological odorant receptors and organic semiconductors developed on flexible substrates. The devices were integrated with radio frequency technologies, for allowing real-time monitoring along with food traceability.

FlexSMELL involved more than five universities and research centres across Europe i.e. the University of Bari (Italy), the Ecole Polytechnique Federale de Lausanne (Switzerland), the University of Tübingen (Germany), the University of Manchester (UK), the University of Sheffield (UK), the Valtion Teknillinen Tutkimuskeskus (Finland) and the Nederlandse Organisatie voor toegepast-natuurwetenschappelijk onderzoek (Nederland).

Two industrial partners involved in food packaging (Carton Pack) and organic electronic sensors (Nanoident) were also part of the project.

The University of Manchester was responsible for the selection and functionalization of different transducers with appropriate sensing materials. Two types of sensing layers were chosen for the project. They included organic semiconductors and olfactory proteins.

As an early stage researcher, I was involved in the synthesis and testing of olfactory proteins for biosensor applications. *Odorant Binding Proteins* (OBPs)

were investigated as bio-recognition elements of the FlexSMELL smart tag due to their unique property to bind chemical molecules in a reversible way. OBPs are soluble proteins mainly involved in the perception of odours and pheromones. The good affinity of OBPs toward odours released by vegetables and spoiled food has been frequently reported. The first Odorant Binding Protein was indeed discovered in cows for its affinity against the strong bell pepper smell, 2-isobutyl-3-methoxypyrazine (2). Other OBPs were described to bind metabolites produced by foodborne pathogens. For instance, OBP1 of *Polistes dominula* showed a good affinity against dodecanol, a long-chain alcohol released from the bacterium *Escherichia coli* (3). Major urinary proteins (MUPs) of mouse bind geosmin. A secondary metabolite produced by both *Penicillium* species (4) and Actinomycetes, which is responsible of a strong earthy flavour in contaminated food (5). Moreover, OBPs can also find applications apart from the food monitoring. In the agriculture, for instance, they can be used for the control of useful insects and pests due to their high affinity against pheromones.

In FlexSMELL, the possibility of using OBPs as bio-recognition elements of different transducers was investigated. Mass and impedimetric sensors were successfully developed for detecting several classes of analytes in both vapour and liquid phases.

OBPs have demonstrated to be a powerful tool for the development of biosensors. They can resist high temperatures and proteases without losing their activity. The OBP-based biosensors showed high performance in selectivity and sensitivity especially against natural ligands when compared to traditional analytical equipment i.e. GC-MS.

1.2 Biosensors

Biosensors are analytical devices that combine biological recognition elements to a signal transducer and convert biological interactions into detectable electric signals (6;7). According to the IUPAC classification, a biosensor can be defined as "*a self-contained integrated device which is capable of providing specific quantitative or semi-quantitative analytical information using a biological recognition element (biochemical receptor) which is in direct spatial contact with a transducer element* " (8).

All biosensors are generally composed of four main elements (Figure 1):

(I) bioreceptor

(II) transducer

(III) amplifier and signal processing

(I) The bioreceptor or recognition element is typically represented by enzymes, receptors, antibodies, DNA/RNA molecules, whole cells or organisms (6). The bioreceptor recognises biological or chemical analytes either in solution or in atmosphere, generating a detectable signal.

(II) The transducer converts biological interactions into a measurable electronic output.

(III) The amplifier and the signal processing are standard electronic components. They are used to process the transducer signal into a final output, which can be displayed using conventional units (7;9).

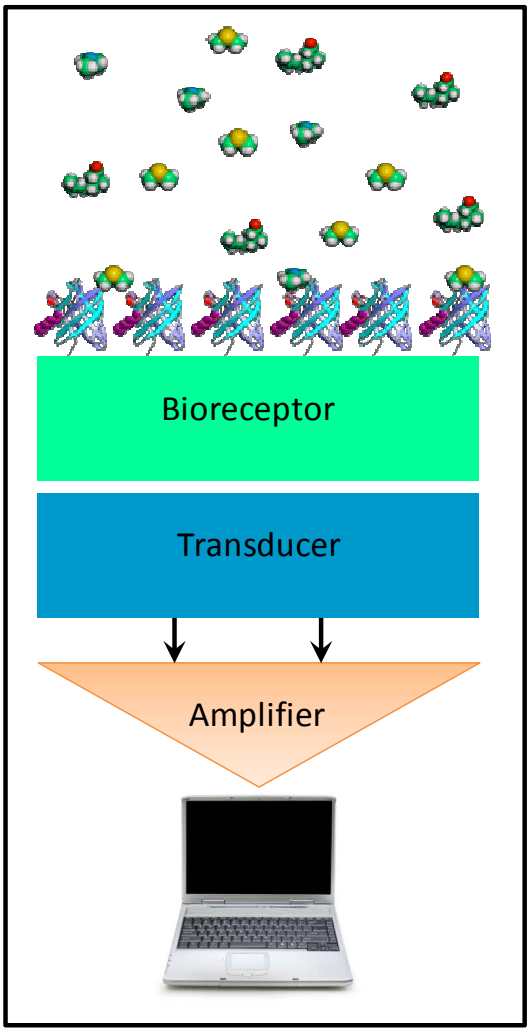

Figure 1. Schematic representation of a biosensor.

Biosensors are highly sensitive, low cost and portable devices that are becoming attractive alternatives to conventional analytic techniques. They can find applications in several areas ranging from disease screening and diagnosis, food quality control and environmental monitoring. In addition, national security departments are aiming to employ biosensor technology in the detection of warfare threat agents and illicit substances (10). The global biosensor market is rapidly growing and it is predicted to reach $ 17.3 billion by the year, as reported in a study of the Global Industry Analysts, Inc., 2015 (11).

1.2.1 Biosensors history

1.2.1.1 First generation of biosensors

Prof. Leland Charles Clark Jr. is considered the pioneer of the biosensor research. In 1956, an early study on the use of a platinum electrode for measuring the oxygen concentration in blood was published. Nowadays, this first amperometric sensor is known as “the Clark electrode” (12). In 1962, at the New York Academy of Sciences symposium, Clark and his colleague Lyons presented the first “enzymatic electrode” for monitoring the glucose in blood. Glucose oxidase (GOx) was immobilised at the interface of a Clark oxygen electrode using a dialysis membrane. The reaction catalysed by the GOx led to the oxygen reduction, considered to be proportional to glucose concentration in the blood (13).

In 1973, Guilbault in co-participation with Lubrano described a blood glucose sensor based on the amperometric detection of hydrogen peroxide. Hydrogen peroxide is produced by the oxidation of the glucose in gluconic acid in the reaction catalysed by GOx (14). The resulting biosensor offered a good accuracy and precision in concomitance with the low volume of blood tested, about 100 µL (15;16).

In 1975, the findings of Clark’s studies became a commercial reality. The Yellow Springs Instrument Company launched on the market the first

commercial glucose analyser, which was based on the detection of hydrogen peroxide (13).

In the same year, Janata introduced for the first time the concept of immunosensors (17). In this work, a sensor based on the protein ovalbumin for studying the interaction against anti-ovalbumin antibodies was developed. The formation of the antigen-antibody complex was detected as a variation of the electrode potential. However, the poor quality of the generated signal did not permit quantitative evaluation of the analyte (17).

The low sensitivity displayed in this first generation of immunosensors was afterward improved by introducing of labels (18). Antibodies and antigens can be conjugated with active labels or probes such as radionuclides, fluorophores and redox enzymes, in order to amplify the intensity of the signal (19). Active probes can generate detectable signals as consequence of the molecular recognition event, providing quantitative information about the ligand. However, the lack of an ideal label along with the long incubation time have limited the use of these types of immunosensors (20;21).

1.2.1.2 Second generation biosensors

In the second generation of biosensors, specific redox 'mediators' were used to improve the accuracy of sensing measurements.

In 1984, Cass et al. developed an amperometric electrode for the detection of glucose. A substituted ferricinium ion was used as a mediator of the electron transfer between the GOx and the electrode. The developed sensor permitted a rapid and reproducible analysis of the glucose in solution, either from plasma or blood, with a minimal sensitivity to oxygen concentrations and to changes in pH (22). The use of mediators could efficiently decrease the potential applied to the biosensor and therefore, reduced the interference from electrochemically oxidisable compounds present in the sample (23).

During the eighties, the second-generation of biosensors were for the first time commercialised. In 1987, MediSense (Waltham, MA) launched a disposable screen-printed enzyme electrode for home blood-glucose monitoring. The pen-sized glucose meter was based on quinoprotein glucose dehydrogenases and a ferrocene derivative mediator (24). Since then, over 40 different enzymatic strips and pocket-sized monitors (16) have been commercialised for the assay of blood glucose (24).

In the same period, optical transducers were harnessed in conjunction with antibodies to develop label-free bioaffinity sensors (25).

In 1983, Liedberg used the Surface Plasmon Resonance (SPR) technique for studying the affinity between immunoglobulin G and antihuman y-globulin, in real-time (26).

Ingemar Lundström and his team together with the BIAcore Company developed a new generation of biosensors based on SPR. In 1990, the Biacore® platform was for the first time launched on the market.

This second generation of immunosensors was based on the direct detection of the antibody-antigen complex by using improved transduction mechanisms. In fact, the use of transducers based on mass, optical and electrochemical methods allowed to convert directly biological interactions into measurable electric signals (21).

1.2.1.3 Third generation biosensors

The third-generation of biosensors involved the immobilisation of redox enzymes directly on to the electrode surface, without the use of mediators. The redox enzyme acts as an electrocatalyst, facilitating the direct electron transfer (DET) between the electrode and the substrate (27).

In 1977, Hill and Kuwana, in two independent studies, reported for the first time, the direct electron transfer propriety between *cytochrome c* and electrode (23). In 1979, DET between large redox enzyme such as laccase and carbon black electrode, was revealed in presence of oxygen (28). Later publications reported also the use of heme-containing oxidoreductase immobilised on carbon black electrodes for the detection of oxygen peroxides, organic hydroperoxides, phenols and aromatic amines (27).

This third generation of biosensors showed a higher selectivity due to the absence of mediators and an operating voltage close to the redox potential of the enzyme. However, only few enzymes exhibit natural DET at the normal electrode surface. This drawback was overcome by the co-immobilisation of proteins and mediators directly on the electrode surface or into a conducting polymeric film (29) as described by Ohara et al. in 1993 (30). The co-immobilisation prevented the mediators from diffusing out of the biosensor film and improved the transport of electrons between the active site of the enzyme and the surface of the electrode(31). In addition, the close proximity of the enzyme and the mediator to the surface of the transducer, minimised the electron transfer distance reducing the response time (29).

1.2.2 Types of biosensors

As mentioned above, a biosensor is commonly composed of a recognition element, a signal conversion unit and an output interface. Biosensors can be classified on the basis of the bioreceptor and transducer utilised as summarised in Figure 2.

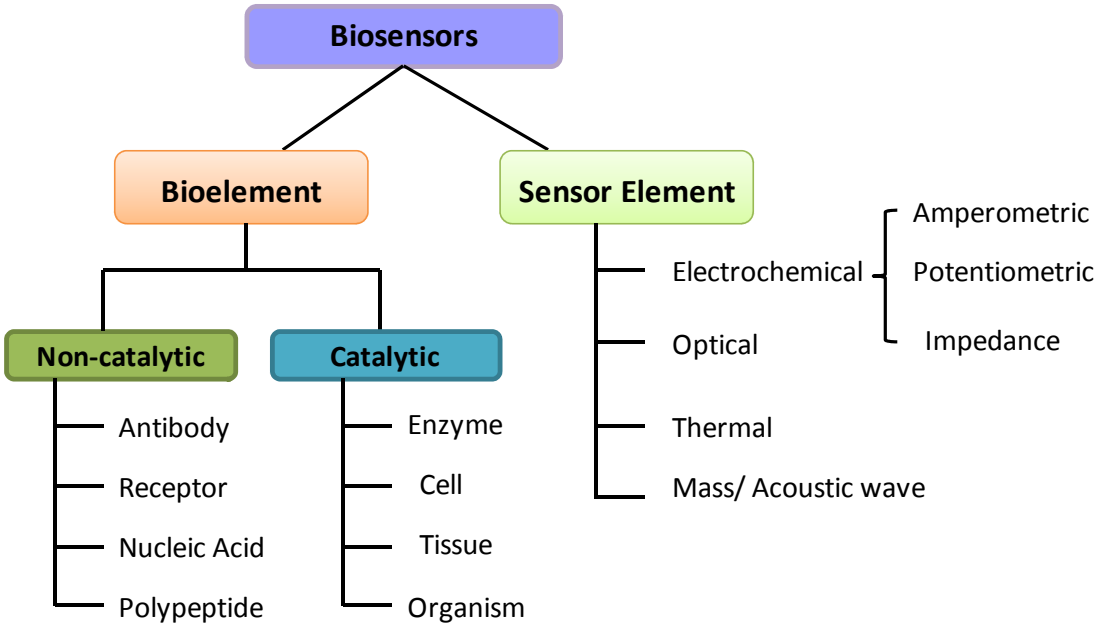

Figure 2. Schematic representation of the main components of a biosensor.

1.2.2.1 Recognition elements

The recognition element is the biological component of the biosensor and it is responsible for the initial events of signal generation. There are various types of recognition elements, ranging from whole cells to nucleic acids. Recognition elements can be divided into two categories: *catalytic* and *non-catalytic* (32).

Catalytic elements include enzymes, whole cells, tissues and microorganisms. They are based on the catalytic transformation of substrates into products, which can be detected at the transducer interface.

Catalytic enzymes are largely used as bio-recognition elements. They can catalyse the formation of a variety of detectable products such as protons, electrons, light and heat with a high substrate-specificity (33). Glucose oxidase and glucose dehydrogenase have been employed for more than fifty years for measuring glucose in blood samples, representing about 90% of the global biosensor market. However, the performance of biosensors based on enzymes can be affected by several factors, such as the enzymatic concentration, the

pH, the temperature and in some cases, the availability of cofactors can limit the enzymatic reaction (34).

Whole cells have gained a special attention for biosensor applications, due to their simplicity of operation (35), their capacity to detect a wide range of chemical substances and to low costs. They are also more tolerant to the environmental conditions that may be harmful for isolated enzymes or proteins. Cells are also a multipurpose catalyst, especially when the process requires the participation of several enzymes in sequence (36). On the other hand, the use of living cells has the disadvantage of longer and less sensitive responses when compared to conventional enzymatic sensors. Substrates have to cross the cell membrane and/or the cell wall in order to reach the cytoplasm where reactions take place (35).

Tissues can be also used as bio-recognition elements as they are sources of enzymes. Several biosensors based on both vegetal and animal tissues have been developed and studied. Ground asparagus tissues and ferrocene were used as a peroxidase sensor (37), homogenates of fresh broad bean tissues were instead investigated to detect phenolic compounds in drinks (38). The porcine kidney tissue was used to determine lactic acid in human plasma and milk (39). However, their poor reproducibility has limited their use for sensing applications (35).

Non-catalytic elements, such as antibodies, receptors, polypeptides and DNA/RNA are also employed in biosensor applications. Chemical interactions, occurring between the bio-recognition element and the analyte, can be detected by the transducer and converted in a detectable electric signal.

Antibodies are complex biological molecules that exhibit a high capability of binding toward specific molecular structures. Antibodies can be used in biosensing in both direct and indirect interaction approaches. In the direct form, antibodies are immobilised on the transducer surface and bind free target compounds.

In the indirect form instead, antigens are linked on the solid surface, interacting with free antibodies (40). Antibodies are generally used for detecting antigens in serum, toxins, bacteria and virus that may affect the health of humans (41). In the last few years, a significant attention has been given to the use of antibodies in assaying the quality of drinking water (42), food (43;44),detection of hazardous materials and illicit drugs (45).

Receptors and carrier proteins are also utilised as recognition elements. These proteins provide a means of molecular recognition, acting as a active site i.e. ion channels or a potential sensitive site (46). Biosensors based on receptors have been developed as point-of-care tests in the detection of potential cancer biomarkers (47) or in monitoring hormone levels in blood (48). Olfactory receptors have also been used in the detection of volatile molecules (49). Receptors show in general a high degree of sensitivity and selectivity toward target ligands, these being essential features for the development of high performance biosensors.

Oligopeptides based biosensors have been successfully employed for detecting mycotoxins (50), biomarkers of hepatotoxicity (51) and dioxins in food (52). They can be either natural peptides or proteins portions (5-10 amino acid residues), such as the active site of a receptor or the single chain variable fragment of antibodies (51). The advantage of using fragments of proteins lies in the fact that their activity is not affected by conformational changes, as it might occur in case of whole proteins.

Nucleic acid biosensors have been primarily employed in clinical diagnostic for the detection of viruses (53) and bacteria such as *E. coli*, *Proteus mirabilis*, *Pseudomonas aeruginosa* and *Enterococcus* spp. (54). The specificity of the interaction dependents on the ability of different nucleic acid sequences to form hydrogen bonds with the complementary probes (55). The system is highly selective and able to detect variations of a single nucleotide in the sequence. However, a pre-treatment step is required for releasing nucleic acids of the sample in the medium.

1.2.2.2 Transducers

The transducer converts bio-recognition events into measurable signals. Transducers can be clustered in four main classes (40) on the basis of the transduction mechanism used.

1) electrochemical
2) optical
3) mass sensing/ acoustic waves
4) thermal

Electrochemical biosensors can be divided into three main groups: potentiometric, amperometric and impedimetric transducers (6).

Amperometric and potentiometric systems typify the most commonly used electrochemical transducers. The detection of analytes, through biological elements, often generates chemical species that can be measured at the electrode interface.

For potentiometric measurements, the relationship between the concentration of the analyte and the potential is governed by the Nernst equation (Equation 1)

$$E = E^0 - \frac{RT}{nF} \ln Q \qquad \textbf{Equation 1}$$

where, E represents the observed cell potential at zero current, E^0 is the standard cell potential, R the universal gas constant, T the absolute temperature in Kelvin, n is the charge number of the electrode reaction, F is the Faraday constant and Q is the ratio of ion concentration at the anode to ion concentration at the cathode (56).

Amperometric biosensors rely instead on a constant potential applied between the working and the reference electrode. The imposed potential promotes redox reactions at the electrode surface, which produce a measurable current. The

magnitude of this current is proportional to the concentration of the electro-active species in the solution (57). The simplest amperometric sensor is the Clark oxygen electrode. This consists of a cathode of platinum and a silver/silver chloride reference electrode. When a potential is applied between the cathode and the reference electrode, a current proportional to the oxygen concentration is then produced (58). The intensity of the current can be used to estimate the oxygen concentration in blood or in biological fluids. Figure 3 shows a schematic representation of a glucose biosensor based on Clark's oxygen electrode.

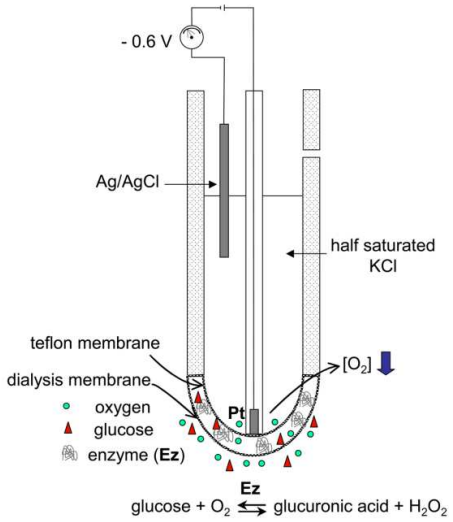

Figure 3. Schematic diagram of a simple amperometric biosensor. A potential is applied between platinum and the silver electrode. This generates a current (I) which is carried between the electrodes by means of a saturated solution of KCl. The enzyme, glucose oxide (GOx) is contained in a membrane at the electrode interface, which is permeable only to oxygen. Figure adapted from Soledad *et al*. (59)

Amperometric biosensors are used on a large scale for the detection of several analytes such as glucose, lactate and sialic acid (60). Moreover, they have been studied for detecting of pesticides (61) and pathogens such as *Bacillus cereus*, *Mycobacterium smegmatis* (62) and *Francisella tularensis* (63).

Potentiometric biosensors are instead based on ion-selective electrodes (ISE) and ion-selective field effect transistors (ISFET). They look at the potential difference between the working and the reference electrode at zero current, monitoring the accumulation of charges generated by biological reactions at the

electrode interface (60). Potentiometric biosensors consist of a perm-selective outer layer and a bioactive element, usually an enzyme. Enzymes catalyse reactions that either consume or generate chemical species, which can be measured by using conventional electrochemical methods. However, potentiometric sensors are more sensitive at lower concentrations, as they rely on logarithmic concentration responses (64). ISFETs based biosensors were used for developing DNA sensors, immunoassays and for monitoring living cells *in vivo* (65). Nevertheless, the incompatibility between the bio-molecule immobilisation protocols and the ISFET fabrication have limited the use of ISFETs for sensing applications compared to other technologies (64).

Biosensors based on impedance are also classified as electrochemical transducers. Impedimetric biosensors are based on the commonly used technique called electrochemical impedance spectroscopy (EIS). In this technique, a low voltage sinusoidal electrical signal is applied at various frequencies to an electrochemical cell. The resulting current is used to determine the impedance as a function of the probed frequencies. The interactions between the bioreceptor and the target compounds lead to changes in the electrical impedance value (64). Impedimetric biosensors have been successfully used for detecting foodborne pathogenic bacteria (66), DNA fragments (67) and as immunosensors (68). The high sensitivity, up to 1 fg ml^{-1} (67) and the simplicity in the interpretation of the result make the impedimetric devices a powerful tool for biosensing applications (64).

Electrochemical transducers are the most commonly used platforms for biosensors, due to fast response time, great simplicity and low costs (58). Nonetheless, the regeneration of the working electrodes, between successive measurements, limited the use of this technology. The commercialisation of single-use disposable screen-printed electrodes (SPEs) has entirely overcame this problem (69).

A wide range of optical techniques has been employed in conjunction with biological elements. Optical detectors can rely on several methodologies, which

include absorption, reflectance, luminescence, chemiluminescence, evanescent wave, surface plasmon resonance and interferometry (70). Amongst several types of optical biosensors available, Surface Plasmon Resonance (SPR) is the more widespread platform (71). SPR is a real-time and label-free optical detection method, which is used for studying the interactions between target compounds and the bio-functionalised surface (72). SPR measures minute changes in the refractive index at and near the surface of the sensing element (Figure 4). In the case of immunosensors, the interaction between antibodies and antigens leads to a change in the reflectance index. The variation of the SPR angle is then directly correlated to the concentration of antibodies in the solution (73).

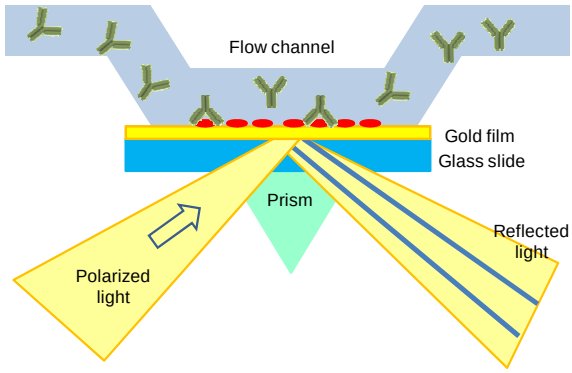

Figure 4. Schematic representation of a SPR device. A glass slide with a thin gold coating is set on a prism. The light diffuses through the prism and the slide, reflects off the gold and passes back through the prism to a detector. Any change in the reflectivity in the angle or in the wavelength, gives a signal that is proportional to the concentration of biomolecules bound on the surface.

Optical biosensors have found applications in several fields. In medical diagnosis, they have been employed for monitoring cancer (6) and cardiac diseases biomarkers (74). In the food industry, they have been used for the detection of pathogenic bacteria, toxins and contaminants (75) as well as for the control of environmental pollution (76).

Mass sensitive transducers, like quartz crystal microbalances (QCMs or QMBs) and surface acoustic waves (SAWs) are highly sensitive devices, able to detect any small change in mass occurring on their surface (40). Mass transducers rely on solid wafers of piezoelectric material that can generate acoustic waves

in the substrate of the sensor. The acoustic waves can propagate on the surface i.e. surface acoustic wave (SAW) or in the bulk of the resonator i.e., quartz crystal microbalances. The adsorption and/or binding of molecules on to the sensor surface lead to changes in the physical proprieties of the acoustic wave. These changes can be detected, providing quantitative information about the amount of the adsorbed material (77).

QCMs are the more widely diffused mass transducers. They are very sensitive transducers able to detect up to picogram mass changes. When an alternating potential is applied to a crystal, it starts to oscillate at a characteristic "resonant frequency". Any modification in the physical proprieties of the crystal, such as changes in the global mass or in the thickness, lead to a proportional variation of the resonant frequency (78). The quantity of mass added to the resonator surface can be easily estimated by using appropriate equations. QCMs transducers are described in more detail in the section 1.3.3.1.

Surface acoustic wave (SAW) sensors consist of one or more interdigitated electrodes built on a piezoelectric substrate, such as quartz, lithium niobate, or lithium tantalate. The electrodes convert electrical signals in to acoustic waves and vice versa. The acoustic waves are propagated along the substrate between the two electrodes with a characteristic speed (77). Mass adsorption, modifications of the viscosity or conductivity can induce variations in the acoustic wave velocity (79;80). Such variations are detected as electrical signals by the system, giving information about any chemical and physical changes that occur on the surface.

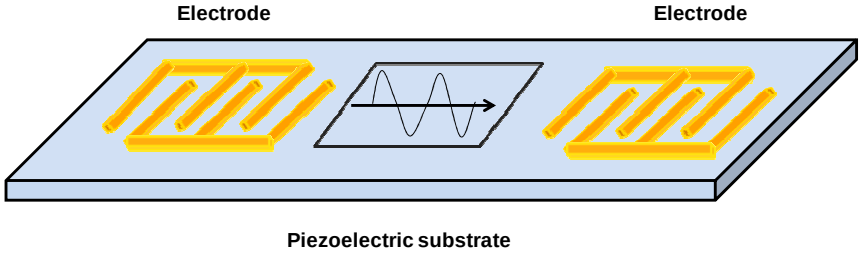

Figure 5. Schematic representation of a SAW transducer.

In the last ten years, mass transducers have been employed in a wide variety of applications, which include detection of low molecular weight ligands (81;82), cancer biomarkers (83), pathogenic bacteria (75), viruses (84), genetic screening (85), protein interactions (86) and for the study of cancer cells (87).

The final category described in this section is that of thermal transducers. Thermal transducers are based on the measurement of the heat produced by the reaction between the receptor element and the analyte. The metabolic activity of the bio-component causes an increase in temperature, which is transformed into a detectable electrical signal. The amount of heat produced is proportional to the concentration of the reactant. All chemical reactions are accompanied by the absorption or evolution of heat. For instance, the immunoreaction between anti-HSA (human serum albumin) and its antigen yields -30.5 kJ/mol (88). Thermal transducers can be classified according to the process of heat transfer. Isothermal calorimeters maintain the reaction cell at constant temperature, measuring the amount of energy required. Heat conduction calorimeters measure the temperature difference between the reaction vessel and an isothermal heat sink surrounding it. The most commonly used is the isoperibol calorimeter that also measures the temperature difference between the reaction cell and an isothermal jacket surrounding it (73).

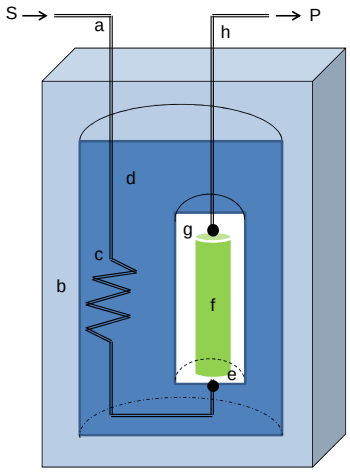

Figure 6. Schematic diagram of a calorimetric biosensor. The sample stream (a) passes through the outer insulated box (b) to the heat exchanger (c) within an aluminium block (d). From there, the sample reaches the reference thermistor (e) and enter into the packed bed bioreactor (f), containing the biocatalyst, where the reaction takes places. The change in temperature is determined by the thermistor (g) determines the difference in the resistance, and hence temperature, between the thermistors.

The diffusion of thermal transducers for sensing purposes is still limited, probably due to the complexity of the instrumentation used (89). However, they have found application in clinical diagnosis (90;91), in on-line food process monitoring (92) and in the control of environmental contaminants (93).

1.2.2.3 Immobilisation methods

The immobilisation of biomolecules onto the transducer surfaces is a crucial step in the development of efficient and high performance biosensors (94). The immobilisation procedure involves the process of making biochemical components insoluble by linking them onto solid surfaces (35). The chosen immobilisation method should not affect any aspect of the structure and conformation of the biomolecules as well as their biological activity. However, it has to ensure that the biomolecules are tightly attached on the surface and that they will not be desorbed during the use of the sensor. An efficient immobilisation strategy is simple, fast and sensor-to-sensor reproducible, moreover, it should improve the bio-element stability to enable long-term applications (95). Intensive efforts have been done to develop successful immobilisation methodologies able to improve important aspects of the biosensor application such as sensitivity and stability (94).

The immobilisation methods used for developing biosensors can be clustered in five main groups (Figure 7):

1) physical adsorption
2) covalent binding
3) entrapment
4) cross-linking
5) affinity

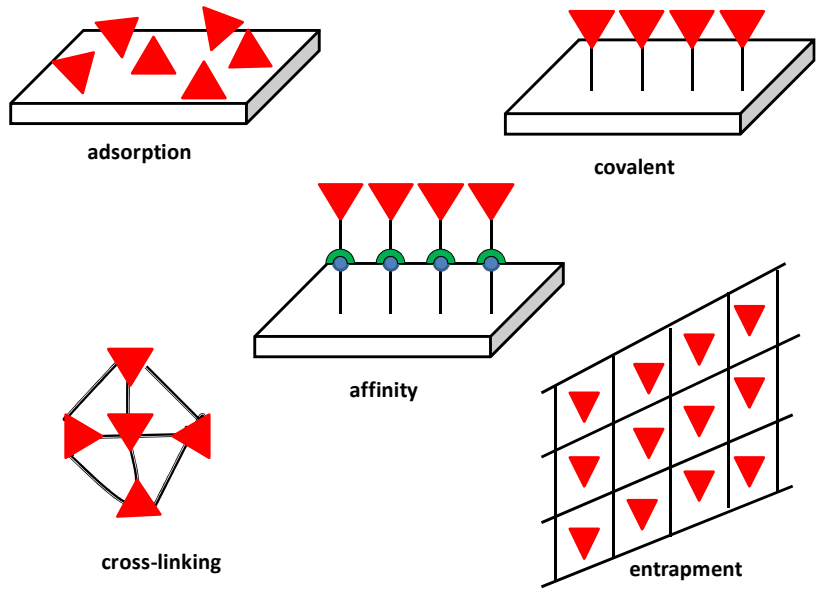

Figure 7. Biological elements and transducers can be coupled by using five different immobilisation methods, including physical adsorption, covalent binding, cross-linking, affinity and entrapment.

The choice of an appropriate immobilisation method is strictly dependent on the nature of the biological element and the type of the transducer used, as well as on the operating conditions of the biosensor (89).

Adsorption of bio-molecules, from solution onto solid surfaces, can proceed via either physical or chemical interactions. The physical adsorption involves van der Waals forces, ionic bonds or hydrophobic forces, whereas in the chemical adsorption there is a sharing or transfer of electrons to form a chemical bond. The main advantage associated with the physical adsorption is due to the simplicity of the method, which can be performed under mild conditions without altering the bio-chemical proprieties of the bio-element. However, biomolecules immobilised through adsorption exhibit a certain degree of reversibility, and with few exceptions, the forces involved in the binding are not very strong. Moreover, an irregular distribution of randomly oriented proteins is commonly observed on the surface (96;97). Despite the low stability and reproducibility of this method, physical adsorption remains the major system in use in clinical assay systems, i.e. ELISA (98).

An alternative approach to graft biomolecules on sensor surfaces is via *covalent binding.* Biomolecules are immobilised on solid surfaces through the formation of defined bonds (99;100). The covalent binding of biomolecules to solid surfaces is a procedure that minimises the loss of the biological activity (101). This method has been employed to improve uniformity, density and reproducibility of bound proteins and nucleic acids on solid surfaces. Proteins, for instance, display many functional groups that can be used for covalent immobilisation. These include amino groups (e.g. lysine), carboxyl groups (e.g. aspartic acid and glutamic acid), sulfhydryl groups (e.g. cysteine), etc. The functional groups involved in the immobilisation reaction should not be part of the active site of the bio-molecule to avoid any possible loss in the activity. Metal surfaces of the transducers, such as gold and silver, can be modified by using hydroxyalkanethiols to generate hydroxyl, carboxyl or amino groups that can react with specific functional groups of the bio-molecule (102). These techniques include the ***Self-assembled monolayers*** (SAMs) method.

SAMs are well organised two- or three-dimensional supramolecular structures formed by the adsorption of an active surfactant on a solid surface (103) (Figure 8). The spontaneous self-assembly is driven by specific interactions between the head of “self-assembling molecules” and the surface, followed by a self-organisation of a monomolecular film (104).

The types of monolayers mainly used for biosensor applications are based on the strong adsorption of disulfides (R–S– S–R), sulfides (R–S–R) and thiols (R–SH) on gold (105). Thiols are chemisorbed on gold, through the oxidation of the S-H bond, followed by a reductive elimination of hydrogen and formation of thiolate ions. The adsorption of disulfides, instead, is due to a simple oxidative addition of the S-S bond on the gold surface. The formation of self-assembled monolayers of thiols on gold surfaces has a biphasic kinetic behaviour. After an initial fast step, which is triggered by the reaction of the sulphur group with the gold surface, a slow second phase begins the formation of a crystallised surface. Alkyl chains of alkanethiols are arranged into unit cells, forming a two-dimensional crystal (103).

SAMs of thiols on gold seem to be the most promising domain for developing biosensors. SAMs of alkanethiols bear carboxylic functional groups, which can be easily activated by using carbodiimides in order to form stable peptide bonds with amino groups of the proteins (106).

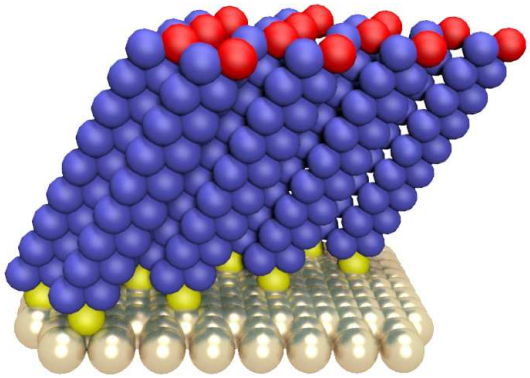

Figure 8. 3D-structure of an organised SAMs of alkanethiols on gold. In yellow are displayed the sulphur groups. Figure adapted from Castangia (107).

Covalent coupling is a technique applied in many biosensor systems described in the literature, resulting in a stable, fast and inexpensive method for linking different types of biomolecules.

The procedure of *entrapping* biological components in three-dimensional matrices has been successfully used for the inclusion of enzymes, cells and organelles (108). The immobilisation of an enzyme in a polymeric gel or behind a membrane is a relatively straightforward process. Enzymes, mediators and additives can be simultaneously deposited in the same sensing layer. The method does not alter the biological element and the biological activity is preserved during the immobilisation process (94). Biosensors based on entrapped enzymes and proteins are often characterised by an increase of the storage stability. However, leakage of the biological species can lead to reduction of their activity (98) and sensitivity (109).

Immobilization of biological components by *cross-linking* with multifunctional reagents is another well-known approach to develop biosensors.

Glutaraldehyde is, so far, the most common cross-linking agent for biosensor applications. Biosensors based on enzymes immobilised in a glutaraldehyde matrix or in combination with natural polymers have been often used (110). This method is simple to perform and lead to strong chemical bounds between biomolecules. However, biomolecules immobilised by using cross-linking can show lowered activity caused by conformational alterations (94).

Affinity immobilisation methods are based on the strong interactions between complementary biomolecules. This technique allows an oriented and site-specific binding of biomolecules on the sensor platforms. Several affinity methods have been described to immobilise proteins, such as (strept)avidin and biotin, antibodies and antigens, lectins and carbohydrates and also chelator agents (94). The affinity interaction involves specific affinity sequences (tag) and complementary affinity ligands. The tag can be either naturally present in the bio-element or artificially added, by using genetic engineering methods. The immobilisation method based on affinity techniques is selective, oriented and highly reproducible. The minimum effect caused to the biological activity along with the possibility to re-use the same platform several times make of this method a promising tool in the biosensors field (111).

1.3 Aims of the research

This research was focused on the development of simple and portable biochemical sensors for the detection of organic compounds in both vapour and liquid phases.

In the last thirty years, great efforts have been made to develop sensors able to mimic the proprieties of the “human nose”. Electronic noses (E-nose) based on either metal oxides or conducting polymers (112) have been widely employed to reproduce the features of the mammalian olfactory system. Unlike most existing chemical sensors, electronic noses do not sense specific compounds, thus arrays of sensors are generally used. Output signals from individual sensors are combined together and processed, in order to produce a distinct response pattern. However, due to the poor selectivity, the high sensitivity to humidity and to the drift in the output signal, E-noses will never completely replace complex analytical equipment or human panels (113).

Mammalian olfactory systems are indeed able to detect thousands of different pure odours and complex mixtures, within seconds after the exposure. The dynamic range of the olfactory system enables the detection of concentrations ranging from saturated vapour to parts-per-billion (114).

Panels of human noses are in fact still widely used as an analytical tool in many industries to assess the quality of food, drinks, perfumes, cosmetics and chemical products (115). Animals, such as dogs, rats (116-118) and honeybees (i.e. the Vasor136 developed by Inscentinel Ltd) (119) are successfully employed for detecting land mines, explosives and diseases. However, even this technology has some drawbacks such as costs and time for training, transportation, limited lifetime and environmental limitations. For instance, heavy rain or snow can affect the detection procedure (120).

The aim of this research was to combine biological components of the olfactory system with simple electronic detectors in order to develop a device with high sensitivity and selectivity, as is the case with the “human nose”. In 2010, when this project started, there was little research published on the use of olfactory proteins for sensing applications. The majority of the research in this area was concentrated with the study of olfactory receptors (ORs) as bio-recognition elements. In 1999, Wu developed one of the early sensors based on ORs. In this work, isolated olfactory receptors from the olfactory epithelium of frogs were conjugated with piezoelectric resonators. The biosensor was studied to detect volatile compounds such as caproic acid, ionone, linalool and ethyl caproate (121).

More recently, several OR-based biosensors have been developed and tested for medical diagnosis and national security purposes. ORs seemed to be the best candidates for the development of high sensitive and selective sensors, due to their unique proprieties. However, the synthesis in large-scale of functional receptors is the main limitation to the adoption of OR-biosensors. A complete review of the state of art of OR based biosensor is described in the section 1.3.4.3.

We believed instead that Odorant Binding Proteins (OBPs) could represent a valid alternative to the use of ORs. OBPs are small proteins able to bind and to release volatile compounds. They are highly expressed in the olfactory structures, where they participate in the perception of olfactory stimuli. OBPs are also ideal tools for developing chemical sensors. They are robust, can be expressed in large quantity in the prokaryote system and show versatile selectivity of binding toward different classes of chemical compounds. Moreover, it is possible to modify the ligand selectivity of the OBPs by replacing single amino acids in the binding pocket.

In this research project, the possibility of employing OBPs as sensing elements was successfully demonstrated. By selecting appropriate transducers, it was possible to develop a device able to generate electric signals directly from the

ligand-binding event, without the use of auxiliary probes. The developed OBP sensors showed important features such as (a) label-free; (b) reusability; (c) real-time detection and (d) portability. OBP biosensors can be used as detectors of organic compounds such as pheromones, where a high sensitivity was demonstrated. Arrays of OBPs were also used for monitoring analytes released by foodstuff i.e. pyrazine derivatives and geosmin as markers of the food quality.

In the following sections, individual components of the developed OBP-biosensors are described and an overview of the structure and the physiological function of the OBPs are provided. This is followed by a general description of the transducers employed for the development of the biosensors, such as quartz crystal microbalances, screen-printed and interdigitated electrodes.

1.3.1 Introduction to the olfactory system

The detection of chemical signals in the environment is essential for the survival of most mammals and insects. Animals have developed a highly sophisticated olfactory system, able to distinguish between thousands of diverse volatile compounds. Humans, for instance, can discriminate more than a trillion of olfactory stimuli (122). Vertebrates and invertebrates detect volatile compounds from the environment and integrate these signals to obtain a complete map of the surrounding background. Considering the vast range of chemicals and the anatomical structures of the olfactory systems, fundamental differences are present in the mechanisms that result in the perception of odorant compounds, especially between vertebrates and invertebrates.

1.3.1.1 Vertebrate olfactory system

In vertebrates, the olfactory sense is involved in many import aspects of life such as finding food, detecting predators and prey, marking the territory and in the mate recognition (123). Odour perception starts in the olfactory epithelium, which is localised in the nose (124). Three types of cell compose the olfactory epithelium, such as the olfactory receptor neurons (ORN), the supporting cells and the basal cells. ORNs are the primary sensing cells involved in the odour recognition. ORNs are bipolar neurons with a single dendrite that extends up to the surface of the epithelium, ending in numerous fine cilia. The cilia, which lie in the layer of aqueous nasal mucus, are the site where the olfactory receptors (ORs) are expressed (125). Each olfactory neuron expresses mainly one type of olfactory receptor (126).

ORs are transmembrane proteins belonging to the family of G-protein-coupled receptors (127). They are the point of contact between the external environment and the olfactory system. Odorants reach and bind to ORs, trigger an intracellular activation cascade, which generates the neuronal olfactory signals.

The axons of ORNs synapse in specialised structures of the olfactory bulb called glomeruli. ORNs expressing the same type of ORs make synapses to the same glomerulus. (128). The olfactory signal is transmitted through the olfactory bulb to the primary olfactory cortex and then to higher order cortical regions; where the olfactory stimuli are perceived and processed (129).

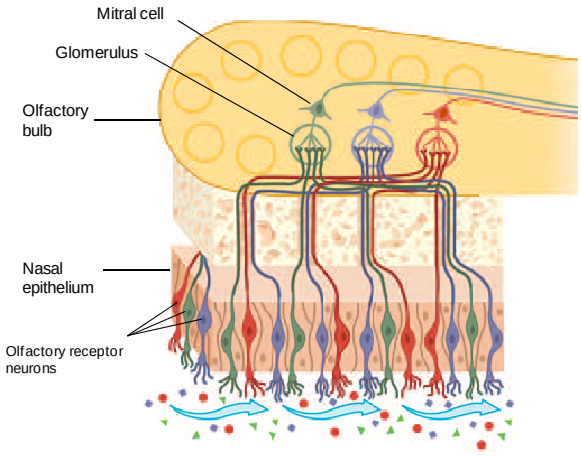

Figure 9. Schematic representation of the mammalian olfactory system. Figure adapted from Rinaldi (130).

1.3.1.2 Invertebrate olfactory system

In insects, olfactory stimuli are perceived through specialised structures called sensilla, which are localised mainly on the antennae (Figure 10). The sensillum is a cuticular sheath with a hair-like shape, which houses olfactory receptor neurons (ORNs) and three auxiliary cells. The surface of the sensillum is covered with tiny pores, through which odorants pass in to reach the ORNs (131). Dendrites of ORNs are contained inside the sensillum cavity surrounded by the sensillar lymph. The cell body of the neuron is tightly enveloped by the glia-like thecogen cell. This is partly enclosed by the trichogen and the tormogen cells (132). These three auxiliary cells are involved in the construction of the cuticular apparatus (133) and in the synthesis and degrading of proteins of the sensillar lymph.

As previously described for vertebrates, olfactory receptors (ORs) are localised on the dendrites of the ORNs, and each neuron expresses one or more odorant receptor genes (134). The invertebrate ORs are atypical seven-transmembrane domain proteins that form ligand-gated ion channels, by assembling a ligand-selective subunit with a common olfactory co-receptor (Orco) (135-137). Once odorant molecules cross the aqueous sensillar lymph and access the ORs a specific recognition mechanism is activated. The neuronal stimulus is transmitted from the ORNs to antenna lobe of the brain where they are processed and trigger behavioural responses (138;139).

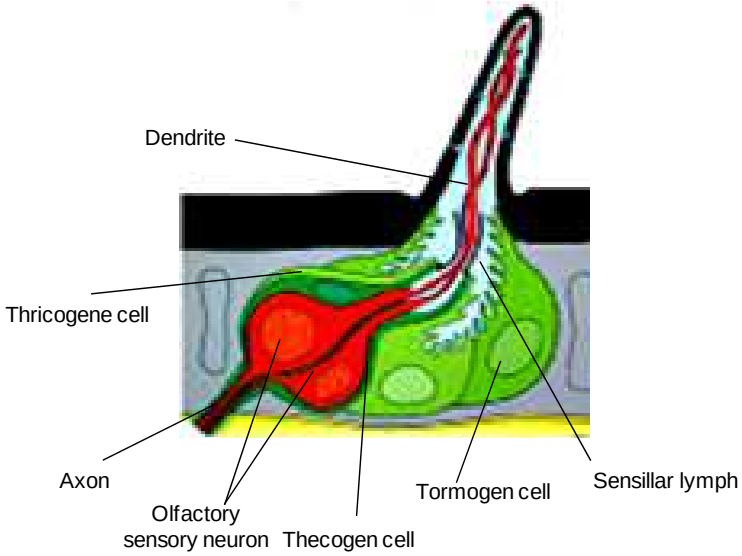

Figure 10. Schematic representation of an antenna sensillum. Figure adapted from Lee et al. (140).

1.3.2 Odorant Binding Proteins (OBPs)

*Odorant Binding Protein*s (OBPs) are small soluble proteins found in the aqueous environment that surrounds the olfactory receptor neurons in both vertebrates and invertebrates. The peculiarity of this family of proteins lies in their ability to bind odorants and pheromones in a reversible way (141).

OBPs were discovered at the beginning of 1980's in vertebrates by Pelosi et al. (2;142) and in insects by Vogt and Riddiford (143). Nowadays, several hundreds of OBPs have been identified and cloned from more than 40 species of insects (144), and from different species of mammals, including cow (145), rabbit (146), pig (147), porcupine (148), mouse (149) and human (150).

In the last thirty years, extensive research has been done to find out the role of OBPs in the olfactory process. Nevertheless, the physiological function of these proteins is not fully understood. When OBPs were isolated for the first time in mammals, it was thought that they were directly involved in the olfactory perception. Following the discovery of transmembrane olfactory receptors in vertebrates (2;127) and their role in olfactory signal transduction (151), experimental evidence proved that olfactory perception did not require the presence of OBPs. Odorant molecules can trigger olfactory stimuli through the direct interaction with the olfactory receptor (152). However, the high concentration of OBPs in the perireceptor space (153;154) strongly suggests their important role in olfaction. The first evidence of the active involvement of OBPs in the olfactory process was provided through knockout experiments performed on *Drosophila melanogaster.* These experiments demonstrated that the OBP LUSH is necessary for the correct recognition of the male pheromone vaccenyl acetate (155).

Other studies instead investigated the contribution of OBPs in the recognition of specific odours in behavioural assays (156-158). The unusual attraction of *Drosophila sechellia* for the distinctive smell of the plant *Morinda citrifolia* was related to two specific OBPs. The exchange of OBPs genes between

D.sechellia and other Drosophila species led to a strongly modified behaviour. Drosophila species that are generally repulsed by odours released by the tropical plant, were attracted when expressed genes coding for the OBPs of *D.sechellia* (158).

In another work, the behaviour of OBPs mutants of *D. melanogaster* was also investigated. Mutated flies, lacking in a specific OBP gene, were tested against the same set of odours. This work clearly demonstrated that the lack of a single gene encoding for a specific OBP was enough to alter the olfactory performance of the fly (156). Moreover, conformational changes in the structure of LUSH were considered responsible of the activation of the specific olfactory receptor. Flies engineered with a mutant version of LUSH, which mimicked their conformations in the complex with the pheromone, were reported to activate the specific olfactory receptor permanently (159).

The evidence clearly proves that OBPs are essential in the perception of the olfactory stimuli. The lacking or swapping of a single OBP can completely alter the behavioural response in the animal. However, further studies and investigations are required to understand the role OBPs play in the olfactory perception process in terms of the physiological mechanism at based of the olfactory receptor interaction.

1.3.2.1 Structure of Odorant Binding Proteins

The tertiary structure of OBPs is widely different between vertebrates and invertebrates.

OBPs of vertebrates belong to the lipocalin superfamily (160) that includes carrier proteins, such as the retinol-binding protein, the β-lactoglobulin and other proteins with different functions. Their three-dimensional structures is organised in a β-barrel domain, with a calyx-shaped cavity, made up of eight antiparallel β-sheets with a short segment of α- helix at the C-terminus (154;161). Cysteine residues can be present or not in the amino acid sequence of the vertebrate

OBPs. For instance, bovine OBPs lack cysteines, while others OBPs like porcine OBPs have a single disulphide bridge. However, the presence of disulphide bridges does not play a major role in the stability of the mammalian OBPs but instead does so in the insect.

The insect OBPs present a completely different tertiary structure. They are constituted by six α-helical domains arranged in a very compact structure, which encloses a hydrophobic cavity (162). The structure of insect OBPs is stabilised by three interlocked disulphide bridges (163), representing the characteristic fingerprint of all insect OBPs. Despite the large variability in amino acid sequences, the structure of the insect OBPs is well conserved across different Orders of insects (164).

Figure 11 displays the tertiary structure of both vertebrates and invertebrates OBPs.

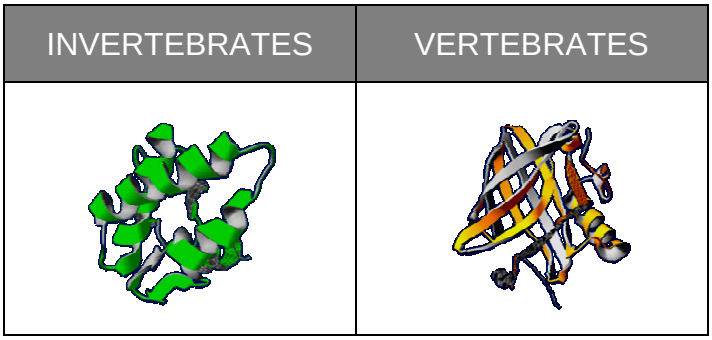

Figure 11. Tertiary structure of invertebrate (left) and vertebrate OBP (right).

1.3.2.2 Classification of Odorant Binding Proteins.

So far, Odorant Binding Proteins have been identified in a large number of vertebrate and invertebrate species. The family of OBPs comprises a heterogeneous group of proteins with different biochemical features, but all associated by the common property of binding chemical compounds. Vertebrate and invertebrate OBPs have been classified in several subgroups on the basis of their amino acid sequences.

In insects, OBPs are clustered in three main groups (144):

a. Pheromone Binding Proteins (PBPs), which are preferentially expressed in the pheromone-sensitive sensilla (165).
b. General Odorant Binding Proteins (GOBPs) are mainly found in the sensilla basiconica, that generally respond to plant odours (166)
c. Antennal Specific Proteins (ASPs), which are highly expressed in the antennal structures (167).

Moreover, according to the length of the sequence and with the number of cysteines, insect OBPs can also be divided in several subgroups. Classic OBPs bear a typical six-cysteine signature. They include PBPs, GOBPs, and ABPs. Tandem OBPs constituted by two classic OBPs linked by a bridge of few amino acids. C-plus OBPs have more than six cysteine residues. C-minus OBPs with only four of the six conserved cysteines. Atypical OBPs have a variable number of additional cysteines and generally a longer C-terminus (168-172).

In mammals, OBPs can be divided instead in four main classes:

a. Pheromone Binding Proteins (PBPs), which are highly concentrated in biological fluids, such as urine, saliva and vaginal secretion (173-175). They are mainly involved in the chemical communication.
b. Classic Odorant Binding Proteins (OBPs) that include proteins normally expressed in large concentrations in the nose.
c. VEG-like proteins. These proteins are expressed in the nasal epithelium and show an amino acidic sequence similar to the von Ebner’s glands proteins. (176).
d. Vomeronasal Secretory Proteins (VNSs), which are mainly expressed in the vomeronasal epithelium. So far, they have been identified only in mice (177).

1.3.3 Transducers

Mass transducers in the form of quartz crystal microbalances and interdigitated and screen-printed electrodes as capacitive transducers were employed for developing different types of OBP-based biosensors.

1.3.3.1 Quartz crystal microbalances (QCMs)

Quartz crystal microbalances (QCMs) are ultra-sensitive mass detectors that have found recently a wide application in the fields of sensors and biosensors (178). Due to the unique piezoelectric property of the quartz, QCMs can detect changes in mass of the order of 10^{-12} grams (179).

In 1880, Jacques and Pierre Curie (180) discovered that applying a mechanical stress to a quartz crystal, it produced a difference of potential across the two surfaces of the material. Nowadays, this phenomenon is known as the piezoelectric effect (181). The piezoelectricity occurs in crystals without a centre of symmetry (182). When a pressure is imposed to a crystal, the crystal lattice is deformed causing the separation of cationic and anionic species, which leads to changes in the dipole moment of the molecules (8). Many types of crystals exhibit the piezoelectric property. However, the electrical, mechanical and chemical features of the quartz make of it the most common material used for analytical applications (183).

QCMs consist of quartz wafers, sliced from a single crystal, with two electrodes deposited on both surfaces. The electrode coating is generally composed of gold or silver prepared by thermal evaporation (183) (Figure 12).

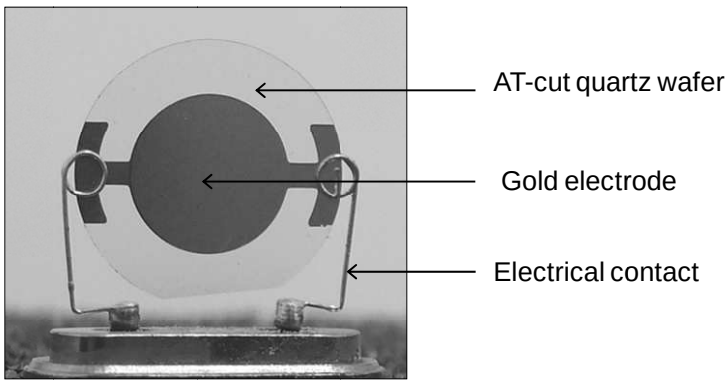

Figure 12. Quartz crystal microbalance.

When a voltage is applied between the electrodes of the QCM, the crystal lattice is deformed, leading the crystal to oscillate at the natural resonant frequency (184). The direction of the oscillation depends on the exact geometry of the cut of the crystal. The most used cut angle is 35º 15' from the Z axis of the crystal, known as AT-cut (185) (through the). AT-cut crystals show a temperature coefficient near to zero, meaning that the resonant frequency is stable over a range of temperatures between 0°C and 50°C (186). Several parameters, such as the thickness and the density of the crystal and the physical properties of the adjacent media i.e. density or viscosity can also affect the oscillation frequency of the quartz crystal.

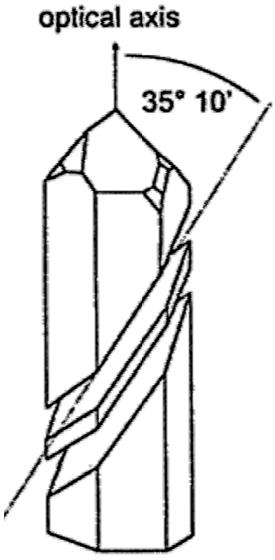

Figure 13. AT-cut quartz crystal. Adapted from Marx (187).

In 1959, QCMs were for the first time used as analytical device thanks to the study carried out by Günter Sauerbrey. Sauerbrey reported a linear relationship between the decrease in frequency of an oscillating quartz crystal and the mass of the deposited metal (187). The quantitative relationship between the relative shift of the resonant frequency and the added mass was derived through the so called Sauerbrey equation (Equation 2) (188).

$$\Delta \mathbf{f} = -\frac{\mathbf{2f_0^2 \Delta m}}{\mathbf{A}\sqrt{\boldsymbol{\mu_q \rho_q}}} \qquad \textbf{Equation 2}$$

where Δf is the measured frequency shift; f_0 is the intrinsic resonant frequency of the crystal; Δm is the mass change; A is the piezoelectrically active area; μq is shear modulus of quartz (2.95 x 10^{11} dyn cm^{-2}); ρq is density of quartz (2.65 g cm^{-3}) (187). The negative sign in the equation indicates that the addition of mass on to the resonator leads to a decrease in the resonant frequency of the crystal and vice versa.

The variations in the resonance frequency of the QCMs can be converted in detectable electric signals. However, Sauerbrey's equation can be applied only when the following assumptions are verified. (a) The mass is uniformly deposited over the entire active area of the QCM (184), (b) the total mass added on the surface of the QCMs does not exceed the 2% of the crystal mass (187) and (c) the measurements are performed in vapour phase. In cases where these assumptions are not met, the equation can give unreliable results.

QCMs have been successfully used either for surface characterisation or for studying biological interactions (189-194). In addition, they have been employed in medical diagnostics (85;190;195;196) and in the detection of hazardous chemicals such as warfare agents (197) and pesticides (198;199).

1.3.3.2 Capacitive transducers

Capacitive transducers have found recently a large interest in the biosensing area, since they offer the possibility to develop label-free sensors, with an easy readout and high sensitivity (200;201).

The simplest configuration of a capacitive transducer consists of two parallel electrodes separated by an insulator layer, called a dielectric. The dielectric may be air, mica, ceramic, fuel or other suitable insulating material (202). The capacitance, usually defined between the two conductors, is determined by the geometry of the electrodes and by the dielectric properties of the material in between (203). For instance, the capacitance of the well known parallel-plate capacitor is approximately equal to the Equation 3.

$$C = \varepsilon_r \varepsilon_0 \frac{A}{d}$$ **Equation 3**

where ε_0 is the dielectric permittivity of the vacuum and ε_r is the relative permittivity of the material between the plates. A is the electrode plate surface area and d the plate distance. From this equation it is evident that a change in the capacitance can be imposed only in three ways: (i) by altering the distance d between the two plates, (ii) by altering the overlapping area between the two plates or (iii) by changing the dielectric permittivity between the plates (204).

In case of capacitive biosensors, the interactions between the bioreceptor and the ligand can affect several parameters such as the dielectric properties, the charge distribution and also the distance between the two electrodes (205). All these variations can be recorded as changes in the initial capacitive value.

Capacitive sensors used in this research belong to two different categories of capacitors: electrode- solution interfaces and interdigitated electrodes (IDEs).

Electrode Solution interface

An electrode, immersed in an electrolyte solution can be described as a capacitor for its ability to store charges. For an applied potential, the electrode will possess a charge q_m and the solution another charge q_s, that will be equal and contrary to q_m. Charged species and dipoles, present in the solution are oriented at the electrode/solution interface, hence forming an electrical double-layer (EDL).

The solution- electrolyte interface has been experimentally demonstrated to behave like a capacitor (204). The total capacitance at the electrode-solution interface can be described as the sum of three capacitors in series as schematised in Figure 14 (200).

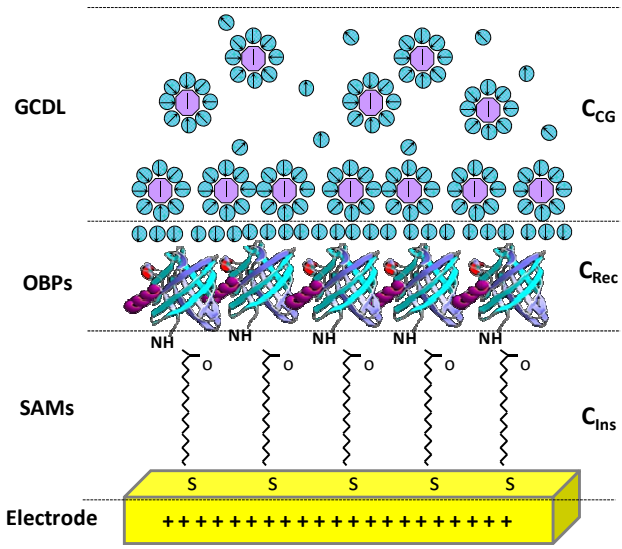

Figure 14. Schematic representation of a polarised protein-based capacitive biosensor and EDL organised at the biosensor/solution interface.

The first capacitor represents the insulating layer (C_{Ins}), that in case of biosensors is often constituted by a self-assembled monolayer of alkanethiols (SAMs) (206). The second capacitor, C_{Rec}, includes the contribution of the bio-recognition element and the Stern layer. The Stern layer consists of bound water molecules, which are present between the recognition elements and the diffuse layers (207). The third capacitor corresponds to the diffuse Gouy and Chapman layer, (C_{GC}) which extends out into the bulk of the solution.

The binding between bioreceptors and target ligands influences the complex capacitance of the recognition layer, C_{Rec}, and thus produces a measurable change in the total capacitance. In summary, the total capacitance can be described through the following equation:

$$1/C_{TOT} = 1/C_{Ins} + 1/C_{Rec} + 1/C_{GC} \qquad \textbf{Equation 4}$$

Equation 4 shows that lower capacitance values dominates the total capacitance. This equation is considered valid when the bio-recognition element covers the electrodes completely, neglecting the presence of holes on the

sensing layer. If the surface is not sufficiently insulated, ions can move through causing short-circuits of the system, which lead to a decrease or absence of the signal. Electrochemical methods such as cyclic voltammetry (CV) and electrochemical impedance spectroscopy (EIS) can be used to study the quality of the insulation layer on the electrode surface.

Interdigitated electrodes (IDEs)

Interdigitated electrodes consist of a series of finger-like parallel electrodes deposited on plane substrates (208). Alternating electrodes are connected together forming a high surface planar capacitor (Figure 15). A broad selection of materials, such as silicon, glass, and polymers plastic, can be used as substrates. When a potential is applied to an interdigitated electrode, the generated electric field travels from one electrode to the other, penetrating the dielectric film and the substrate underneath the electrodes (209).

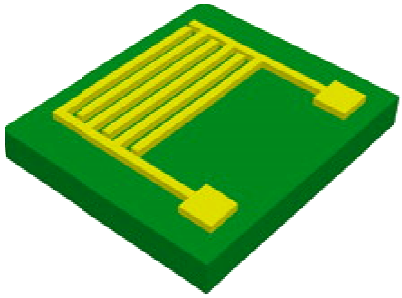

Figure 15. Schematic representation of an interdigitated electrode. Figure adapted from Tsouti et al. (204)

The capacitance measured between the two electrodes can be generally described using Equation 5.

$$C = 2n\varepsilon_r\varepsilon_0 \frac{A}{d}$$ **Equation 5**

where ε_r is the dielectric constant of the medium between the plates, ε_0 is the permittivity of free space, A is the area of the electrodes and d is the distance

between the two electrodes, n is the number of electrodes and finally the factor 2 in this equation represents each electrode forming the capacitor.
Interdigitated electrodes, compared to other capacitors, offer a larger electrode area, a higher sensitivity and more rapid reaction kinetics, due to proximity of the cathodic and anodic electrodes (210). Additionally, IDEs do not need to use a reference electrode, providing a simple tool for obtaining a steady-state response (211).

Interdigitated capacitive transducers used for biosensing applications rely on the detection of changes in the dielectric constant. The interaction between target analytes and biomolecules immobilised on the sensor surface, leads to changes in the capacitance value between the two electrodes (204). Such capacitance variations are detected as output signals.

IDE biosensors has been applied for both label-free and non label-free detection methods. They have been successfully used for the detection of *picomolar* concentrations of cancer biomarkers in human blood (212), for monitoring contaminants in drinking (213) and for the detection of harmful foodborne bacteria such as *E. coli* O157:H7 (214).

Capacitive biosensors have established a new niche of electrochemical sensors. Due to their high sensitivity, high selectivity, reusability and fast response, they have attracted increasing interest during the past few years (215). Moreover, their low power consumption along with the possibility to be realised in micro-scale make them even more interesting for developing portable biosensors (204).

Nowadays, capacitive transducers have shown great promise as immunosensors device (206), for the detection of heavy metal ions (205) as well as platforms for nucleic acid biosensors (216).

1.3.4 Biosensors based on olfactory elements: state of the art.

The excellent capacity of the olfactory system to detect thousands of chemical compounds has raised the interest of specialists of both engineering and biology fields, for developing devices able to mimic the performance of the human nose.

The knowledge achieved in the olfactory system has also allowed the improvement of the performance of chemical sensors based on biological olfactory elements. Moreover, new generations of transducers, with higher signal amplification and nano-scale dimensions have enabled the realisation of portable devices able to detect very small inputs.

However, artificial olfaction devices have not reached the sensitivity and selectivity of biological olfactory systems yet (217). Several structures belonging to the olfactory system, such as olfactory tissues, olfactory cells and olfactory-related proteins have been successfully used as sensing layers of biosensors for the detection and discrimination of odorant molecules. In the following sections, selected biosensors based on olfactory structures are reviewed and described on the basis of the olfactory element employed.

1.3.4.1 Mammalian olfactory tissues and insects' antennae

Mammalian olfactory tissues and the antennae of insects have often been combined with various transducers to investigate electrophysiological responses to odour molecules.

Microelectrode arrays (MEA) were employed by Chen (218) and Liu (219) for studying the electrophysiological activities of the olfactory bulb (OB) and the olfactory epithelium (OE) of rat, respectively. The use of an array of electrodes allowed recording of the signals originated from different regions of the neuronal tissue, simultaneously. In the work carried out by Chen, the response of

different layers of OB to the neurotransmitter glutamic acid was investigated. Liu instead tested the OE of rat towards four different analytes. Acetic acid, butanedione, ethyl ether and acetone were used as odour stimuli. Each odour evoked a potential with a characteristic frequency and amplitude in the olfactory epithelium, showing odour discrimination. Both biosensors kept the original neural network, seeking to reproduce systems close to the physiological scenario as much as possible.

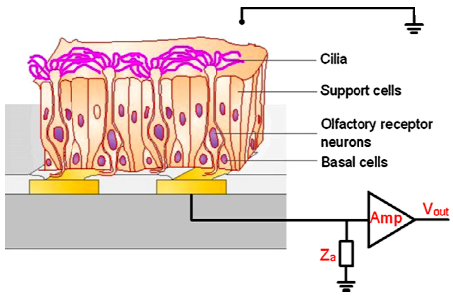

Figure 16. Schematic representation of the rat OE based biosensor developed on MEA. Adapted from Liu et al. (220).

The ability of the olfactory epithelium to discriminate among analytes was also confirmed in a work previously published by Liu et al (221). The olfactory mucosa of the rat was used to investigate the response to both acetic acid and butanedione by means of a light-addressable potentiometric sensor (LAPS). A characteristic firing mode was recorded in presence of a specific analyte, demonstrating the ability of the sensor to discriminate between the two compounds.

Antennae from different species of insects were also employed for developing portable sensors. Antennae of the Colorado potato beetle were combined with a field-effect-transistor (FET) for detecting volatiles released by damaged potatoes. Potato plants liberate (Z)-3-hexen-1-ol in the environment, when they are subjected to mechanical and pests damages. The antenna based biosensor was extremely sensitive and able to detect 1 *ppbv* concentrations of (Z)-3-hexen-1-ol in air at 10 metres from the source (222).

Myrick instead developed a more complex sensor, combining antennae of different species of insects. The array showed a rapid response, within 15-75

milliseconds from the odour exposition. However, the sensor had a short lifetime, less than 90 minutes, after which the response lost reliability (223).

Tissue and antenna -based sensors showed in general a good sensitivity, up to *parts per billion*, and ability to discriminate among several analytes in both vapour and liquid phases. Despite that, the wide usage of this type of sensors in large scale is limited by two main factors: (a) the realisation of these biosensors always required the sacrifice of the animal and (b) the short lifetime of the device, less than few hours after the preparation, does not allow application in the field.

Table 1 summarises the main features of the olfactory tissue and antenna-based biosensor discussed above. The tested analytes and the respective concentrations are reported as well.

Bioelement	Transducer	Analyte	Concentration tested	Ref.
Olfactory bulb slices	Microelectrode array (MEA)	Glutamic Acid	10^{-5} M	(218)
Olfactory epithelium	Microelectrode array (MEA)	Butanedione; Acetic Acid; Ethyl Ether; Acetone	10^{-7} M	(219)
Olfactory mucosa	light-addressable potentiometric sensor (LAPS)	Acetic Acid Butanedione	2.5 10^{-4} M	(221)
Whole antenna	Field- effect transistor (FET)	(Z)-3-Hexen-1-ol	0.01 ppbv	(222)
Antennae array	Multi-channel electroantennogram (EAG)	(Z)-11-Hexadecenal; (E,E)-8,10-Dodecadien-1-ol; (E)-11-Tetradecen-1-ol; Indole; Butyric Acid; Citronellal; Thujone; Acetophenol; Methyl- Salicylate; Phenylethyl Alcohol; (Z)-3-Hexenyl; Acetate	N.A.	(223)

Table 1. Summary of the major forms of olfactory tissue and antenna-based biosensors.

1.3.4.2 Olfactory receptor neurons (ORNs)

Olfactory receptor neurons have also been successfully utilised for sensing applications. ORNs can be cultured directly on the surface of transducers in order to develop sensors able to detect analytes in both vapour and liquid environments (224;225).

LAPs chips was used by Wu to record in real- time the electrochemical signals of 26 ORNs, in presence of a mixture of analytes i.e. acetic acid, octanal, cineole, hexanal, 2-heptanone (225).

MEA chips were also used as platforms for growing ORNs. Ling at al. studied the response of an array of olfactory receptor neurons to the vapour of both limonene and isoamyl acetate. Each compound excited the olfactory neurons population with a characteristic pattern, with the possibility to discriminate between the two chemicals (224).

In addition, ORNs can be also customized in order to create olfactory neurons able to detect specific analytes with high sensitivity. Du et al. (226) demonstrated that olfactory receptors of *Caenorhabditis elegans* can be successfully expressed in rat ORNs. The bioengineered ORN responded to 0.1 µM concentrations of diacetyl, the natural ligand of OR-10 of *C*. *elegans*.

However, several practical issues have limited the use of olfactory receptor neurons for sensing applications. The extraction of ORNs from the olfactory epithelium is a complex process that also in this case implicates the sacrifice of animals. This makes large-scale production impossible. On the other hand, growing ORNs *in vitro* is an expensive practice, which requires aseptic rooms and specialised technical staff.

Table 2 reports the main features of the described sensors, with reference to the tested analytes and concentrations.

Bioelement	Transducer	Analyte	Concentration tested	Ref.
Olfactory Sensor Neurons of rat	LAPS	Acetic Acid; Octanal; Cineole; Hexanal; 2-Heptanone	10^{-3} M	(225)
Bioengineered Olfactory Sensor Neurons of rat	LAPS	Diacetyl; Isoamyl- Acetate; Acetic Acid	10^{-7} - 10^{-4} M 5 10^{-7} M	(226)
Olfactory Sensor Neurons of rat	MEA	DL-Limonene; Isoamyl- Acetate	10^{-6} M	(224)

Table 2. Summary of the major olfactory receptor neurons based biosensors present in literature.

1.3.4.3 Olfactory receptors

In the last few years, a growing interest in the use of mammalian and insect olfactory receptors for developing artificial noses has been recorded. An increasing number of papers were published on the use ORs as bio-recognition, from the 2005 to 2013, as Figure 17 shows. However, despite this growing interest, the research in this field is still limited.

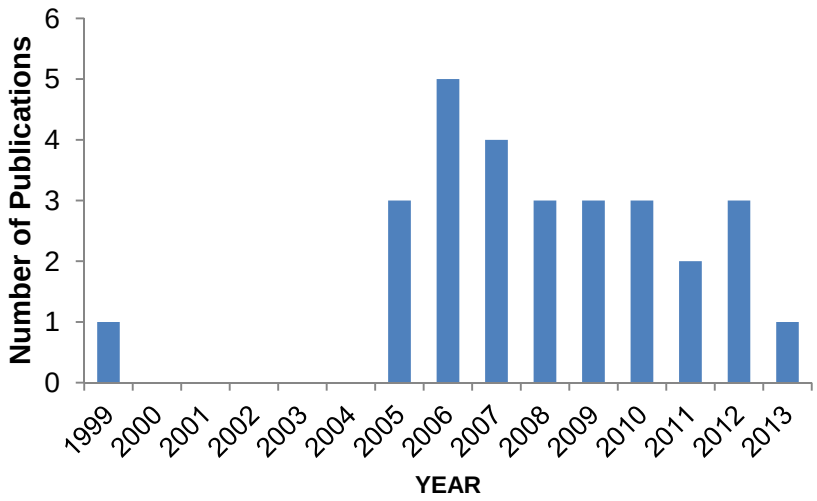

Figure 17. Number of publications per year found using Web of Science. The search was performed using the term "biosensors" refined by "olfactory receptor". The abstracts of each publication were examined to ensure that the paper was related to this topic.

The total number of papers, where ORs are used for sensing applications, is lower than 30 spread across a period of fourteen years. A large gap is observed between 2000 and 2004, where no scientific research in this area was published.

In 1999, Wu published the first scientific work on a biosensor based on olfactory receptors (121). The sensor employed ORs, extracted from bullfrogs, as sensitive layer of QCMs for detecting volatiles. *Parts per million* concentrations of n-caproic acid, isoamyl acetate, n-decyl alcohol, β-ionone, linalool and ethyl caproate were successfully detected specifically. Since then, several biosensors have been developed utilising ORs as sensing materials.

ORs biosensors can be constructed by using either whole cell expressing ORs or liposomes carrying ORs. Liposomes can be generated by fragmentations of heterologous system expressing the receptor or by extraction from living olfactory epithelium. Oocytes of Xenopus, human embryonic kidneys and yeast cells expressing ORs have been used combined with different transduction systems for detecting chemical compounds.

Missawa et al. used living oocytes of Xenopus expressing ORs, to build an artificial bio-nose. The sensor was integrated inside a robot head. *Parts per billion* concentrations of analyte were enough to trigger the response of the sensor, which led to motions of the head of the robot (227). However, the system had high noise levels and a relatively short lifetime. Oocytes do not survive more than 2-3 weeks after removal from the frog (228).

More simply, Lee et al. (229) grew, on planar electrodes, human embryonic kidney (HEK)-293 cells bearing rat olfactory receptors. The interaction between the receptor and the ligand octanal was directly detected as variation in the membrane potential.

Saccharomyces cerevisiae bearing the human olfactory receptor OR17-40 were combined with interdigitated electrodes in a work published by Marrakchi et al. (230). In this case, the interaction between the ligand and the receptor was recorded as changes in the conductance at the surface of the electrode. The sensor was highly sensitive, able to detect down to 10^{-14} M concentrations of the analyte. The sensitivity of this OR-sensor was further increased by co-expressing the human olfactory receptor OR-17-40 together with the α-subunits of G_{olf} protein (231).

The use of field effect transistors (FETs) instead allowed the development of highly sensitive and selective devices as demonstrated by Kim at al. (232). Femtomolar concentrations of analyte were detected by the OR-FET biosensor, with a resolution close to a single-carbon-atom.

Surface acoustic waves (SAWs) and quartz crystal microbalances (QCMs) have been also employed for studying the activity of several olfactory receptors. *C.elegans* OR-10 grafted on to the gold surface of SAW chips were used in vapour phase in the work carried out by Wu et al (82). The developed sensor showed a high sensitivity with a detection limit of 1.2 10^{-14} M. However, the lifetime of the biosensor was only a week, time that cannot be considered enough for long-term sensing applications. The same ORs were also

investigated as sensing layer of QCMs. This study confirmed the good sensitivity and repeatability of the biosensor, with a detection limit lower than 1.5 ppm (v/v). Also in this case, loss of sensing performances were observed after seven days from the first usage, possibly due to conformational changes that could affect the ORs (233).

Surface plasma resonance was also utilised for evaluating the response of ORs in cell and non-cell based systems. Nanosomes bearing human OR 17-40 and α-subunits of G_{olf} protein were used in SPR experiments. The interaction between receptors and ligands was detected through the desorption of G_{olf} subunit from the lipid bilayer. The sensors that resulted were stable over time, with the possibility to be reused for more than eight times (234). The dose-response curve calculated for the sensor, did not follow the classic sigmoid behaviour, which is usually observed for G-protein-coupled-receptors (230). However, in presence of the Odorant Binding Proteins OBP-1F, the typical dynamic of binding of ORs was re-established (235).

ORs seem to own all the features required for developing high performance biosensors. They have a high selectivity, with resolution close to a single carbon atom, and sensitivity that can reach femtomolar concentrations. However, the short lifetime of the OR-biosensors along with the difficulties of synthesis ORs in large quantity, represent the main drawbacks of these devices. In addition, the use of suitable medium conditions is fundamental for retaining the structure and the functionality of these transmembrane proteins.

Table 3 summarises the main olfactory receptor-based biosensor found in literature. Details about the transducer used, analytes tested and concentrations are reported as well.

Bioelement	Transducers	Analyte	Concentration tested	Ref.
Bullfrog ORs	QCMs	N-Decyl- Alcohol; Isoamyl- Acetate; N-Octyl- Alcohol; β-Ionone; N-Caproic Acid; Linalool; Ethyl- Capronate	10- 6500 ppm	(121)
Rat I7 on HEK cells	Plate micro-electrodes	Octanal	10^{-3}-10^{-2} M	(229)
BmOR1, BmOR3, PxOR1, and DOr85b, in Xenopus oocytes	two-electrode voltage clamping	Bombykol; Bombykal; (Z)-l1-Hexadecenal; 2-Heptanone	10^{-8}-10^{-6} M	(227)
Human olfactory receptor	swCNT-FET	Amyl- Butyrate; Butyl- Butyrate; Propyl- Butyrate; Pentyl- Valerate	10^{-12}- 10^{-10} M	(232)
***S. cerevisiae* with human OR17-40**	IDEs	Helional; Heptanal	10^{-14}- 10^{-8}M	(230)
Human OR17-40 and α-subunits of G_{olf} protein	EIS	Helional; Heptanal	10^{-11}- 10^{-7} M	(231)
***C. elegans* OR-10**	SAWs	Diacetyl; Butanone, 2,3-Pentanedione	10^{-13}- 10^{-7} M.	(82)
***C. elegans* OR-10**	QCMs	Diacetyl; Isoamyl- Acetate; Anisole; Lavender; Butanone; 2,3-Pentanedione	10- 100 ppm	(233)
HEK cells expressing Rat I7	QCMs	Hexanal; Heptanal; Octanal; Nonanal; Decanal	10^{-11}- 10^{-4} M	(236)

Human OR17-40 and α-subunits of G_{olf} protein in nanosomes	SPR	Octanal; Nonanal; Heptanal; Diacetyl; Cyclohexyl- Acetate; Octanol; Octanone; Octanoic acid; Isoamylacetate; Pyridine; Helional; Cassione; Piperonyl- Acetate; 3,4-Methylenedioxyphenyl; Acetone; 3,4-Methylenedioxy-Propiophenone; Lilial	10^{-10}- 10^{-5} M	(234)

Table 3. Summary of the main olfactory receptor based biosensors.

1.3.4.4 Odorant Binding Proteins (OBPs)

OBPs are becoming an attractive tool for sensing applications due to their ability to binding chemical compounds in a reversible way with resistance to temperature and denaturation. Despite these key features, the research carried out on the use of OBPs in sensing area is still narrow, when compared with ORs.

Biosensors based on OBPs are mainly combined with both resonant and electrochemical transducers.

Polypeptides that mimicked the binding site of LUSH of *D. melanogaster* were used by Sankaran et al. for detecting *Salmonella* contaminations in packaged beef (237). Alcohols such as 3-methyl-1-butanol and 1-hexanol were used as markers of the bacterial contamination. The sensor, developed using QCMs, showed a good sensitivity, with a detection limits calculated between 1 and 3 ppm.

An array of mammalian OBPs was instead developed by Di Pietrantonio for studying the response to the analytes carvone and octenol (238). Recombinant porcine and bovine OBPs were used as sensing layers of SAW resonators. The high affinity of the porcine OBP toward the octenol allowed discrimination between the two compounds. The biosensor response was fast, within 30 seconds from the analyte exposure, and fully reversible. The array could be reused for several assays without losing performance.

The OBP binding events can be also electrochemically detect as demonstrated in the work published by Lu et al. (239). Lu immobilised recombinant honeybee OBPs on gold IDEs and tested them against pheromones and floral odours in liquid phase. The interaction between OBPs and ligands was recorded as the variation in the electron transfer resistance (R_{ct}) of the biosensor, in presence of the redox probe ferro/ferricyanide The presence of bound ligands led to a reduction in the R_{ct}. Ligand concentrations ranging from 10^{-6} M to 10^{-3} M were successfully detected by the OBP-sensor, showing linear concentration response curves for all the tested analytes.

Interdigitated electrodes were instead employed for detecting chemical compounds in vapour phase. Porcine OBPs, covalently linked on the gold surface of IDEs, were tested against *parts per million* concentrations of ethanol and methanol. Decreasing in the charge-transfer resistance was observed in presence of the analyte. The observed variation in the impedimetric curve was likely due to conformational changes of OBPs caused by the interaction with the analyte (240).

Ultrathin films of OBPs of rat deposited by Langmuir-Blodgett techniques were studied by Hou et al. (241). The interaction between the analyte, isoamyl acetate and the OBP-film was monitored by electrochemical impedance spectroscopy. Decreases in resistance were observed in presence of the analyte, confirming the findings described by other authors.

So far, the research performed on the use of OBPs as bio-recognition elements of biosensor have demonstrated the possibility to develop highly sensitive and stable devices. The use of arrays of OBPs belonging to different species of animals can improve the selectivity of the system and the ability to discriminate among several ligands.

Contrary to the previously described olfactory elements, OBPs can be easily expressed in bacterial system in a relatively inexpensive way and with high yield, reducing the biosensor costs.

In Table 4 the main features of the described OBPs based biosensors are summarised.

Bioelement	Transducer	Analyte	Concentration tested	Ref.
Binding site of LUSH *D.melanogaster*	QCMs	3-Methyl-1-Butanol; 1-Hexanol	10-100 ppm	(237)
Wt bovine OBP **Dm bovine OBP** **Porcine OBP**	SAW	Octenol; R-(-)-Carvone	9-80 ppm 13-61 ppm	(238)
***Apis cerana cerana* ASP2**	IDEs (EIS)	Methy-*p*-Hydroxyl; Benzoate Isoamyl; Acetate; Linalool; Geraniol; β-Ionone; 4-Allylveratrole; Phenylacetaldehyde; Dibutyl- Phthalate; Butanedione	10^{-6}- 10^{-3} M	(239)
Porcine OBPs	IDEs (EIS)	Ethanol; Methanol	20 ppm 10 ppm	(240)
Rat OBP-1F	EIS	Isoamyl- Acetate	840 ppm	(241)

Table 4. Summary of the main OBP-based biosensors.

In the last few decades, extensive work has been carried out to study Odorant Binding Proteins in both vertebrate and invertebrate systems. The binding activity of OBPs toward a large number of chemical compounds has been well characterised by using fluorescence binding assays. Dissociation constants of both insects and mammals OBPs, against different classes of chemicals, are now available in literature. Moreover, structural characterisation of OBPs-ligands complexes, performed by crystallography techniques and circular dichroism, has allowed identification of the amino acid residues involved in the binding process. The information collected on the structure and function of these proteins has been employed for developing different types of biosensors.

The emerging research in the use of OBPs as sensing material has already provided encouraging results. OBPs based biosensors have been successfully utilised for the detection of odours and pheromones in vapour and liquid phases.

Inspired by the promising potentialities of OBPs, we decided to investigate further their ability to bind chemical compounds, studying different type of OBP-based biosensors. Our aim was to develop simple and label-free sensors, which may be used as analytical devices for the control of perishable food along the transport and storage or in agriculture, for the monitoring of useful insects and pests. The development of portable, high sensitivity and low cost devices can be very appealing in the biosensor market especially in the food and agriculture areas, where expensive analytical equipment are usually used for the quality control.

2 Materials and Methods

All chemicals used were purchased from Sigma-Aldrich, UK. All reagents used for the protein synthesis were from Biorad UK. The proteins, porcine OBP-C and *Locusta migratoria* OBP1, were kindly provided by Prof. Paolo Pelosi (University of Pisa, Italy). The major urinary protein of the mouse (MUP-10) was provided by Prof. Carla Mucignat (University of Padova, Italy).

2.1 Odorant Binding Proteins: gene design, expression and purification

Table 5 shows a list of proteins expressed during the project. With the exception of the Green Florescence protein (GFP) of *Aequorea victoria*, these proteins were tested as sensitive layers of different transducers for the detection of organic compounds in vapour and liquid phases.

	LIST OF PROTEINS EXPRESSED	ABBREVIATION
1	Porcine OBP F88W	pOBPF88W
2	Porcine OBP W16F-F88W	pOBPW16F-F88W
3	*Apis mellifera* OBP14	A.melOBP14
4	*Polistes dominula* OBP1	P.domOBP1
5	*Bombyx mori* PBP1	B.moriPBP1
6	*Bombyx mori* GOBP2	B.moriGOBP2
7	*Aequorea victoria* GFP	GFP

Table 5. List of the proteins synthesised in our laboratory and used for the realisation of biosensors.

2.1.1 The gene design

The gene coding for the General Odorant Binding Protein 2 (GOBP2) of *Bombyx mori* was synthesised by the company Eurofin MWG Operon (Germany). The gene was designed in accordance with the mRNA sequence annotated in GenBank database (accession no. NM_001044033). The amino acid sequence was analysed by using the software package SignalP 4.1, in order to identify the noncoding sequences.

A tag of six histidines (His-tag) was added to the 5' end of the sequence. The presence of the His-tag fused with the recombinant OBP facilitated the purification process from the bulk of other proteins (242). His-tags are the most widely used affinity tags. The imidazole ring of the histidine shows a high affinity for chelated metal ions, such as nickel (Ni^{2+}). Metal ions complexed with chelating agents are strongly fixed to solid supports, usually agarose beads. The protein separation occurs on the basis of interactions between the imidazole of the histidine and the metal ions fixed on a solid matrix (243).

At the 5' and 3' end of the gene, the restriction sites for NdeI and EcoRI were inserted respectively. The restriction site is a nucleotide sequence, which is recognised by a restriction enzyme. The restriction enzyme cut the site, leaving an overhang at each end (sticky end). The expression vector is then cut with the same restriction enzymes, generating the same sticky ends. Using a DNA-ligase, both extremities of the gene were joined within the expression vector. For the GOBP2 the pET-30a (Novagen) was used. Figure 18 displays the schematic representation of the gene construct used for the synthesis of the GOBP2 of *Bombyx mori.*

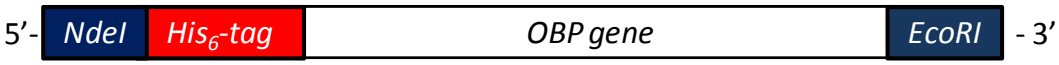

Figure 18. Schematic representation of the gene construct used for the synthesis of GOBP2 of *B.mori.*

The other vectors, used for the expression of proteins were kindly provided by Prof. Pelosi, University of Pisa, Italy.

2.1.2 Protein expression

For protein expression, *E. coli* BL21(DE3) cells (Agilent Technology) were transformed with 2 µL of the expression vector pET containing a specific OBP (unknown concentration). Bacteria colonies were grown overnight in 10 ml of Luria-Bertani/Miller broth containing 100 mg L^{-1} of ampicillin or kanamycin, depending on the type of vector used. The culture was diluted 1:100 with fresh medium and grown at 37°C until the absorbance at 600 nm reached 0.7 AU. At this stage, 0.4 mM isopropylthio-D-galactoside (IPTG) was added to the culture to induce expression. After 2 h at 37°C, the cells were harvested by centrifugation, resuspended in 50 mM Tris-Cl pH 7.4 and lysed by sonication.

The recombinant porcine OBPs were present at this stage in the supernatant while the insects' OBPs were found in an insoluble form, as inclusion bodies. The protein were solubilised by dissolving the pellet obtained from 1 L of culture in 5 ml of 8 M urea, 1 mM of dithiothreitol (DTT) in 50 mM Tris-Cl buffer, pH 7.4, then diluting the solution to 50 ml with Tris-Cl buffer and dialysing three times against Tris-Cl. (244)

2.1.3 Protein purification

The proteins were purified by two chromatographic steps on anion-exchange resin DE-52 (Whatman), using a gradient of 0.5 M NaCl in Tris buffer, followed by gel filtration on Superose-12 (GE-Healthcare). Protein bearing the His-tag was purified by using a nickel-affinity chromatography (GE-Healthcare). 0.5M imidazole in Tris-Cl buffer was used to elute the protein.

The fractions were analysed by SDS-PAGE and by UV spectroscopy to evaluate the amount of DNA co-eluted with the protein. At the end of the purification procedure, the proteins were more than 95% pure, as judged by SDS-PAGE, and virtually free from DNA.

Protein samples were delipidated at acidic pH (pH 4-5) using a suspension of Sephadex LH-20 (Pharmacia Fine Chemicals) and mixing for 2 hours at 4˚C (245). The delipidation step was essential to remove any possible ligands present in the binding site of the protein. The proteins were then dialysed against 50 mM sodium phosphate buffer at pH 7.4.

2.2 Fluorescence measurements

Emission fluorescence spectra were recorded on a Perkin Elmer LS55 instrument at 25°C in a right angle configuration, with a 1 cm light path quartz cuvette and 5 nm slits for both excitation and emission. The protein was dissolved in 50 mM Tris-Cl buffer, pH 7.4 or 50 mM sodium phosphate buffer pH 7.4.

2.2.1 Fluorescence binding assays

OBPs	PROBE	LIGANDS
Porcine OBP F88W	1-AMA	geosmin 2-phenylethanol S-(+) carvone R-(-) carvone 2-isobutyl-3-methoxypyrazine
Porcine OBP W16F-F88W	1-AMA	
Polistes dominula OBP1	1-NPN	
Bombyx mori PBP1	1-NPN	bombykol bombykal
Bombyx mori GOBP2	1-NPN	bombykol bombykal

Table 6. List of probes and ligands tested in fluorescence binding assays.

The binding activities of the expressed OBPs were measured using the fluorescent ligands 1-aminoanthracene (1-AMA) and 1-N-phenylnaphthylamine (1-NPN). OBPs display a high affinity of binding toward these probes. They can be used to calculate the dissociation constants of ligands that compete for the protein binding. A micromolar concentration of the protein in buffer was titrated with aliquots of 1 mM of probe prepared in methanol to final concentrations of 2-

16 μM. The probes were excited at specific wavelengths. 1-NPN was excited at 337 nm and the emission spectrum was recorded between 380 and 450, while 1-AMA was excited at 375 nm and the fluorescence recorded between 400 to 570 nm. The main feature of these probes is the ability to change the emission wavelength peak when shift from the free to the bound form. For instance, 1-AMA when excited at 375 nm presents a weak fluorescence emission with a maximum at 537 nm, but in the presence of the protein, this maximum shifts to 480-490 nm, allowing visualisation of the binding process (147). In Table 6 are listed the different OBPs used in our research together with the probes and the ligands tested.

The binding constants for the OBP-probe complex were calculated using *Sigma Plot™ software* and the number of binding sites were set equal to one. The following equation was used: $y=(B_{max} * x)/(K_D+ x)$, where y is the degree of saturation, B_{max} is the number of maximum binding sites and K_D is the dissociation constant (246).

The affinity of the ligands was measured in competitive binding assays. A solution of the protein and probe, both at the same concentration was titrated with 1 mM solutions of each competitor to final concentrations of 0.5-16 μM. Dissociation constants of the competitors were calculated from the corresponding IC50 values, using the equation: $K_D=[IC50]/1+[Probe]/K_{Probe}$, where [Probe] is the free concentration of the fluorescence probe and K_{Probe} is the dissociation constant of the complex Protein/Probe (244) .

2.3 Quartz crystal microbalances (QCMs)

Quartz crystal microbalances were purchased from the National Research Council (CNR) of Rome, Italy. Piezoelectric AT-cut quartz crystals, with a resonance frequency of 20 MHz and 7.95 mm diameter were used. The crystals were coated on both sides with a layer of gold (Au geometric surface 4.9 mm of

diameter). The gold was deposited on the quartz wafer through an adhesion layer of titanium.

2.4 Screen-printed electrodes (SPEs)

Disposable screen-printed electrodes were acquired from Metrohm AG (Switzerland). The screen-printed electrodes were in a three electrodes configuration, with a gold working electrode (4 mm diameter), an auxiliary carbon electrode and a reference electrode of silver, all printed on the same ceramic strip.

2.5 Interdigitated electrodes (IDEs)

Gold interdigitated electrodes realised on flexible platforms were provided by L'École polytechnique fédérale de Lausanne (EPFL), Switzerland. The IDEs were realised by thermal evaporation on Upilex® substrates. The gold was evaporated on the polyimide surface utilising an adhesion layer of chromium. The IDEs used for our experiments had 5 µm gaps between electrodes and dimensions of 2.29 mm x 2.84 mm.

2.6 Protein immobilisation methods

Proteins were immobilised on the gold surfaces by self-assembled monolayers (SAMs). Two different alkanethiols were used:

- thioctic acid (TA)
- 16-mercaptohexadecanoic acid (MHA)

The used of thioctic acid was preferred to 16-mercaptohexadecanoic acid for immobilising proteins on quartz microbalances. The short alkyl chain of TA

minimized the dissipation phenomena that can happened on the surface of the QCMs. SAMs of 16-mercaptohexadecanoic acid was used to graft OBPs on screen-printed electrodes and interdigitated electrodes. Electrochemical studies demonstrated the formation of a more compacted and insulated layer on the electrode surfaces when 16-mercaptohexadecanoic acid was used.

2.6.1 Cleaning procedure

Quartz crystal microbalances (QCMs):

Before the protein immobilisation, the gold surface of the QCMs was cleaned by dipping the crystal in Piranha solution (1:3= 30% H_2O_2: H_2SO_4) for few minutes to remove any organic residues from the surface. The QCMs were then rinsed with ddH_2O and ethanol and dried with a nitrogen stream.

Screen-printed electrodes (SPEs)

The gold surfaces of screen-printed electrodes were cleaned by cyclic voltammetry (CV) from -1.4 to 1.4 V at a rate of 100 mV s^{-1}, with a 10 mV potential step. The electrode was dipped in a solution 0.5 M sulphuric acid, and the CV was run approximately for five cycles until a stable CV signal was reached (247). After that, they were rinsed with ddH_2O and ethanol and dried in a nitrogen stream.

Interdigitated electrodes (IDEs)

The gold interdigitated electrodes were cleaned by dipping the electrodes in a 0.5 M sulphuric acid solution for few minutes and then were rinsed several times with ddH_2O. After that, the electrodes were immersed in a 30% solution of H_2O_2 for few minutes to keep the surface hydrophilic. IDEs were rinsed with ddH_2O and ethanol and dried with a nitrogen stream.

2.6.2 OBPs immobilisation by Self-assembled monolayers

Quartz crystal microbalances:

Two protocols were used to link OBPs on both gold electrodes of QCMs by using thioctic acid as SAMs.

Protocol 1:

The QCMs were dipped in an ethanolic solution of 10 mM thioctic acid (TA) for at least 20 hours, under nitrogen flow. The gold electrodes were then rinsed with absolute ethanol to remove the unbound molecules of thioctic acid and were left to dry at air. The activation of carboxylic acid groups of the SAMs was carried out using 20 µL of a solution of ethyl(dimethylaminopropyl)carbodiimide (180 mM) and N-hydroxysuccinimide (180 mM). The reaction was left for 2 hours at room temperature. The solution was then rinsed with ddH_2O and dried at air.
The immobilisation of the proteins on the activated SAM layer was performed by pipetting 10 µL of a 1 mg mL^{-1} OBPs solution onto the gold surface of the QCMs. The protein solution was left to react for an hour before gently rinsing with ddH_2O and drying in air. This step was repeated twice.

The same process was repeated on both sides of the quartz microbalance.

Protocol 2:

SAMs of thioctic acid were prepared by a drop-casting technique (248). An ethanolic solution of 100 mM thioctic acid was drop-casted on both gold electrodes at least ten times. The surfaces were allowed to dry in air, before activating the carboxylic groups with a water mixture solution of EDC: NHS in ratio 1:2, for at least two hours.

After that, the surface of the QCMs was gently rinsed with ddH_2O before pipetting 10 µL of a 1 mg mL^{-1} OBPs solution on the electrode surface. The OBPs were incubated for an hour and then rinsed several times with ddH_2O. Freshly prepared biosensors were stored at 4°C until use.

Screen-printed electrodes and Interdigitated electrodes:

The SPEs and IDEs were dipped in an ethanolic solution of MHA at the concentration of 2 mM for at least 20 hours, under nitrogen flow. The electrodes were then rinsed with absolute ethanol to remove the unbound molecules of MHA and left to dry at air.

The carboxylic groups of the MHA were activated by using a mixture solution of EDC (100 mM) and NHS (200 mM) in phosphate 10 mM buffer pH 7. The SPEs or IDEs were dipped in the EDC/NHS solution for 3 hours, and then they were rinsed with ddH_2O and dried at air.

Proteins were immobilised on the working electrode of SPEs by pipetting about 10 µL of a 1 mg mL^{-1} OBPs solution onto the gold surface and left for an hour before gently rinsing with ddH_2O and drying in air. This step was repeated twice.

In case of IDEs, the electrodes were immersed in the protein solution and were kept at 4°C until the use. Before testing, IDEs were rinsed several times with ddH_2O and left to dry at air.

2.7 Instrumentation and Setup

2.7.1 Electrochemical surface characterisation

The electrochemical experiments were performed using a CompactStat Instrument (IVIUM Techology), interfaced with the IviumSoft software provided by the same company. The electrodes were inserted in to an interface box connected directly to the potentiostat (Figure 19).

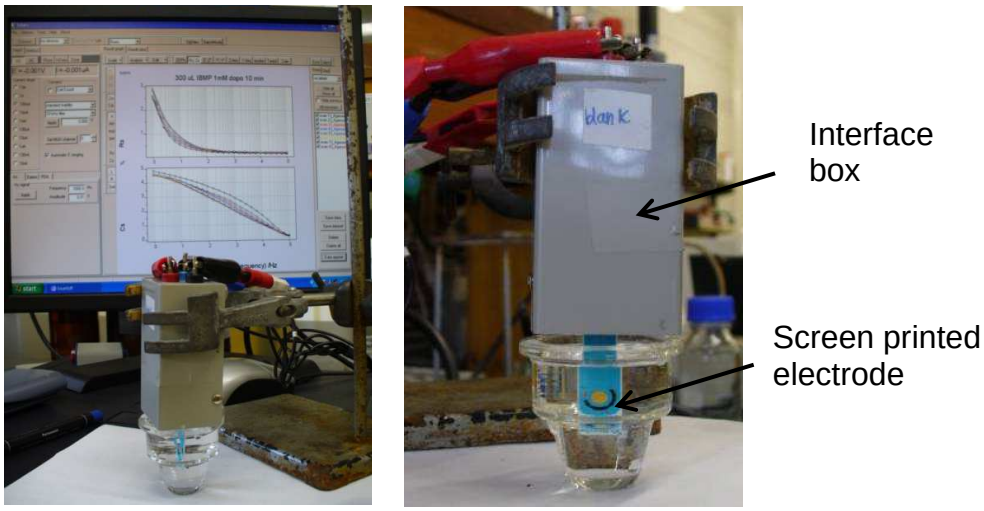

Figure 19. Electrochemical system set-up.

The electrochemical characterisation of the sensors was performed by cyclic voltammetry (CV) and electrochemical impedance spectroscopy (EIS).

CV experiments were performed in 5 mM $Fe(CN)_6^{3-}$/ $Fe(CN)_6^{4-}$ (1:1) in 0.1 M aqueous solutions of KCl with a scanning range from 0.18 V to -0.2 and then to 0.5 V at a scan rate of 0.1 V s^{-1}.

Electrochemical impedance spectroscopy was carried out using the same solution of 5 mM $Fe(CN)_6^{3-}$/$Fe(CN)_6^{4-}$ (1:1) in 0.1 M KCl over a frequency range of 0.025 Hz to 1 MHz with 10 mV amplitude. The potential was fixed at 0.18 V (249).

2.7.2 Vapour phase measurements with Quartz crystal microbalances (QCMs)

2.7.2.1 Quartz crystal microbalances

Measurements with quartz crystal microbalances were recorded using two miniaturised 4-channel frequency counters developed by JLM Innovation, interfaced by “MultiSens” Software.

In order to introduce volatile organic compounds (VOCs) to the quartz crystals, a self-designed flow-cell was attached to the frequency counter having the configuration as shown in Figure 20.

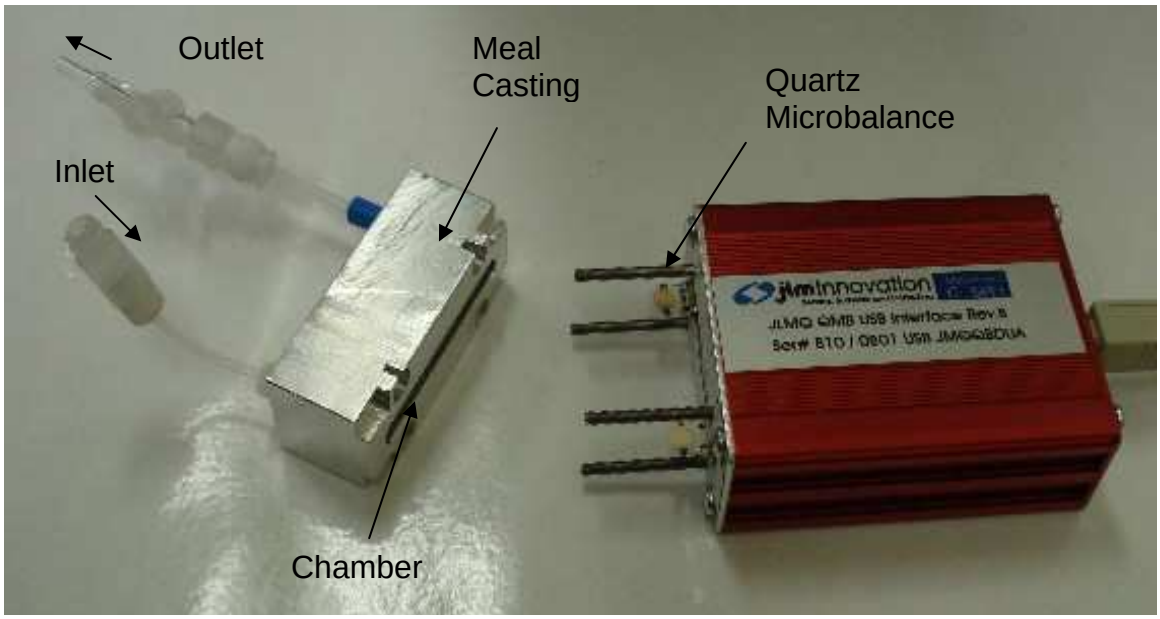

Figure 20. QCMs connected to the frequency counter.

The inlets to the flow-cell of two counters were merged together and connected to a 'flow-switch', which switched from the VOCs to air and vice versa. The whole system was set up in an incubator chamber at 30°C. Measurements were performed under a constant flow rate. The flow from the air cylinder was regulated by a flow meter at the desired rate and controlled by a 3-way valve as shown in Figure 21.

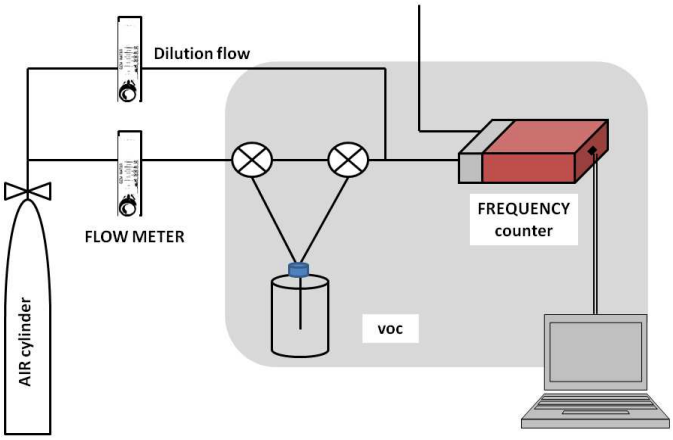

Figure 21. Schematic representation of the delivery system.

Volatile compounds tested were introduced into the sample chamber of the frequency counters. The stock for the vapour sample was prepared by pipetting a known amount of compounds into a bottle having a volume of 0.6 L and sealed. In this case, all the amounts taken for the different VOCs were above the volume that can produce saturated vapour. The sealed bottle was then transferred into the incubator at 30°C.

In order to test the biosensor with different concentrations of the analyte, the VOC flow channel was increased from 10% to 100% of the initial saturated concentration by mixing with a separate flow of air, maintaining by the way the same total flow rate. Upon achieving a stable baseline signal, under a constant flow of air, the analyte was introduced in the counter chamber for a time of about 10 minutes followed by a regeneration step of 20 minutes with cleaned air.

2.7.2.2 Interdigitated electrodes

Capacitive/Impedimetric measurements were performed using a CompactStat Instrument (IVIUM Techology), interfaced with the IviumSoft software provided by the same company. The IDEs were connected to the potentiostat through a ZIF connector. The IDEs were placed inside a self-designed cell (Figure 22).

The inlet of the flow-cell was connected to a three-way valve, which switched from the VOCs to the air and vice versa. Measurements were performed under a constant flow rate. The flow from the air cylinder was regulated by a flow meter at the desired rate and controlled by a 3-way valve.

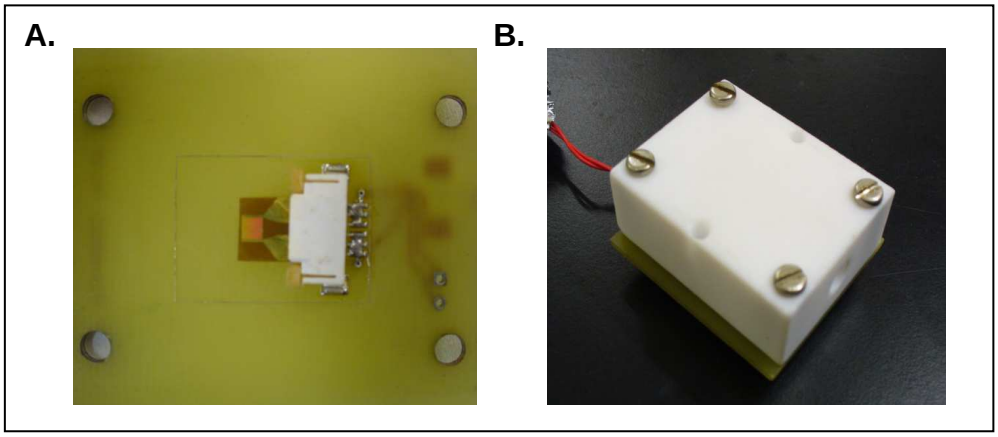

Figure 22. (A) Interdigitated electrode located inside a zif connector. (B) Interdigitated electrode incubation chamber

The capacitance measurements were recorded at the frequency of 100 Hz. A potential of 1 volt was applied with an amplitude of 20 mV. The delivery system used was the same described for the quartz crystal microbalances measurements (see section 2.7.2.1). The total flow rate used was 180 ml min^{-1} with a relative humidity of about 25%. The biosensor was stabilised for about an hour before starting the measurements under a constant flow of humid air. The analyte was introduced in the flow cell for about 10 minutes followed by a cleaning step of 10 minutes.

2.7.3 Capacitive measurements in liquid phase

Capacitive measurements were performed using a CompactStat Instrument (IVIUM Techology), interfaced with the IviumSoft software provided by the same company. The electrode was located inside a self- designed flow cell, shown in Figure 23. The system was connected to a peristaltic pump, which was set at constant flow rate of 0.5 ml min^{-1}.

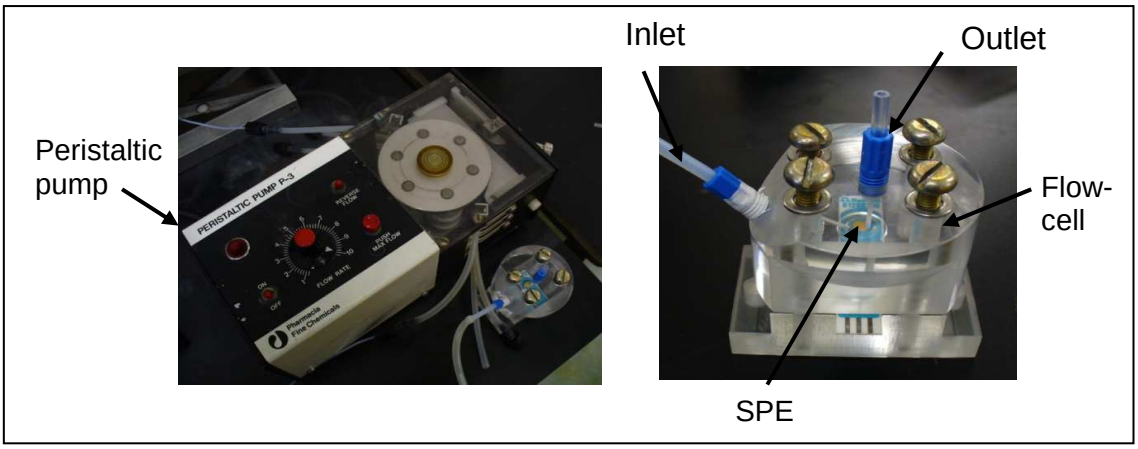

Figure 23. Flow-cell system used for capacitive measurements in liquid phase

The capacitance was recorded at the frequency of 96 Hz. A potential of 0.1 volt was applied with amplitude of 20 mV. Measurements were performed under constant flow of 10 mM phosphate buffer at pH 7. The analyte was introduced in the flow cell at different concentrations (0.05; 0.1; 0.5; 2.5 and 5 µM) for a time of 15 minutes followed by a cleaning step of 20 minutes. The biosensor was stabilised under constant flow of buffer for at least 50 minutes before starting the measurement.

2.8 Gas Chromatography- Mass spectrometry analysis

A Gas Chromatograph–Mass spectrometer (GC-MS) (Varian Saturn 2200) equipped with a DB-Wax column (0.25 mm i.d. 60 m, Agilent Scientific) was used to estimate the relative volatility of the bombykol and bombykal. The injector and ion source of the GC-MS were maintained at 230°C, and the ionization voltage was 70 eV. Helium (1.0 ml min^{-1}) was used as the carrier gas. The column oven temperature was held at 120°C for the first 2 minutes, increased at 12°C min^{-1} to 180°C, and then at 5°C min^{-1} to 240°C (250). The gas injections were performed by using a CombiPAL Autosampler. The vials containing the ethanolic solutions of bombykol and bombykal were incubated at 145°C for an hour before injecting in the gas chromatographer. The syringe was heated at the temperature of 150°C.

Pure bombykol and bombykal were purchased from Pherobank (The Netherlands).

2.9 Fluorescence microscopy

Green fluorescent proteins (GFPs) grafted on gold surfaces were imaged on an upright microscope (Olympus BH2-RFL) using an AM7023 Dino-Eye camera (Dino-Lite)) with the Image Acquisition and Analysis software (DinoCapture 2.0). The sample was illuminated from the epifluorescence port with a Xenon lamp and the excitation and emission light was filtered by a fluorescent filter set (Olympus, excitation BP490 nm; dichroic 500 nm; emission 515 nm).

3 RESULTS

The aim of our research was to investigate the possibility of using OBPs as bio-recognition elements of biosensors, for the detection of organic compounds in both vapour and liquid phases. OBPs were identified as suitable candidate for the development of the FlexSMELL smart tag due to their unique biochemical properties. OBPs are able to bind in a reversible way a wide range of chemical compounds (176); they are resistant to high temperatures and proteolytic attacks (251) and they can be synthesised in large amounts on a laboratory scale. These features made of the OBPs a promising tool for realising biosensors to be used in field.

In order to have a quantity of OBPs for carrying out our research, OBPs belonging to different species of vertebrates and invertebrates were heterologously expressed and purified in our laboratory.

3.1 Protein expression and characterisation

Six different OBPs were synthesised in large quantity during the project. These included two mutant forms of the porcine OBP1, *Apis mellifera* OBP14, OBP1 from *Polistes dominula*, GOBP2 and PBP1 of *Bombyx mori*. In addition, the gene coding for the Green fluorescence protein of *Aequorea Victoria* was expressed for studying the reliability of the protein immobilisation method.

Porcine OBPs were selected for their ability to bind different classes of chemical compounds, most of them related to foodstuff, such as pyrazine derivatives, carvone, menthol, dihydromyrcenol, etc (147;154;252;253). The mutated porcine OBP F88W and W16F-F88W were preferred to the wild type form of the porcine OBP1, for their higher affinity against the fluorescence probe 1-AMA (254), suggesting a better binding performance.

Insect OBPs were also used in our research. Amongst the wide range of insect's OBPs, *Polistes dominula* OBP1 was selected for its good affinity against the ligand dodecanol (255). This alcohol can be used as markers of food borne pathogens since it is released by several gram-negative bacteria as *Escherichia coli, Citrobacter freundii, Klebsiella pneumoniae*, *Salmonella typhimurium*, etc (256). *Apis mellifera* OBP14 was picked for its atypical structure. OBP14 belongs to the C-minus class of OBPs, bearing only five cysteine residues (257). Moreover, this OBPs displays a binding affinity in the micromolar range for compounds released by food as 2-heptanone, which is related to the gorgonzola smell. (258).

General Odorant Binding Protein 2 (GOBP2) and Pheromone Binding Protein 1 (PBP1) of *Bombyx mori* were instead synthesised with the purpose to develop biosensors for agriculture applications. Useful insects and pests can be monitored and controlled by using pheromones. Pheromones are substances secreted by an individual and detected by others of the same species, which can produce changes in sexual or social behaviour (259). We used these two proteins as model for developing an analytical sensor for detecting the two main components of the pheromone blend of the silk moth *Bombyx mori*, bombykol and bombykal.

3.1.1 Protein expression

Odorant Binding Proteins were expressed in a bacterial system, using the protocol described in Materials and Methods section. The proteins were expressed in good yields (around 15 mg of OBPs per litre of bacterial culture) and in soluble form in case of mammalian OBPs (porcine) while the OBPs of insects (Polistes, Apis and Bombyx) were contained in insoluble inclusion bodies. In order to make them soluble, the proteins were denatured and renatured with urea and DTT. This process were previously reported to yield the OBPs in their native folding configuration with the six cysteines correctly paired (260;261).

Figure 24 shows the electrophoretic analysis under denaturing conditions (14% SDS-PAGE) of crude bacterial cultures expressing OBPs, sampled before (–) and after (+) induction with isopropyl-beta-D-thiogalactopyranoside (IPTG). The expressed protein showed a molecular weight of about 15 kDa in the case of insect OBPs and 18 kDa for mammalian OBPs, in according with the literature (254;255;257;262;263).

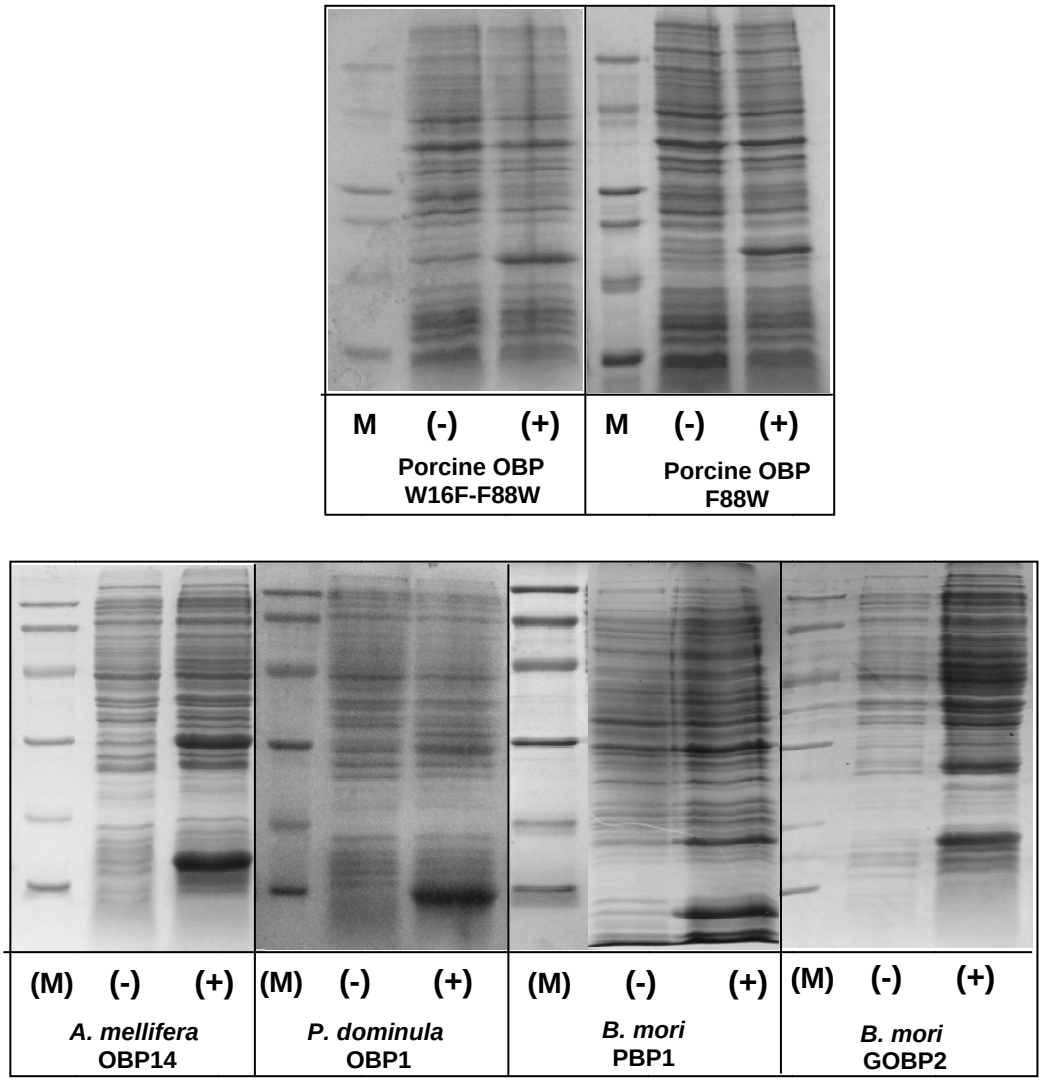

Figure 24. SDS-PAGE at 14 % of acrylamide. (-) Cellular pellet before induction; (+) cellular pellet after induction. Molecular weights of markers (M) were from the top: 97.4, 66.2, 45, 31, 21.5 and 14.4 kDa

The green fluorescent protein from the jellyfish *Aequorea Victoria was* expressed following the same protocol used for the OBPs. The protein was expressed with very good yield (about 25 mg of protein for litre of bacteria culture) and in a soluble form.

Figure 25 shows the electrophoretic analysis in denaturing conditions (14% SDS-PAGE) of crude bacterial cultures expressing GFPs, before (–) and after (+) induction with IPTG.

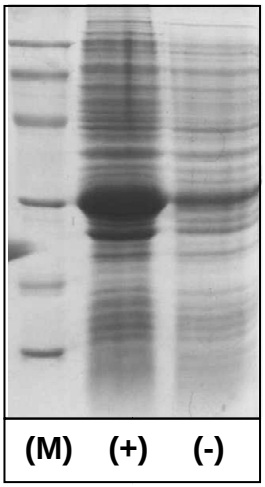

Figure 25. SDS-PAGE at 14 % of acrylamide. (-) Cellular pellet before induction; (+) cellular pellet after induction. Molecular weights of markers (M) were from the top: 97.4, 66.2, 45, 31, 21.5 and 14.4 kDa.

3.1.2 Purification of recombinant OBPs by chromatography

The proteins were purified, using a combination of anion-exchange chromatography and gel filtration. Fractions obtained after each chromatographic steps were analysed by electrophoresis in denaturing conditions (Figure 26).

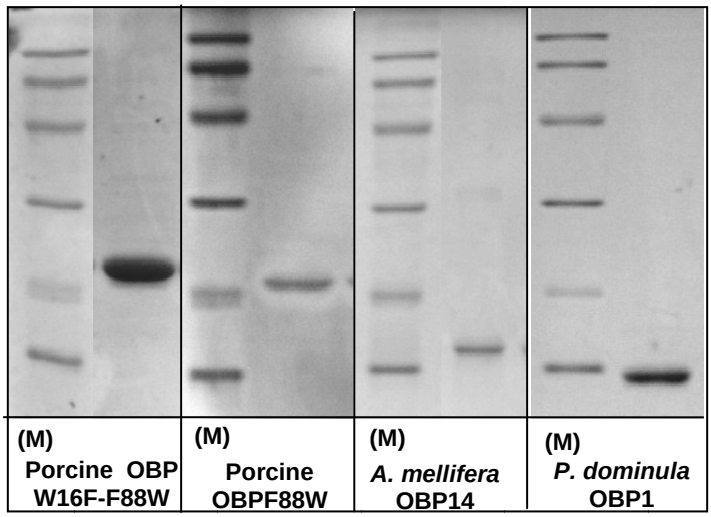

Figure 26. SDS-PAGE (13%) of the fractions of recombinant OBPs purified by DE-52 anionic exchange chromatography and subsequently gel filtration. Molecular weights of markers (M) were from the top: 97.4, 66.2, 45, 31, 21.5 and 14.4 kDa

GFPs of *A.victoria*, PBP1 and GOBP2 of *B.mori* were purified using a Nickel affinity chromatography (Figure 27). These proteins bore a tag of six histidines at the amine-terminal end, which interacted with the Nickel ions immobilized on the stationary phase of the chromatography resin.

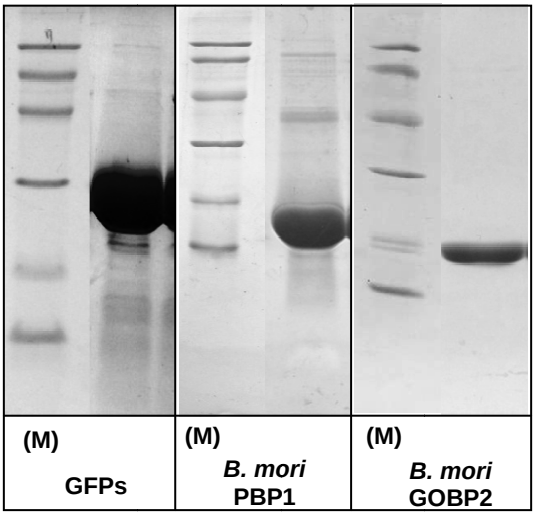

Figure 27 . SDS-PAGE (13%) of the fractions of recombinant OBPs purified by Nickel affinity chromatography. Molecular weights of markers (M) were from the top: 97.4, 66.2, 45, 31, 21.5 and 14.4 kDa.

The use of affinity chromatography increased the yields of the purified OBPs. The concentrations of the proteins that resulted were more than twice when compared with fractions purified using anion- exchange and gel filtration chromatography.

The amino acid sequences of the expressed Odorant Binding Protein are displayed in Figure 28. The conserved cysteine residues, which represent the characteristic fingerprint of the OBPs, are highlighted. Generally, two residues of cysteine are present in the vertebrate OBPs, as shown in Figure 28 B, while in the insect there are usually six (Figure 28 A). These cysteines are interlinked by disulfide bridges, which give to the proteins high stability. The OBP14 of *Apis mellifera* is an exception, since it bore only five cysteines. This protein belongs to the class of OBPs named “C-minus” (257;264) with only two disulfide bridges. The C-minus class OBPs are more abundant in the ancient insects such as

Drosophilidae, Bombyx and Apis lineages (169) and they might be ancestral proteins from which the classic OBPs were evolved.

A.

```
B.moriPBP1       MGSSHHHHHHSSGLVPRGSHMSQEVMKNLSLNFGKALDECKKEMTLTDAINEDFYNFWKE 60
B.moriGOBP2      MFSFLILVFVAS--VADSVIGTAEVMSHVTAHFGKTLEECREESGLSVDILDEFKHFWSD 58
P.domOBP1        ------------------MDSDIAVKKYLHAVPEPVLAKCLKESGLEADK----DKLLSD 38
A.melOBP14       ----------------------MTIEELKTRLHTEQSVCKTETGIDQQK---ANDVIEG 34
                                       . . :          *  *  :         .. .

B.moriPBP1       GYEIKNRETGCAIMCLSTKLNMLDPEGNLHHGNAMEFAKKHGADETMAQQLIDIVHGCEK 120
B.moriGOBP2      DFDVVHRELGCAIICMSNKFSLMDDDVRMHHVNMDEYIKGFPNGQVLAEKMVKLIHNCEK 118
P.domOBP1        ESTVDQGKFSCLIACTLKDNGALVN-GELKYDVLSELLSKLLTN-KEDKLQERLEKACIP 96
A.melOBP14       NIDVEDKKVQY-CECILKNFNILDKNNVFKPQGIKAVMELLIDE----NSVKQLVSDCS- 88
                    : . :      *  .. . :     ::        .         :    :   *

B.moriPBP1       STPANDDKCIWTLGVATCFKAEIHKLNWAPSMDVAVGEILAEV- 163
B.moriGOBP2      QFDTETDDCTRVVKVAACFKKDSRKEGIAP--EVAMIEAVIEKY 160
P.domOBP1        EGANAKNDCEYIGKIMQCKLSKAKEMGL---------------- 124
A.melOBP14       -TISEENPHLKASKLVQCVSKYKTMKSVDFL------------- 118
                       :       :  *         .
                  .     . .     :      :  .:
```

B.

```
pOBPwt             EEPQPEQDPFELSGKWITSYIGSSDLEKIGENAPFQVFMRSIEFDDKESKVYLNFFSKE 59
pOBPF88W           MQEPQPEQDPFELSGKWITSYIGSSDLEKIGENAPFQVFMRSIEFDDKESKVYLNFFSKE 60
pOBPW16F-F88W      QRASPEQDPFELSGKFITSYIGSSDLEKIGENAPFQVFMRSIEFDDKESKVYLNFFSKE 60
                   :...**********:****************************************

pOBPwt             NGICEEFSLIGTKQEGNTYDVNYAGNNKFVVSYASETALIISNINVDEEGDKTIMTGLLG 119
pOBPF88W           NGICEEFSLIGTKQEGNTYDVNYAGNNKWVVSYASETALIISNINVDEEGDKTIMTGLLG 120
pOBPW16F-F88W      NGICEEFSLIGTKQEGNTYDANYAGNNKWVASYASETALIISNINVDEEGDKTIMTGLLG 120
                   ******************.*******:*.****************************

pOBPwt             KGTDIEDQDLEKFKEVTRENGIPEENIVNIIERDDCPA- 157
pOBPF88W           KGTDIEDQDLEKFKEVTRENGIPEENIVNIIERDDCPAK 159
pOBPW16F-F88W      KGTDIEDQDLEKFKEVTRENGIPEENIVNIIERDDCPAK 159
                   ************************************
```

Figure 28. Alignment of Odorant Binding Protein sequences performed by ClustalW2 software (http://www.ebi.ac.uk/Tools/msa/clustalw2/). The cysteines were highlighted in yellow.

The porcine OBPs expressed were two mutated forms of the wild type OBP1. Figure 28 B shows the alignment of the mutants against the wild type form. The porcine OBP F88W bore a mutation in position 88, where a phenylalanine (F) was replaced by a tryptophan (W). The replacement of an aromatic amino acid with another aromatic residue (tryptophan) did not affect the protein folding. X-ray structure of porcine OBP-ligand complexes showed that phenylalanine 88 is located rather close to ligands but seems not to be involved in the uptake and

release of ligands. The porcine OBP W16F-F88W bore a second mutation in position 16, in this case a tryptophan (W) was substituted by a phenylalanine (F). Both mutations were localised in the binding pocket of the protein. However, these mutated OBPs showed an higher affinity of binding than the wild type toward the probe 1-AMA and in particular against compounds with aromatic structures (254).

3.1.3 Fluorescent binding assay

The OBPs expressed in our laboratory were tested using fluorescence-binding assays as described in the Materials and Methods section 2.2.1

Fluorescence binding assays were employed to study two important parameters:

- the dissociation constant (K_D) between the protein and the probe
- the affinity of binding of target ligands

The dissociation constant, besides giving information about the affinity between the protein and the probe, can be also used to evaluate the correct expression and activity of the proteins. Since the OBPs employed in this research are all known, it was possible to compare the values of the calculated K_D with the values reported in literature. In this way, the correct expression of the recombinant protein was proved and the activity of the OBPs in different media can be studied.

In addition, fluorescence analyses can be used to estimate the affinity of binding of selected ligands through competitive binding assays. In competitive binding, the K_D is calculated as reduction of the fluorescence intensity emits from the probe. A fixed concentration of fluorescent probe is used, while the concentration of the test ligand is increased gradually. If the affinity of the ligand for the protein is higher than the probe, a reduction in the emitted fluorescence is observed. Such reduction is caused by the displacement of the probe from

the binding site. The dissociation constant for the target ligand can then calculated using the following formula K_D=[IC50]/1+[Probe]/K_{Probe}, where [Probe] is the free concentration of the fluorescence probe and K_{Probe} is the dissociation constant of the complex Protein/Probe (244). The K_D value is important parameter for evaluating the affinity of binding of OBPs toward target ligands in order to select the best proteins for the purposed application.

3.1.3.1 Calculation of the dissociation constant (K_D)

3.1.3.1.1 Porcine OBPs

Porcine OBPs, OBP F88W (pOBPF88W) and OBP W16F-F88W (pOBPW16F-F88W) were tested against the fluorescent probe 1-aminoanthracene (1-AMA) (254). Figure 29 and Figure 30 show the binding curve obtained by plotting the concentration of 1-AMA bound to the protein over its total concentration. Assuming that in saturating conditions, the concentration of bound 1-AMA is equal to the concentration of the protein, we can use the fluorescence intensities around 480 nm to calculate the concentration of bound 1-AMA. The dissociation constant (K_D) of both proteins was estimated by using the formula described in the section 2.2.1.The calculated values corresponded to 2.25 µM ± 0.91 for pOBPW16F-F88W and 0.045 ± 0.037 µM for pOBPF88W. The pOBPF88W underwent a delipidation treatment, before the binding assay, that considerably improved its binding activity.

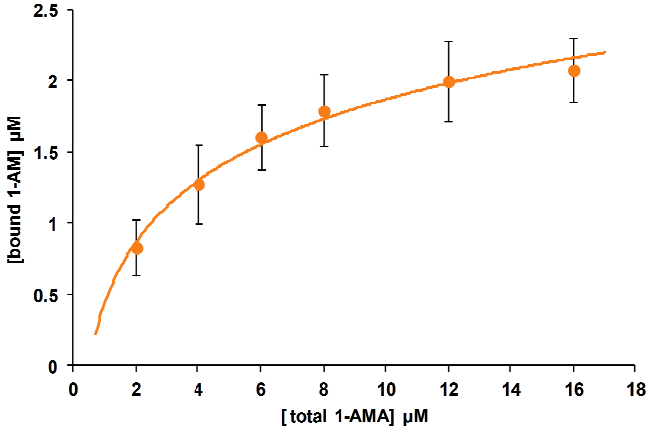

Figure 29. Binding curve of porcine OBP W16F-F88W with the fluorescent probe 1-AMA. The OBP was solubilised in Tris-Cl buffer at pH 7.4 with a final concentration of 2 µM. n=3.

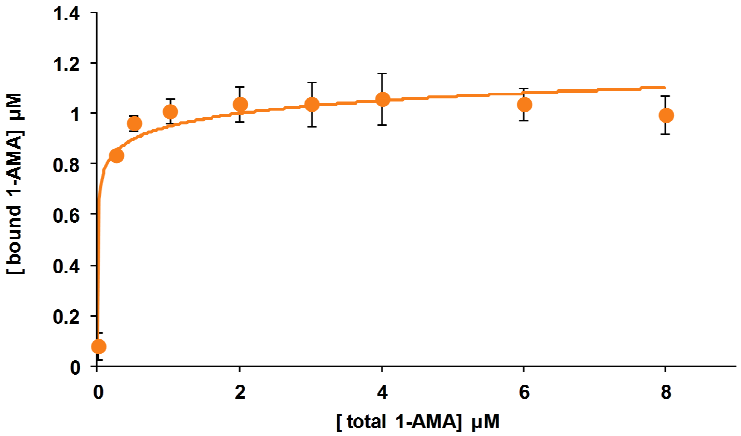

Figure 30. Binding curve of porcine OBP F88W with the fluorescent probe 1-AMA. The OBP was solubilised in Tris-Cl buffer at pH 7.4 with a final concentration of 1 µM. n=3.

An interesting property of the OBPs is their exceptional stability to high temperatures. OBPs can withstand temperatures up to 80 °C, and even 100 °C, for several minutes without suffering irreversible denaturation and recover their binding activity when returned to room temperature (147;251). This feature is important for the realisation of biosensors that can be used at room temperature, without altering the performance of the bio-recognition element.

Porcine OBP F88W solutions were kept at 95°C for 5 minutes in order to test their stability near the boiling point. After cooling down to room temperature, the affinity of binding of the OBPs toward the fluorescence probe 1-AMA was tested (Figure 31).

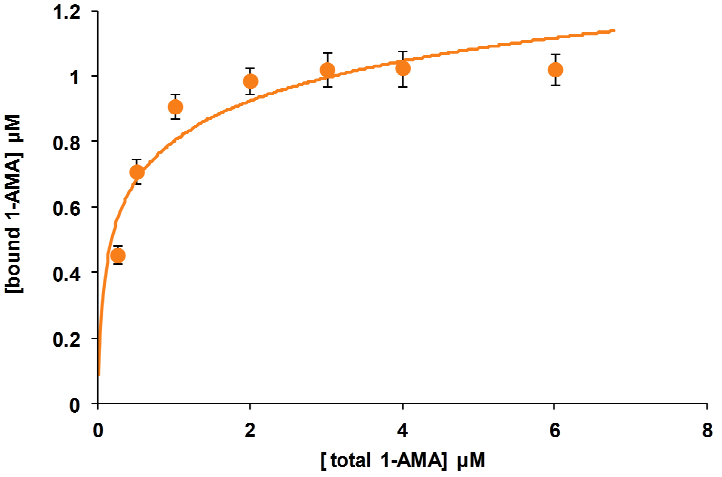

Figure 31. Binding curve of porcine OBP W16F-F88W, after boiling, with the fluorescent probe 1-AMA. The OBP was solubilised in Tris-Cl buffer at pH 7.4 with a final concentration of 1 µM. n=3.

The estimated dissociation constant of the pOBPF88W after treating at 95°C was 0.721 µM ± 0.049. The high temperature reduced the activity of the OBP; however, the calculated dissociation was still below 1 µM, demonstrating an extremely good binding affinity.

3.1.3.1.2 Polistes dominula OBP1

The binding activity of the recombinant OBP1 of the paper wasp *Polistes dominula* (PdomOBP1) *was* also tested with fluorescence binding assays by using the probe N-phenyl-1-naphthylamine (1-NPN). The emission spectrum of 1-NPN in aqueous medium show a maximum around 480 nm, while in presence of a binding protein the maximum is shifted at 405-410 nm, when excited at 337nm (255;265). The activity of PdomOBP1 was tested in 50mM Tris-Cl buffer pH 7.4 using 1-NPN at the concentration of 1 mM (Figure 32). The dissociation constant was calculated as previously described and the estimated value was 1.150 µM ± 0.888.

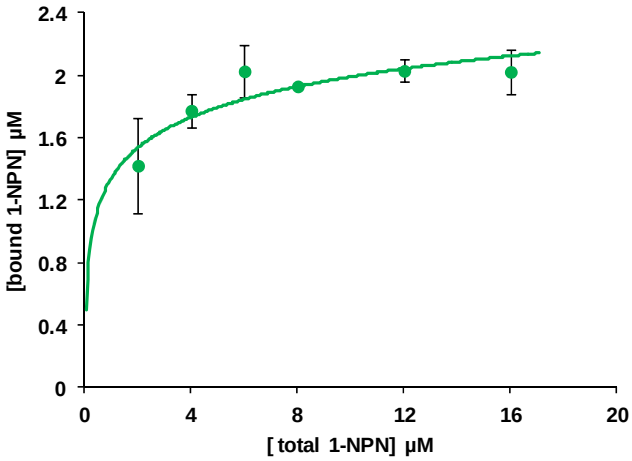

Figure 32. Binding curve of *Polistes dominula* OBP1 with the fluorescent probe 1-NPN. The OBP was solubilised in Tris-Cl buffer at pH 7.4 with a final concentration of 2 µM. n=3.

The activity of PdomOBP1 toward 1-NPN was also investigated in the medium tetramethyl orthosilicate (TMOS) (Figure 33). TMOS sol-gel can be used to entrap proteins onto the surface of transducers for sensing applications. The affinity of binding of the PdomOBP1 dissolved in TMOS liquid sol-gel was

tested. The value of K_D was 3.357 µM ± 1.755, higher than the value calculated in Tris-Cl buffer at pH 7.4. Such a decrease in the activity could be attributed to the low pH of the TMOS solution (pH around 4). In fact, it was observed that the activity of binding of some OBPs decreases in acidic environment. For the PBP of *B.mori* it was indeed demonstrated that the C-terminus folds into an α-helical domain and enters in the binding site at pH of 4.5 (266), blocking the entrance to ligands.

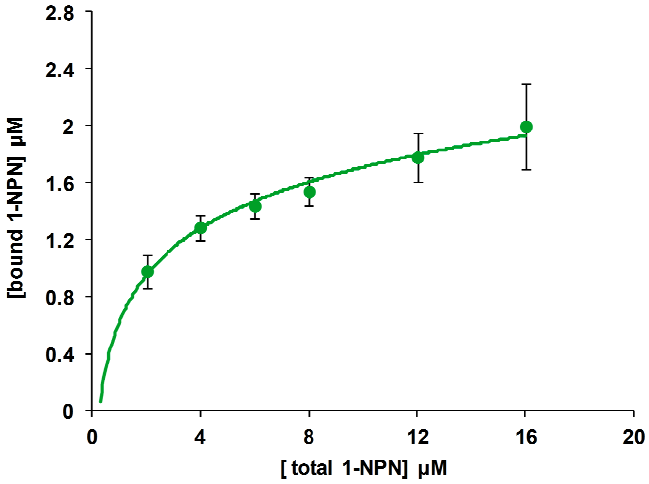

Figure 33. Binding curve of *Polistes dominula* OBP1 with the fluorescent probe 1-NPN. The OBP was dissolved in TMOS Sol-gel pH 4 at the concentration 2 µM. n=3.

The same fluorescent experiment was repeated dissolving the protein in 50mM acetate buffer, pH 4.5 (Figure 34). In this case, the dissociation constant of the PdomOBP1 was of 6.340 µM ± 5.557, higher than in TMOS solution. The activity of the OBPs was found to be better in the sol-gel compared to the acetate buffer, maybe due to the medium composition.

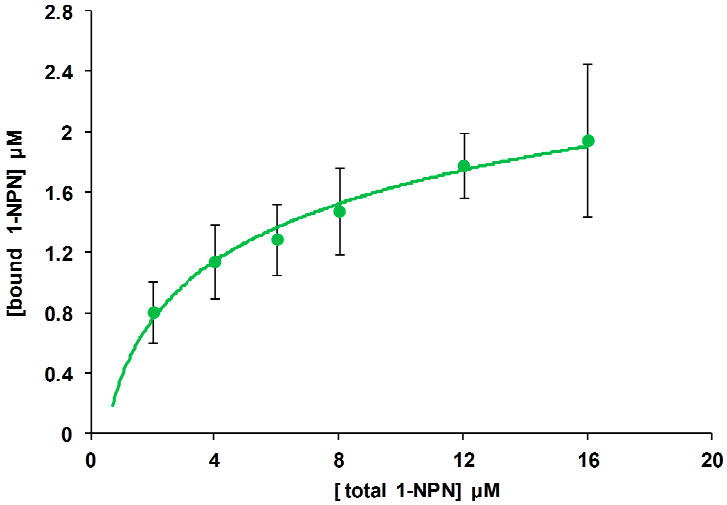

Figure 34. Binding curve of *Polistes dominula* OBP1 with the fluorescent probe 1-NPN. The OBP was solubilised in acetate buffer pH 4.5 at the final concentration of 2 µM. n=3.

TMOS sol-gel was studied during the project for immobilising OBPs, since it maintained an acceptable protein activity. Nevertheless, problems related to the polymerisation of the gel and to the appearance of cracks on the surface addressed us to seek alternative methods.

3.1.3.1.3 Bombyx mori Pheromone Binding Proteins (PBP1) and General Odorant Binding Proteins 2 (GOBP2)

The affinity of binding of the recombinant PBP1 and GOBP2 of *Bombyx mori* was investigated in fluorescent assays against the probe 1-NPN (Figure 35). The proteins at the final concentration 0.5 µM were dissolved in 50mM phosphate buffer, pH 7.4. The K_D calculated were 0.336 µM ± 0.032 for PBP1 and 0.147 µM ± 0.023 for the GOBP2.

Both proteins were delipidated before the binding experiments, as described in the Materials and Methods section. The delipidation step improved the affinity of binding of the PBP1 against the probe 1-NPN by about six times (from 1.9 µM before delipidation to 0.3 µM after delipidation).

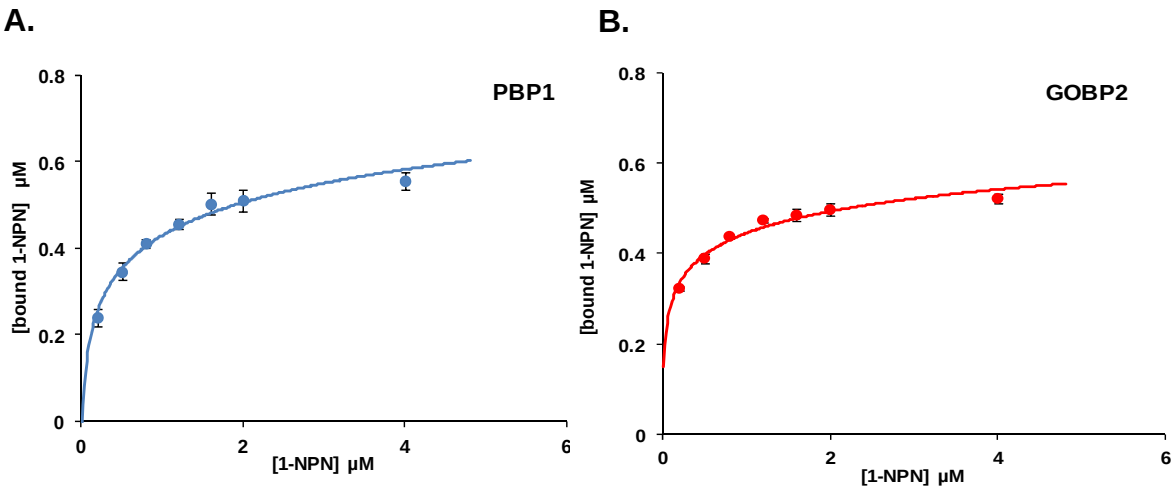

Figure 35. Binding curve of *B.mori* PBP1 (A) and GOBP2 (B) with the fluorescent probe 1-NPN. The OBP was solubilised in phosphate buffer at pH 7.4 with a final concentration of 0.5 µM. n=3.

3.1.3.1.4 Apis mellifera OBP14

It was not possible to calculate the dissociation constant for the OBP14 of *Apis mellifera*. The OBP14 did not show any signs of binding activity to the probe in the fluorescence assay. Such results could be attributed to an incorrect refolding of the protein during the solubilisation process, given that the OBP14 was expressed as inclusion bodies. Furthermore, OBP14 bears only five cysteine residues and that may affect the correct formation of disulfide bridges and consequently the tertiary structure.

3.1.3.2 Competitive binding assays against target ligands

Fluorescence binding experiments were also used to evaluate the affinity of several OBPs against target ligands by means of competitive binding assays. After determining the dissociation constant as previously described, the proteins were tested against different ligands by using a fluorescence probe as reporter. The displacement of the fluorescent probe from its complex with the protein, in presence of increased concentrations of the ligand, leads to a reduction of the fluorescence intensity emitted by the probe. These variations can be graphically displayed as percent reduction of the initial fluorescence intensity emitted by the probe versus the ligand concentration. The dissociation constant for each

compound was then calculated from the concentration value that halved the initial 1-NPN fluorescence signal, [IC50] (see section 2.2.1).

The results of the competitive binding assays performed using recombinant porcine OBP F88W, GOBP2 and PBP1 of *B.mori* are displayed in the next sections.

3.1.3.2.1 Porcine OBP F88W (pOBPF88W)

Using 1-AMA as the fluorescent reporter, the affinity of pOBPF88W toward five chemical compounds was measured. The ligands were selected on the base of their chemical features. Two enantiomeric forms of the carvone were chosen, in order to test the ability of OBPs to discriminate between enantiomers. 2-phenylethanol was selected as a control as a putative weak ligand for the porcine OBPs. Geosmin was tested since it is a marker of food quality and 2-isobutyl 3-methoxypyrazine (IBMP) was instead assayed because considered one of the best ligand for porcine OBPs (2).

Figure 36 reports the displacement of 1-AMA from the complex with pOBPF88W by those compounds. The dissociation constants (K_D) were calculated for each compound from the concentration value that halved the initial 1-AMA fluorescence intensity ([IC50]). The data of the estimated K_D are reported in Table 7.

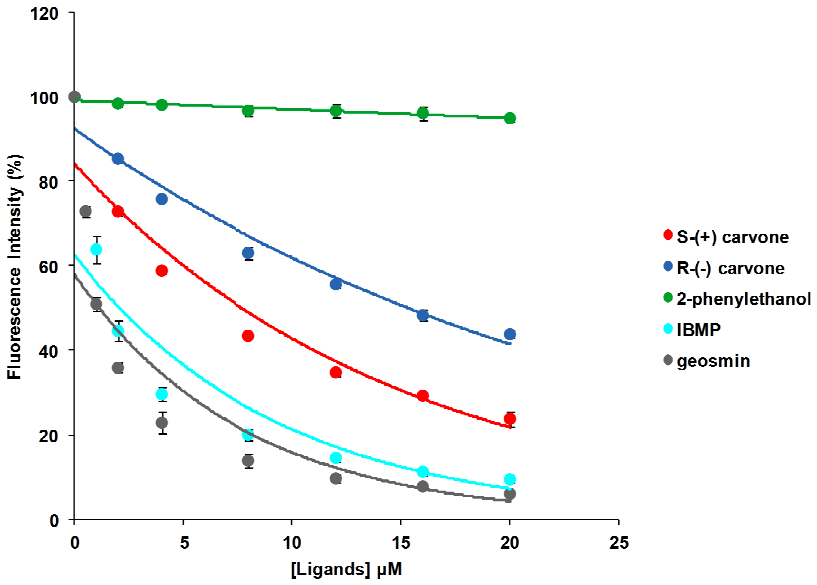

Figure 36. Competitive binding of selected ligands to pOBPF88W. A mixture of the protein and 1-AMA in phosphate buffer, both at the concentration of 1 µM, was titrated with 1 mM solutions of each competing ligand to final concentrations of 2–20 µM. The fluorescence intensity at 480 nm was reported as percent value of the initial signal, recorded in absence of competing ligand. When increasing concentrations of ligand were added to the mixture, the fluorescence probe was displaced from the OBP, leading to a reduction of its fluorescence intensity. n=3.

Ligand	K_D(µM)
2-phenylethanol	>> 28 µM (N.A.)
R-(-) carvone	1.219 µM ± 0.055
S-(+) carvone	0.500 µM ± 0.009
IBMP	0.141 µM ± 0.006
Geosmin	0.097 µM ± 0.007

Table 7. Dissociation constants (K_D) of the complex recombinant pOBPF88W with the different ligands tested.

The competitive binding assays showed a good affinity of the pOBPF88W toward geosmin, IBMP and both the isomeric forms of the carvone. A slight preference for the S-(+) form was observed compared with the R-(-) carvone. 2-phenylethanol was confirmed to be a weak ligand for the porcine OBP. The exact K_D value for 2-phenylethanol was not possible to be determined, due to the low response. It is important to note that, the solutions of 2-phenylethanol,

S-(+) and R-(-)carvone were prepared in 1mM phosphate buffer, instead that the traditional methanol. The use of the buffer was driven by the fact that we wanted to keep same conditions in both fluorescence and electrochemical measurements, avoiding possible interfere in the detection of the electric signal. These organic compounds, however, show a poor solubility in water and/or buffer solutions. Ultraviolet (UV) spectrophotometry was used to estimate the solubility of S-(+) and R-(-) carvone in aqueous solution as described by Smyrl and LeMaguer (267). The saturated solution of S-(+) and R-(-) carvone achieved a final concentration of 16 mM and 16.6 mM, respectively at room temperature. The solubility of 2- phenylethanol in water was previously reported to be about 200 mM at the temperature of 19°C (268).

3.1.3.2.2 Pheromone Binding Protein 1 (PBP1) and General Odorant Binding Proteins 2 (GOBP2) of Bombyx mori

Bombykol and bombykal are the two main components of the pheromone blend of the silk moth *Bombyx mori*. The affinity of binding of the PBP1 and the GOBP2 against these two compounds was tested in competitive binding assays by using the fluorescence probe 1-NPN. PBP1 and GOBP2 were tested at 0.5 µM concentration in 1:1 ratio with the probe. Table 8 reports the values of the dissociation constants for both proteins against the pheromones bombykol and bombykal. The K_D were estimated using the equation K_D= [IC50]/1+[1-NPN]/$K_{1\text{-}NPN}$, previously described.

	Bombykol (K_D)	**Bombykal (K_D)**
PBP1	0.053 µM ± 0.015	0.053 µM ± 0.020
GOBP2	0.056 µM ± 0.009	0.034 µM ± 0.009

Table 8. Dissociation constant (K_D) calculated in competitive binding assays of PBP1 and e GOBP2 against the pheromones bombykol and bombykal

The K_D of bombykol and bombykal are graphically displayed in Figure 37.

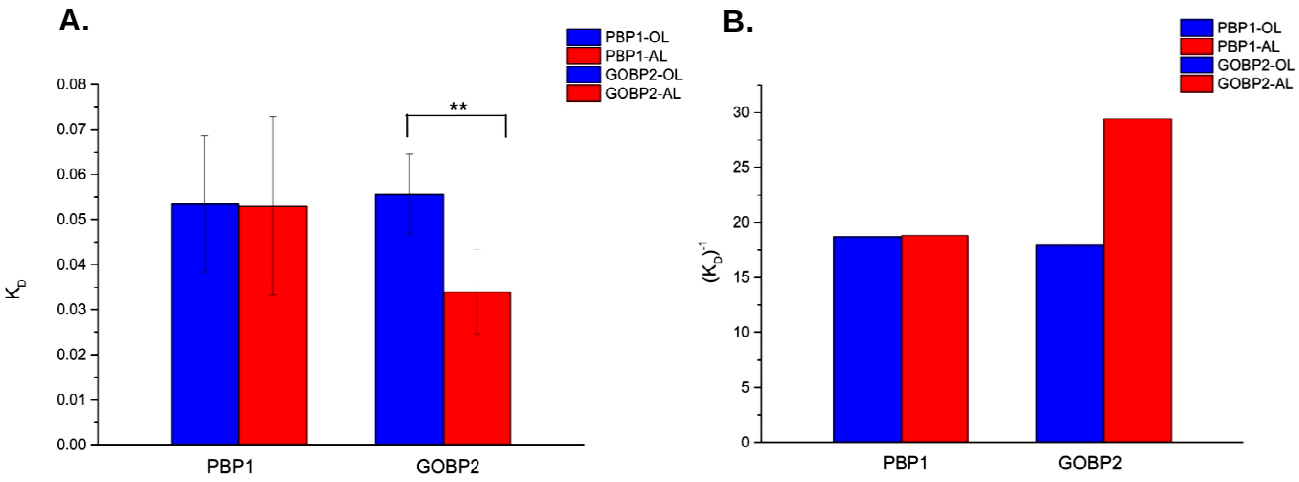

Figure 37. (A) Dissociation constants, K_D. (B) Affinity constants $(K_D)^{-1}$ of PBP1 and GOBP2 toward bombykol and bombykal. Each column is the average of three replicates and the bar denotes the standard error. n=3.

Analysing the binding data, a difference in the response of the two proteins was observed. Both proteins showed a high affinity of binding toward both pheromones. PBP1 bound bombykol and bombykal with the same intensity, without significant difference, as estimated with paired sample t-test with $p< 0.05$. However, GOBP2 showed a significant difference in the binding between bombykol and bombykal ($p<0.05$; paired sample t-test). GOBP2 bound bombykal two times better than bombykol. GOBPs may be able to discriminate between the two compounds.

Table 9 summarises all the recombinant OBPs expressed and the values of dissociation constants calculate against the fluorescent probes and ligands.

OBPs	Expression	K_D (Probe)	K_D (Ligands)
Porcine OBP F88W	X	0.045 µM ± 0.037 0.721 µM ± 0.049 (after boiling)	R-(-) carvone 1.219 µM ± 0.055
			S-(+) carvone 0.500 µM ± 0.009
			2-phenylethanol >> 28 µM
			geosmin 0.097 µM ± 0.007
			IBMP 0.141 µM ± 0.006
Porcine OBP W16F-F88W	X	2.250 µM ± 0.910	N.A.
Apis mellifera OBP14	X	N.A.	N.A.
Polistes dominula OBP1	X	1.150 µM ± 0.888 µM (pH 7.4)	N.A.
		3.357 µM ± 1.755 (in TMOS)	
		6.340 µM ± 5.557 (pH4.5)	
Bombyx mori PBP1	X	0.336 µM ± 0.032	bombykol 0.053 µM ± 0.015
			bombykal 0.053 µM ± 0.020
Bombyx mori GOBP2	X	0.147 µM ± 0.023	bombykol 0.056 µM ± 0.009
			bombykal 0.034µM ± 0.009
Green fluorescent proteins	X	N.A.	N.A.

Table 9. Summary of the OBPs expressed and tested using fluorescence-binding assays.

3.2 Development of OBP-biosensors

After the synthesis of OBPs in large quantities, the next step of our research was to develop an immobilisation method suitable for different types of transducer without affecting the binding activity of the OBPs. In the next sections, the different method studies for grafting OBPs are described. The activity of OBPs was evaluated by performing preliminary measurements in vapour or liquid phase by using QCMs, SPEs and IDEs.

3.3 Protein immobilisation method

Enzyme immobilisation is a key factor for developing efficient biosensors with appropriate performances such as good stability, high sensitivity and a good reproducibility (94). The choice of a proper immobilisation method is depended to the nature of the bio-molecules, the configuration of the transducer and the detection method used for recording the signal. The immobilisation does not have to affect the structure and the biological activity of the biomolecules. Further, the bioreceptors have to be tightly bound to the surface of the transducer and should not be desorbed during the use of the biosensor.

Biomolecules can be immobilised by using various strategies such as adsorption, entrapment, covalent binding, cross-linking or affinity (269). However, each immobilisation method has either advantages and drawbacks. Therefore, the best method is strictly dependent on the application of the biosensor and on the parameters required, for instance maximum sensitivity or rather stability (94) .

In the research that we carried out several immobilisation methods were investigated:

- Physical adsorption
- Covalent binding by alkanethiols on gold surface (SAMs)
- Entrapment in sol-gel or water-gel
- Cross-linking by using glutaraldehyde

Covalent binding by using alkanethiols is resulted the best technique for grafting OBPs on gold platforms. This method was suitable for both liquid and vapour phase sensing experiments. Proteins were uniformly distributed on the entire surface of the electrode forming an insulation layer, as described in the sections 3.4.1 and 3.4.2. Moreover, the use of self-assembled monolayers for linking biomolecules on solid surfaces is an easy, not expensive and fast technique. The main disadvantage of using this method was a random and not-oriented immobilisation of biomolecules on the transducer surface that could slightly affect the sensor performance.

Physical adsorption was the first method employed for immobilising OBPs on mass transducer. Physical adsorption is an ideal method for investigating the possibility to use OBPs as sensitive layer of sensors. It is an easy and fast technique, do not require the use of chemicals and do not affect the structure and function of the protein. OBPs solutions were simply dropped on both gold electrodes of quartz crystal microbalances and allowed to dry at air. After drying, the biosensors were tested in vapour phase against several analytes. The biosensors developed using this method showed a good response toward target analytes. This was the first evidence that OBPs could be used as the sensitive layer for vapour sensors.

Figure 38 compares the response of a QCM-based biosensor to the ligand bombykol when the OBPs were linked via physical adsorption or through SAMs.

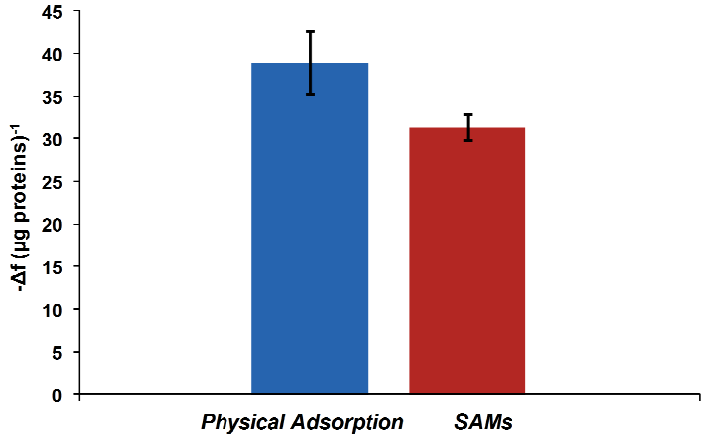

Figure 38. Comparison of the response of OBP-QCMs biosensors developed by physical adsorption or by SAMs. Each column is the average of the response of three different sensors normalised for the micrograms of protein bonded on the QCMs surface. The responses were of PBP1 of *B.mori* toward bombykol. n=3.

Both biosensors showed the same sensitivity to the tested analytes. However, a better reproducibility and increased stability in the signal were observed when the PBP1 was linked by SAMs.

The entrapment of OBPs in gel, such as tetramethyl orthosilicate (TMOS) or tetraethyl orthosilicate (TEOS), was also investigated for the immobilisation OBPs. Entrapment in polymer matrices is based on the growing of siloxane polymer chains around the biomolecules within an inorganic oxide network. The porous nature of the sol-gel network allows external analytes to reach and interact with the entrapped bio-molecules. However, sol-gel based sensors suffer of some disadvantages. The chemical and biological properties of the entrapped biomolecules may change due to reduced degrees of freedom (270).

Two different sol-gel networks were studied to immobilise OBPs. (I) TMOS sol-gel was prepared following a modified protocol described by Nogala et al. (271). A mixture of TMOS, dH_20 and 0.04 M aqueous HCl in a volume ratio of 18:4.5:1 was sonicated for 20 minutes and then diluted 1:1 with dH_20. The obtained stock solution was then sonicated for further three minutes and the diluted 1:100 with dH_20 and sonicated again for three more minutes. (II) TEOS sol-gel network was instead prepared according to Lovino et al (272). A mixture of

TEOS:PBS buffer:HCl (0.62 M) in a volume ratio of 2.9:5:0.07 was stirred vigorously until a clear solution was obtained. The sol-gel was stored at 4° C, until the use.

OBPs was added to the sol-gel solution and incubated for at least half hour. After that, the sol-gel/OBP solution was drop-casted on polymeric surfaces. The activity of OBPs in the sol-gel was initially investigated through the fluorescence binding assay (3.1.3.1.2). The fluorescence results showed a reduced activity of the wasp OBPs when dissolved in TMOS sol-gel, mainly caused by the acidic environment. However, the activity of binding was still considered good. The main limitation to the use of the sol-gel was caused by the instability and poor adhesion of the sol-gel on polymeric surfaces. Cracks appeared on the surface of the biosensor after dehydration of the gel, leaving several parts uncovered. For these reasons, the use of sol-gel for immobilising OBPs was abandoned.

Agarose was also studied for the immobilisation of the OBPs due to its natural features (273). Agarose is a polysaccharide with an average molecular weight of 120 kDa, consisting of 1,3-l-d-galactopyranose and 1,4-linked 3,6-anhydro-k-l-galactose units (274). In hot solutions, agarose chains exist in a rigid and disordered configuration. Upon cooling below 40°C, the coils form orderly helices which subsequently aggregate into thick bundles, which keeps large pores of water (275). Agarose gel has been used for entrapping several bioreceptor/biomolecules for biosensor applications (276).

OBPs buffer solution was mixed with a solution of agarose (0.4 % in double distilled water) and dimethylformamide (DMF) in ratio 1:1 (277). The obtained mixture was used as the sensing layer of SPEs. The measurements were performed dipping the electrode in Tris-Cl buffer 50 mM pH 7.4 and adding increasing concentration of analyte. Electrodes coated only with agarose-DMF solution were used as control. The signal was recorded as change in the capacitance value at the frequency of 1 kHz. The impedance measurements were performed at potential of 0 V with amplitude of 20 mV. Figure 39 shows the response of the sensor to increasing concentrations of 2-isobutyl-3-

methoxypyrazine (IBMP). Each point of the plot is the average of the values recorded from two different sensors; the standard deviation was reported as the error bar.

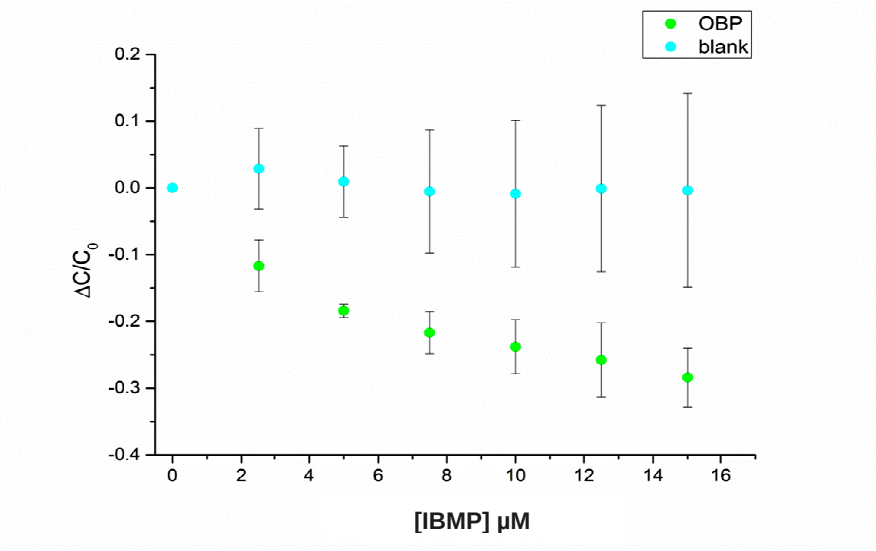

Figure 39. Impedimetric response of the pOBPF88W immobilised by agarose-DMF hydrogel to increase concentrations of IBMP. Screen-printed electrode coated only with agarose-DMF mixture was used as control (blank). n=2.

The OBP-biosensor responded to increasing concentrations of the analyte. The variation in capacitance increased with the increasing of the concentration of the analyte, until the saturation was reached. However, further investigations and studies on the use of agarose hydrogel for immobilising OBPs were not carried out due to the poor adhesion of the biofilm on the electrode surface. During the measurement, the biological film often peeled off and the biosensor activity was completely lost.

OBPs were also immobilised by using glutaraldehyde (GA) as a cross-linker. Glutaraldehyde reacts rapidly with amine groups of the proteins forming a compact network (278). Porcine OBPs cross-linked with 2.5% water solution of GA (279) on interdigitated electrodes (IDEs) were assayed against volatiles. The biosensor was tested toward 2-isobutyl-3-methoxypyrazine (IBMP) at the concentration of 150 ppm with 18% of relative humidity. A potential of 4 volts was applied to the system. Figure 40 shows the response over the time of the

IDE-OBP biosensor toward IBMP. When the analyte was introduced in the incubation chamber, a reduction in the current was observed. The baseline current value was then restored after cleaning with fresh air.

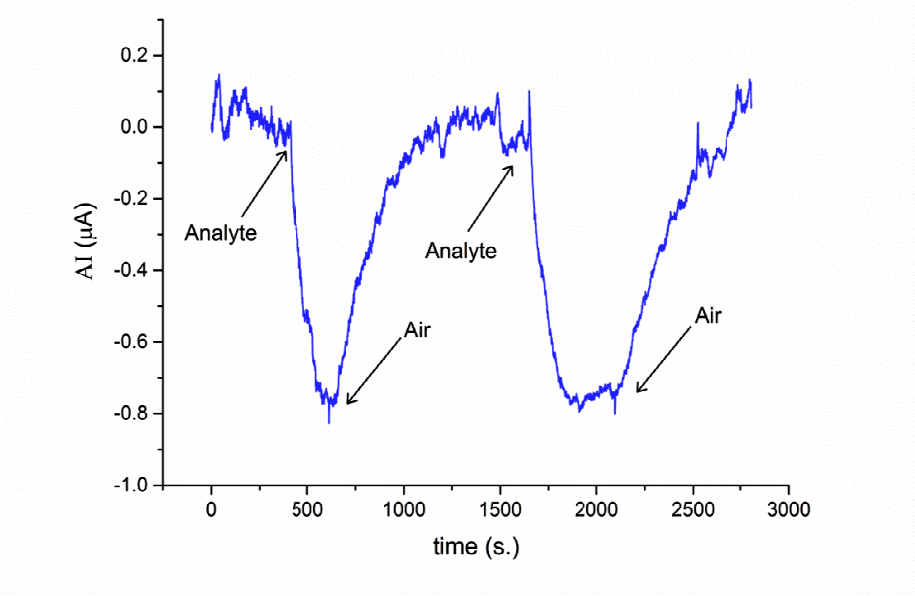

Figure 40. Response of IDEs functionalised with the porcine pOBPF88W to 150 ppm of 2-isobutyl-3-methoxypyrazine. The measurements were performed in vapour phase, applying a potential of 4V to the system.

The reproducibility in the response was quite good. It should be noted that the high voltage applied to the system (4 volts) could affect the structure of proteins and in consequence their activity (280).

After an investigation on the several methodologies that could be used for immobilising OBPs, we decided to focus our research on the covalent binding of proteins by Self-assembled monolayers. Two different alkanethiols were studied:

- thioctic acid (TA)
- 16-mercaptohexadecanoic acid (MHA)

Thioctic acid was preferred to 16-mercaptohexadecanoic acid for immobilising proteins on mass transducers. The short alkyl chain of TA minimised the dissipation phenomena that can happen on the surface of the microbalance.

SAMs of 16-mercaptohexadecanoic acid were instead used for grafting OBPs on screen-printed electrodes and interdigitated electrodes due to its insulation property. SAMs were formed on the gold surface of the transducers by dipping them in an ethanolic solution of the alkanethiol for at least 20 hours, in a controlled environment. The incubation times guaranteed the formation of a compact and uniform monolayer on the sensor surface. The carboxylic groups of both SAMs were then activated by using an aqueous solution of 1-ethyl-3-(3-dimethylaminopropyl)-carbodiimide (EDC) and N-hydroxysulfosuccinimide (NHS) as described in the Materials and Methods section (2.6.2). OBPs were tightly attached on the transducer surface by peptide bonds, which were formed between the free amino groups of the OBPs and the activated carboxylic groups of alkanethiols.

The surfaces of the biosensors developed by using both SAMs were characterised by using electrochemical techniques such as cyclic voltammetry (CV) and electrochemical impedance spectroscopy (EIS). Moreover, green fluorescence proteins were employed to assess whether the immobilisation method affected the activity and the structure of the protein.

3.4 Biosensor-surface characterisation

3.4.1 Cyclic voltammetry

Cyclic voltammetry (CV) is an electroanalytical technique, that can be used to obtain information about the redox potential and electrochemical reaction rates of analyte solutions (281). Therefore, cyclic voltammetry (CV) is often used to characterise the performance and the surface of electrochemical biosensors.

CV together with electrochemical impedance spectroscopy (EIS) are used to characterised the surface of transducers during process involved in the biosensor realisation (282;283). CV is broadly applied for the monitoring of SAMs properties, since it gives information on the distribution of defect structures, kinetics and mechanism of the monolayer formation process, etc (284;285). The compactness of the self-assembled monolayer is very important parameter to take in account for the realisation of a functional biosensor. The compactness of the monolayer can be affected by several factors, one of them is the morphology of the surface of the electrode (286).

An ideally smooth gold electrode surface allows the formation of highly ordered and regularly packed monolayers (287). The surface roughness factor usually is estimated before modifying the gold electrode. This index gives a clear indication of the surface morphology and can be even used for the determination of the real area of gold electrode. The surface roughness factor is the ratio of the real surface area to the geometric area, by definition (286). In this work, the real surface area of the gold working electrode of screen-printed electrodes was measured by using the redox probe $K_3Fe(CN)_6$/ $K_4Fe(CN)_6$ and Randles-Sevcik equation (284):

$$i_{pa} = kn^{3/2}A\sqrt{Dv}\,C_{ox}$$ **Equation 6**

In this equation, k is a constant of 2.69 x 10^5 with units of C mol^{-1} $V^{-½}$ at 25°C, n is the number of electrons appearing in the half-reaction for the redox couple, A is the electrode area (cm^2), D is the analytes diffusion coefficient (cm^2 s^{-1}) and v is the rate at which the potential is swept (V s^{-1}) (288). The diffusion coefficient for ferricyanide in a KCl solution is 7.63 X 10^{-6} cm^2 s^{-1} (284).

Figure 41 shows a typical voltammogram of the redox couple $Fe(CN)_6^{3-}$ /$Fe(CN)_6^{4-}$ at the bare gold working electrode of SPEs. The SPEs was dipped in a 0.1M KCl solution containing $Fe(CN)_6^{3-}$/$Fe(CN)_6^{4-}$ at the final concentration of 5mM (1:1). The potential was scanned between -0.2 V and 0.5 V and the current generated between the working and the counter electrode was measured. Using the Equation 6 and an anodic peak current of I_{pa} =9.82 x10^{-5} A (point 2 of Figure 41), the real surface area of gold electrode was calculated to be 0.167cm^2. The surface roughness factor resulting from the ratio of real to geometric surface area was of 1.34. The calculated surface roughness factor was found to be within the reported values for gold electrodes used for SAM modification (289).

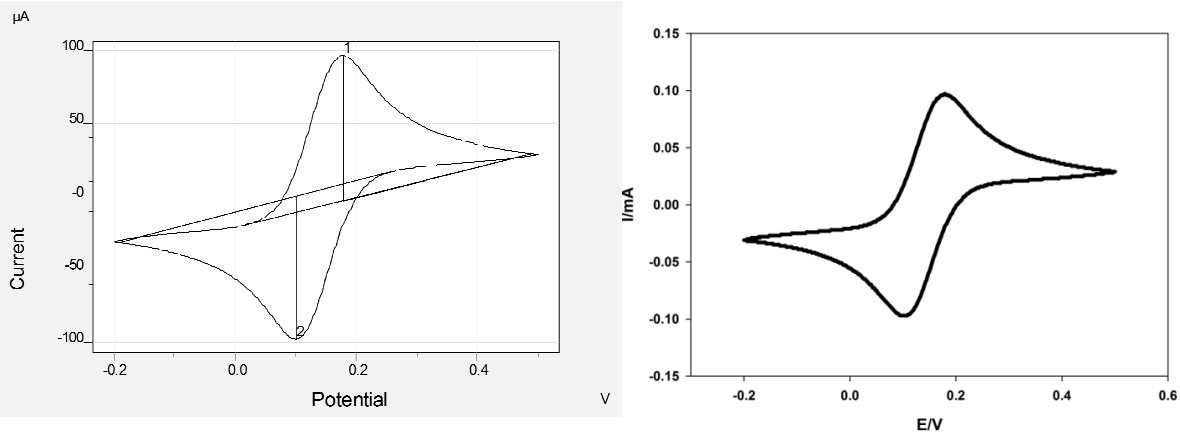

Figure 41. Cyclic voltammogram for 5 mM $K_3Fe(CN)_6$/$K_4Fe(CN)_6$ (1:1) in 0.1 M KCl solution. Scan rate = 100 mVs^{-1}.

Cyclic voltammetry was also used to characterise the density and compactness of the protein biofilm formed on the gold surface of the electrodes. The oxidation

and reduction processes of the ferro-/ferricyanide were investigated at different steps of the sensor preparation and then, they were compared with the same redox processes at the bare gold working electrode.

Figure 42 shows three different cyclic voltammograms carried out at different steps of the sensor fabrication. The first voltammogram was of an uncoated gold electrode (a), the second after treating the electrode with a SAMs of thioctic acid (TA) at the concentration 10mM (b) and the final one, after OBPs immobilisation (c).

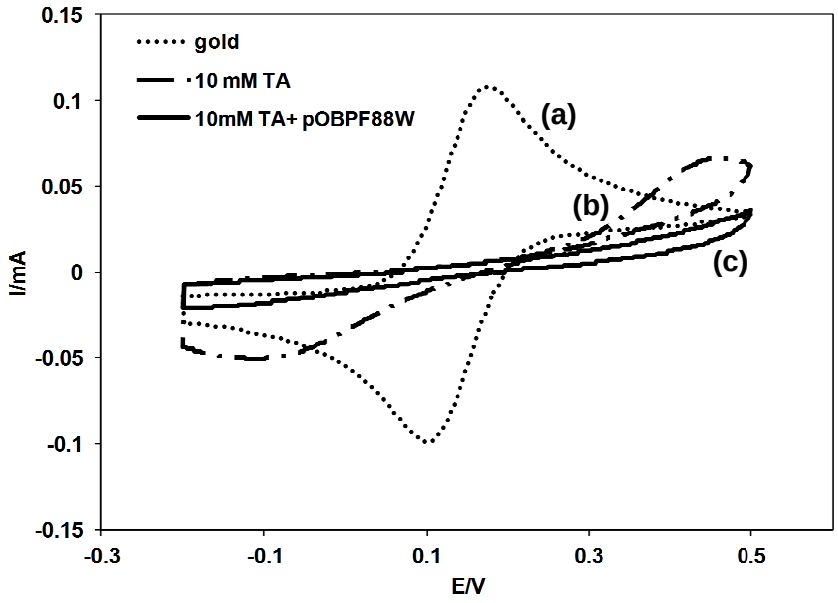

Figure 42. Cyclic voltammograms performed in a 5 mM $K_3[Fe(CN)_6]$/ $K_4[Fe(CN)_6]$ solution containing 0.1 M KCl at a scan rate of 100 mV s^{-1}. (a) Bare gold electrode; (b) after SAMs of thioctic acid (TA); (c) after immobilising of OBPs

Figure 43 shows three different cyclic voltammograms carried out at different steps of the sensor formation, when SAMs of 16-mercaptohexadecanoic acid was used for grafting the OBPs on the electrode surface.

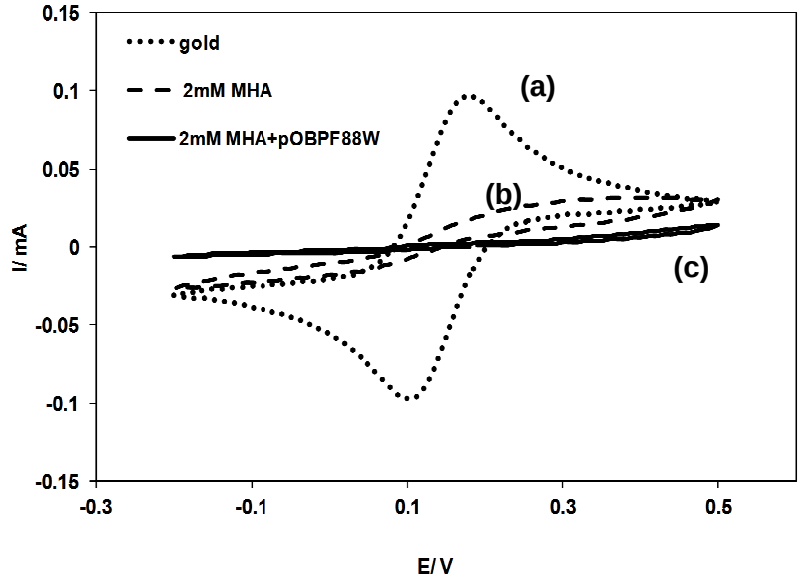

Figure 43. Cyclic voltammograms performed in a 5 mM $K_3[Fe(CN)_6]$/ $K_4[Fe(CN)_6]$ solution containing 0.1 M KCl at a scan rate of 100 mVs^{-1}. (a) Bare gold electrode; (b) after SAMs of 16-mercaptohexadecanoic acid (MHA); (c) after immobilising of OBPs.

At the bare gold electrode, a high current at the cathodic (i_{pc}) and anodic peak (i_{pa}) was observed. After the electrode was dipped in the SAMs solution, the CV curve changed drastically due to the sluggish electron-transfer kinetics through the alkanethiols layer (283). After linking the proteins, the cyclic voltammogram appeared almost as a straight line. The electron transfer of the $Fe(CN)_6^{3-/4-}$ was completely blocked. The reduction of the current intensity was caused by the increasing of the layers deposited on the electrode. The hindrance of the electrode (B) was evaluated as index of the layer density. The hindrance was calculated by using the following equation (290):

$$\mathbf{B = 1 - \frac{i_p^f[SAMs-Prot]}{i_p^f\,[Au]}} \qquad \textbf{Equation 7}$$

where $i_p^f[SAMs - Prot]$ and $i_p^f\,[Au]$ were the forward (reduction of ferricyanide) peak currents measured at both the modified and the bare electrodes, respectively. Increasing the layers deposited on the gold electrode, the value of the hindrance increased as well (Figure 44).

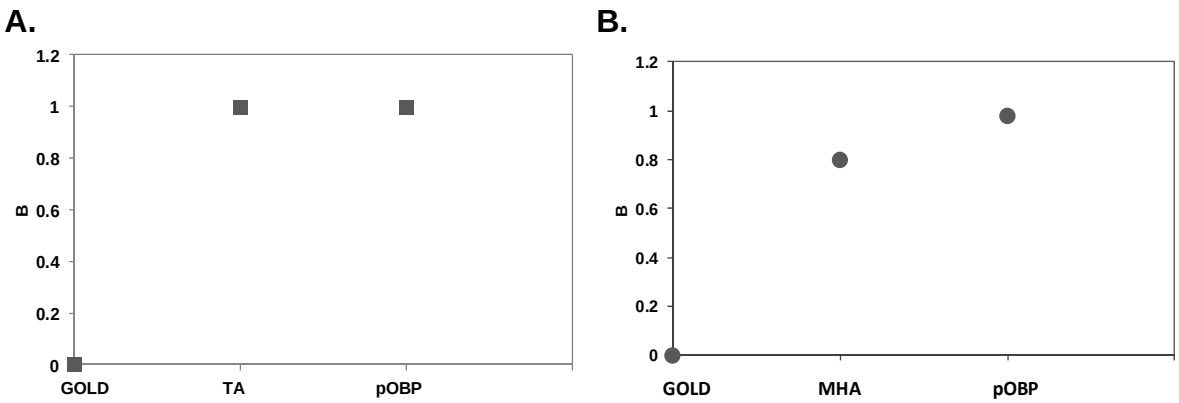

Figure 44. Calculated hindrance (B) versus different steps of the biosensor formation. (A.) Biosensor developed by using a SAMs of TA 10 mM. (B.) Biosensor realised by using SAMs of MHA 2mM.

3.4.2 Electrochemical impedance spectroscopy (EIS)

Electrochemical impedance spectroscopy (EIS) can be used to investigated thin films which allows charge transfer between a redox active probe in the solution and the electrode surface (291). The main advantage, of this technique compared to the CV, is that does not affect the surface and the specimens can be used for further applications (284).

EIS techniques are well-established and known techniques used for the characterisation of electrode-solution interfaces. EIS studies reveal charges of transfer processes which occurring at the electrode-solution or at modified electrode-solution interfaces. Any change in the EIS spectra can be related to the change in interface properties, thus can be utilised for surface characterisation.

The EIS was employed in our studies to evaluate the surface coverage of the modified gold working electrode of SPEs by using the ferro/ferricyanide redox probe.

Figure 45 shows the impedance spectra reported in the form of Nyquist plot of different phases of the sensor preparation. In the Nyquist plot the impedance is

presented as the sum of the real (Z') and imaginary (Z") components, which are originate from the resistance and capacitance of the cell. The diameter of the semicircle, lying on the real component, corresponds to the electron transfer resistance (R_{ct}) of the redox probe at the electrode interface. It reflects the blocking behaviour of the electrode surface toward the redox couple.

The Nyquist plot of a bare gold, which was plotted as red circles in Figure 45, shows the typical shape of a faradaic impedance spectrum for conductive electrodes. A very small semicircle at high frequencies correlated to a very low electron transfer resistance, followed by a 45° straight line, which is typical of a diffusion limited electron-transfer process (292). The impedance plots of the electrodes modified by SAMs significantly differs from the bare gold. At high frequencies, the responses of both electrodes modified with MHA and TA showed a semicircle with a wide diameter, due to the increasing of the charge-transfer resistance. Diffusion processes can be still observed at low frequencies due to imperfections of the SAM.

The values of electron-transfer resistance for the gold bare and modified electrodes were obtained by modelling the EIS spectra with the Randles equivalent circuit. Data related to the bare gold surface and the SAMs-modified electrodes were fitted by means of the circuit displayed in the inset of Figure 45.

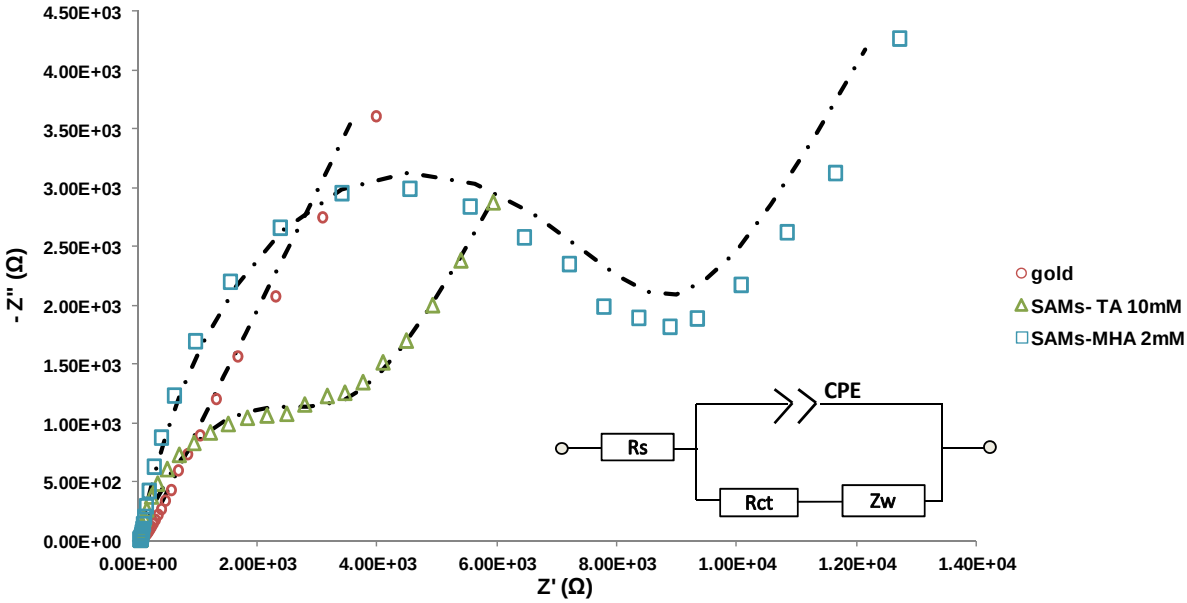

Figure 45: Nyquist plot of the blank Au electrode (○); electrode modified with MHA (□) and TA (△). The test solution contained 5 mM $K_3Fe(CN)_6/K_4Fe(CN)_6$ in 0.1 M KCl. The dotted lines correspond to the fits modelled by using the Randles equivalent circuit.

The elements presented in the circuit are:

- R_s: the ohmic resistance of the electrolyte solution;
- R_{ct}: the electron-transfer resistance of the ferro/ferricyanide redox probe;
- Z_w: the Warburg impedance, resulting from the diffusion of ions from the bulk to the electrode interface;
- CPE: the constant phase element, which takes into account deviations from the ideal capacitance behaviour (292).

The diameters of the semicircles of the EIS spectrum were significantly enlarged after the immobilisation of the Odorant Binding Proteins (Figure 46). The proteins formed a complete insulating layer on the modified electrode, which inhibited the passage of redox couples dissolved in the solution (48). Diffusive processes at lower frequencies were not observed indeed. The EIS spectra were modelled by using the Randles equivalent circuit showed in the insert of Figure 46. The equivalent circuit kept the same elements of the circuit described above but without the Warburg impedance (Z_w).

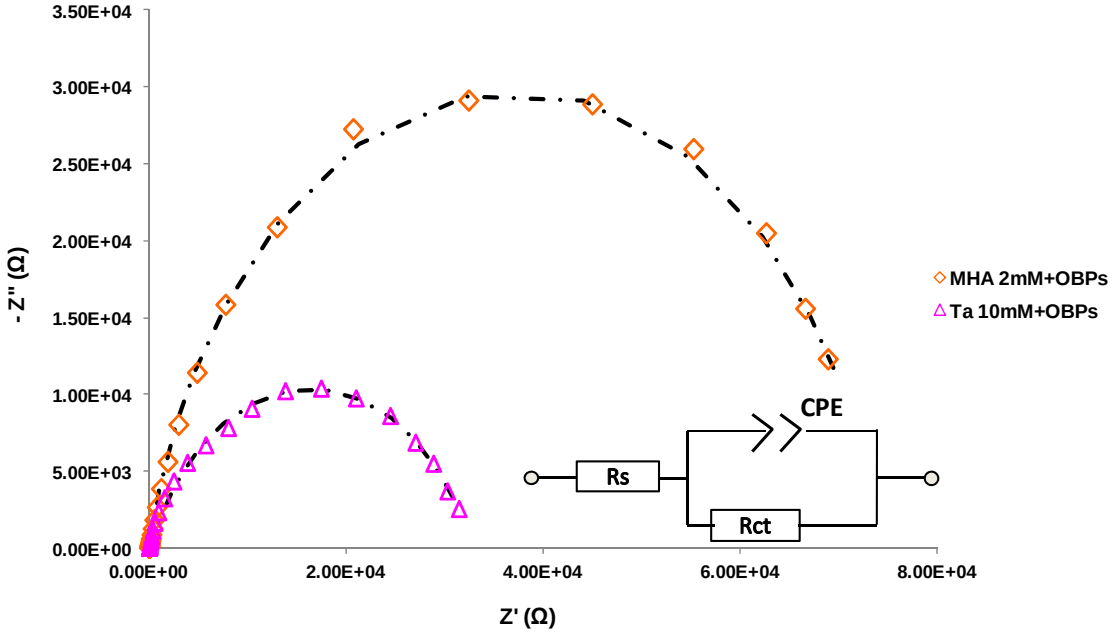

Figure 46. Nyquist plots of OBPs immobilised on electrodes modified with TA self-assembled monolayers (△) and MHA self-assembled monolayers (◇).The test solution contained 5 mM $K_3Fe(CN)_6/K_4Fe(CN)_6$ in 0.1 M KCl. The dotted lines correspond to Randles equivalent circuit fits.

The surface coverage of the modified electrodes was evaluated from the blocking properties of the film for the electron transfer reaction of the ferro/ferricyanide redox probe. We assumed that electron transfer reactions occur only at bare spots on the electrode surface and that diffusion to these defect sites is planar. If the above assumption is correct, the apparent electrode coverage (θ) can be related to the charge-transfer resistances using the following equation (293):

$$\theta = 1 - \frac{R_{ct}^{0}}{R_{ct}}$$ **Equation 8**

Where R_{ct}^{0} and R_{ct} are the charge-transfer resistances of the bare and modified gold electrodes, respectively.

	Gold Bare	SAMs (TA 10 mM)	SAMs (TA10 mM) +OBP	SAMs (MHA 2mM)	SAMs (MHA 2mM) +OBP
Rct (kΩ)	0.057 (0.838%)	3.553 (0.031%)	32.900 (0.008%)	8.377 (0.133%)	74.300 (0.009%)
CPE ($\mu S\ s^n$)	0.370 (2.45%)	0.130 (0.368%)	0.169 (0.158%)	0.351 (0.197%)	1.637 (0.130%)
n	0.760 (0.418%)	0.647 (0.754%)	0.717 (0.022%)	0.786 (0.029%)	0.859 (0.014%)

Table 10. Values of circuital parameters obtained by the impedance analysis with the corresponding errors in bracket.

Table 10 summarises the parameters obtained by fitting the EIS spectra, along with the corresponding errors. The data clearly showed that the charge-transfer resistance increases with the modification of the gold surface from a value of 0.057 kΩ for the bare electrode to 3.553 and 8.337 kΩ after modification with SAMs of thioctic acid and 16-mercaptohexadecanoic acid, respectively. A further increase of the charge-transfer resistance was observed after the immobilisation of the OBPs on the modified electrodes.

The fractional coverage (θ) was calculated using the Equation 8, and the relative values are reported below.

	TA	TA+OBPs
θ	0.984	0.998
	MHA	**MHA+OBPs**
θ	0.993	0.999

θ close to 1 was obtained when the OBPs was immobilised by using a SAMs of 16-mercaptohexadecanoic acid, indicating that the film covered completely the whole surface. The estimated surface coverage, in case of OBPs immobilised by using a self-assembled monolayer of thioctic acid, was of 0.998. The protein films covered more than the 99 % of the electrode surface. Both the alkanethiols studied can be considerate suitable for linking the OBPs on gold surface since that a complete coverage of the electrode surface was achieved.

The immobilisation of OBPs through the SAMs generated a complete insulator layer on the surface of the electrode as demonstrated by CV and EIS. This property was fundamental for the development of capacitive biosensors.

3.4.3 Fluorescence microscopy

A common problem with the protein immobilisation is the occurrence of surface induced denaturation and consequent loss of function (294). Green fluorescence proteins (GFPs) were used as model proteins since they possess an intrinsic chromophore that is only functional when the protein is structurally intact. Studies performed on the spectral properties of the GFPs demonstrated the importance of the intact structure of the protein in order to keep unaltered the fluorescence features. Chromophores in solution, separately from the proteins, have shown to lose fluoresce. The tertiary structure of the GFPs is important not only for autocatalysis, but also for protecting the chromophore from substances present that can have a quenching effect (295). Green fluorescent protein has a barrel-shaped conformation with a central p-hydroxybenzylidene-imidazolidone chromophore. The formation of the chromophore results from an oxidative backbone cyclization involving the residues Serine 65, Tyrosine 66 and Glycine 67.

The wild-type GFP isolated in the jellyfish *Aequorea victoria* has a characteristic dual-peak excitation spectrum with a major absorption maximum at 395 nm and a minor peak at 477 nm. Excitation at either wavelength results in the emission of green fluorescence around 507 nm. This dual absorption of GFP stems from the existence of two interconvertible states of the chromophore. The neutral phenol state of the chromophore absorbs at 395 nm, whereas the deprotonated phenolate anion absorbs at 477 nm (Figure 47) (296).

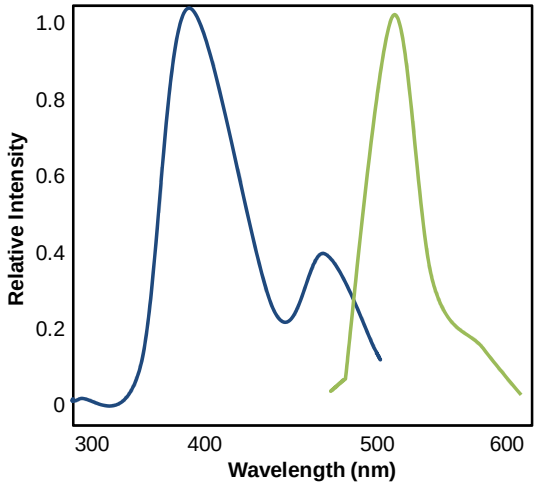

Figure 47. The excitation spectrum of native GFPs from *A. victoria* (blue) shows two excitation states i.e. 395 nm and 477 nm. The fluorescence emission spectrum (green) has a peak at 507 nm and a shoulder at 540 nm. Adapted from Chelfie et al. (297)

By using fluorescence microscopy, we demonstrated that the GFPs kept their own fluorescence after immobilising on the SAM-modified gold electrode.

Figure 48 shows the images recorded after immobilisation of GFPs on both self-assembled monolayers of thioctic acid (A) and 16-mercaptohaxedacanoic acid (B). The immobilisation was performed by using the same method employed for the OBPs, described in the Materials and Methods section (See section 2.6.2).

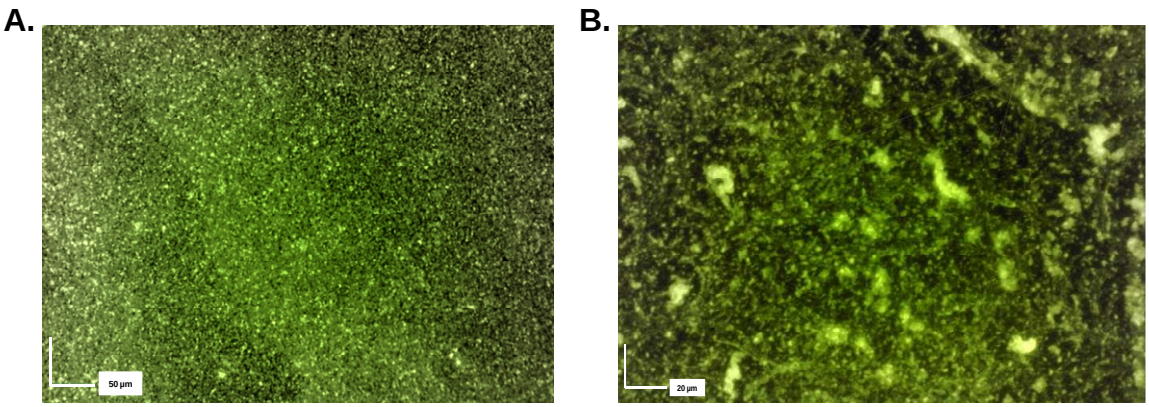

Figure 48. Fluorescence microscopy images of GFPs immobilised by using (A) a SAMs of thioctic acid at the concentration 10 mM, and (B) a SAMs of 16-mercaptohexadecanoic acid at the concentration 2 mM.

In both cases, a compact green layer was observed on the gold surfaces. The thioctic acid seemed to form a monolayer of proteins while, in presence of 16-mercaptohedecanoic, agglomerations of GFPs were observed. The difference

found between the two types of SAMs, can be due not only to their chemical proprieties, but also to the roughness of the gold surface used, which can affect the quality of the SAMs.

A SAM of 1-dedecanethiol was used as control. This thiol differs from the thioctic acid and 16-mercaptohexadecanoic acid since it has a methyl group at the terminal end. The methyl moiety cannot react with the free amino groups of the protein even in presence of carboxyl activating agents such as EDC and NHS; therefore the fluorescence protein cannot be covalently bound to the SAM surface (Figure 49).

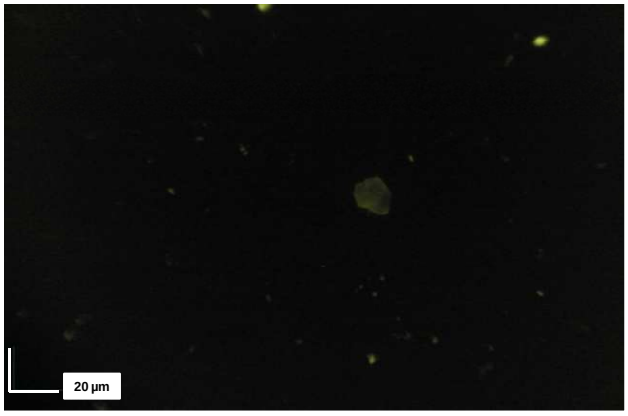

Figure 49. Fluorescence microscopy image of a control experiment performed using a SAM terminating with -CH_3 groups. The methyl moiety is not reactive against the EDC/NHS activating groups; therefore, the coupling reaction with GFPs cannot occur. Hence, fluoresce signal was not observed.

The control experiment with 1-dedecanethiol, demonstrated that the linking between proteins and SAMs occurred only through peptide bonds. Only few fluorescence spots were observed on the gold surface, as displayed in Figure 49, likely due to unspecific interactions.

The results found for the GFPs could be applied to the vertebrate OBPs as well, since they share several biochemical proprieties. Both proteins have a β-barrel organisation. The molecular weight is relatively close, 19 kDa for OBPs against 27 kDa for GFPs and the isoelectric point (pI) is at slightly acid pH for both proteins (Table 11).

	Porcine OBP	GFP
MW	18.8 kDa	26.8 kDa
pI	4.55	5.67

Table 11. Comparison of chemical proprieties of porcine OBP and GFP. The parameters was calculated by using Expasy ProtParam tool (http://web.expasy.org/protparam/).

Considering the similarities between GFPs and OBPs, it was thought that the results found for GFPs, could be valid for the OBPs as well.

Surface characterisation experiments demonstrated that SAMs were a suitable method for attaching OBPs on gold electrode surface. A compact and insulator layer of OBPs was present on the transducer surface due to the presence of covalent bonds formed between the amino groups of the proteins and the carboxylic groups of the alkanethiol. Furthermore, the structure of the protein was not altered as demonstrated in the fluorescence experiment.

3.5 OBP-based biosensors

Odorant Binding Proteins were used in our studies as sensitive layer of three different types of transducers such as quartz crystal microbalances (QCMs), screen-printed electrodes (SPEs) and interdigitated electrodes (IDEs) for both vapour and liquid phase application. Figure 50 summarises the different kinds of biosensors developed.

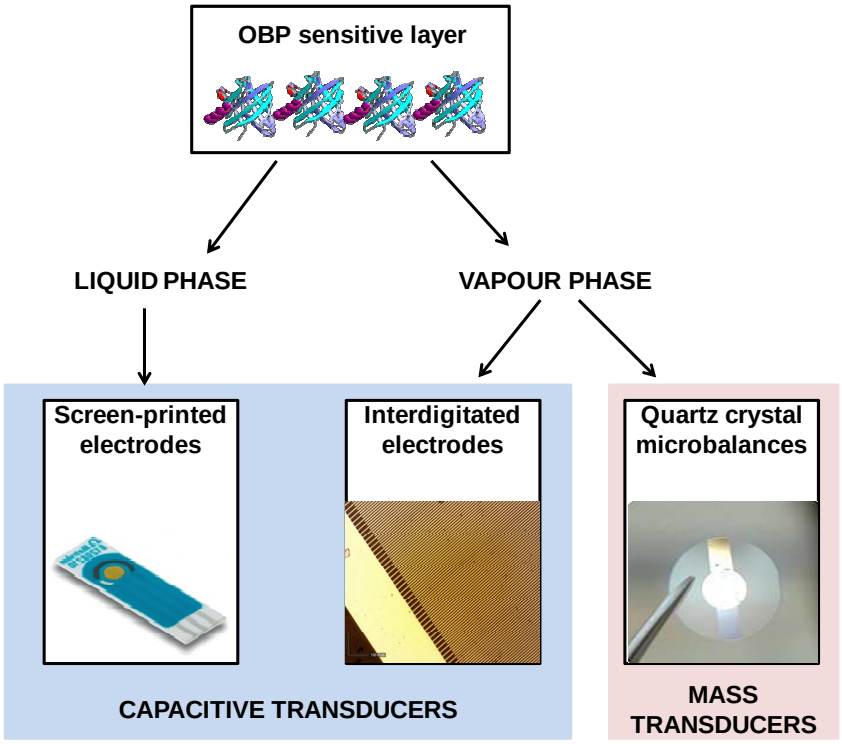

Figure 50. Schematic representation of the different OBP- biosensors developed.

Quartz crystal microbalances were used as mass transducers to investigate the sensitive and the selectivity of different OBPs in vapour phase. Recombinant OBPs, obtained from different species of vertebrates and invertebrates, were linked on both sides of QCMs and tested against target analytes dissolved in vapour. The use of QCMs as transducers allowed the detection of any interaction occurring between proteins and ligands in real-time. Such interaction was recorded as variation in the resonance frequency of QCMs. The increase in

mass on the surface of the QCMs, due to the presence of bound ligands, leads to a proportional reduction in the resonance frequency of the microbalance.

Six different QCMs were tested simultaneously in vapour phase against target analytes aiming to develop a sensor able to discriminate food related ligands.

Capacitive biosensors realised on IDEs and SPEs were employed to investigate the binding activity of the OBPs in vapour and liquid phase. The interaction between protein and ligand was monitored by means of electrochemical signals.

Screen-printed electrodes functionalised with OBPs were tested in liquid phase, by using a self-designed flow cell system. OBPs were grafted on the gold working electrodes of SPEs forming a compact insulator layer. The measurements were performed in AC mode and a small voltage was applied to the device. The signal was recorded as a variation in the capacitance value. When the analyte was injected in the flow cell, a reduction of the capacitance was observed. The initial capacitance value was re-established after eluting away the ligand from the sensor surface. The biosensor showed an excellent selectivity, a good sensitivity- concentration in the order of nanomolar was detected and a good reproducibility. Moreover, the use of a liquid medium mimicked the natural environment of the OBPs, maintaining the biochemical features of the proteins. After proving that the interaction between OBPs and ligands can be detected with electrochemical method, the system developed for SPEs was transferred to interdigitated electrodes (IDEs). IDEs functionalised with OBPs were tested in vapour phase against the ligand S-(+) carvone. In this instance, only few tests were performed due to time constraints. However, it was possible to show as a proof of principle that the interaction between OBPs and ligands can be electrochemically detected also in vapour phase.

The working principles and the tests performed on the developed OBP-based biosensors are described in detail in the next sections.

3.6 Label-free impedance/capacitive biosensors

The biological interaction between an electrical biosensor and a target analyte can be detected in a variety of ways i.e. capacitance, resistance, voltage and current. Due to their low cost, low power consumption and possibility of miniaturization, electrical biosensors hold great promise in applications where minimizing size and costs are crucial. In particular, capacitive biosensors have shown great promises in immunology field, for the detection of heavy metal ions and for DNA sequencing, providing high selectivity and low detection limits (298).

In a capacitive biosensor, the electrode surface is generally covered with an insulating layer and the bio-recognition element is immobilised on it. Electrodes immersed in an electrolyte solution can be described as a re-assembled capacitor (200). Charged species and dipoles present in the solution will be oriented at the electrode-solution interface, generating the electrical double-layer (EDL).

The assaying principle of capacitive biosensors is simple and does not require the use of labelled compounds (299). Any physiochemical change, which happens at the interface of the sensing element, can be detected as variation of the capacitance value (300). When a target molecule interacts with the bioreceptor, solvated ions and water are pushed out from the electrode surface, resulting in a change of the sensor capacitance. The decrease in the biosensor capacitance is proportional to the amount of bound molecules (299). Furthermore, conformational changes of the bio-recognition element, caused by the interaction between proteins and ligands, can lead to decreases in the capacitive signal as well. Also in this case, the change in capacitance is generated by modifications in the EDL distance (301).

The selectivity and the sensitivity of the OBP-based biosensor developed by us, was investigated towards several analytes selected on the basis of their binding affinity.

The sensors were developed on disposable screen-printed electrodes. Porcine OBP, pOBPF88W, were immobilised on the gold working electrode by using a self-assembled monolayer of 16-mercaptohexadecanoic acid (see Section 2.6.2). The insulating proprieties of the sensors were investigated through electrochemical methods. Both CV and EIS showed the presence of a compact insulation layer on the surface of the sensor, especially after the immobilisation of OBPs.

3.6.1 Sensing experiments

The capacitive measurements were performed in liquid phase under a constant flow rate of sodium phosphate buffer. The working electrode was polarised at 0.1 volt against the silver reference electrode. Each scan was performed in the frequency range between 1 Hz and 0.1 MHz. Figure 51 shows the raw response of the OBP-sensor at different concentrations of the tested analyte S-(+) carvone.

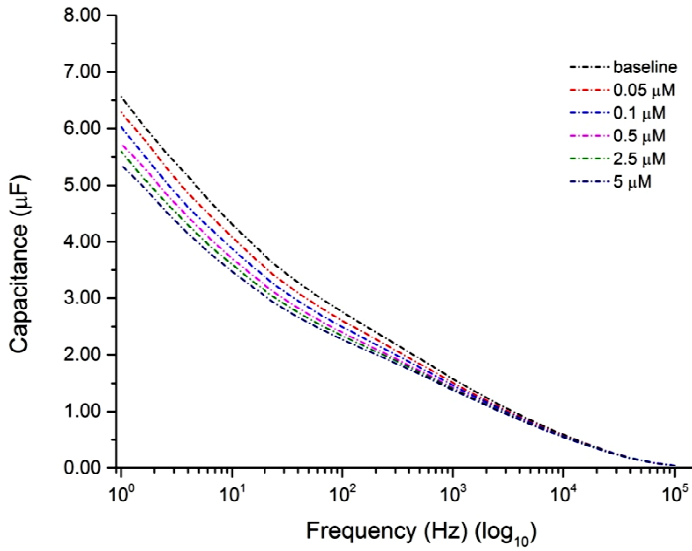

Figure 51. Raw response of pOBPF88W-biosensor to different concentrations of S-(+)-carvone. A voltage of 0.1 V was applied. The frequency was scanned between 1 Hz and 0.1 MHz with 20mV amplitude.

When increased concentrations of analyte were injected in to the flow cell system, a decrease in capacitance was observed.

The measurements were performed using a “step by step” procedure. The analyte was introduced in the flow cell for 15 minutes after a stabilisation time of about 50 minutes. This was followed by a cleaning step of 20 minutes with phosphate buffer to reequilibrate the system.

In Figure 52, the typical behaviour of the OBP-capacitive biosensor with increasing concentrations of analyte is shown. The capacitance was recorded at a frequency of 96Hz.

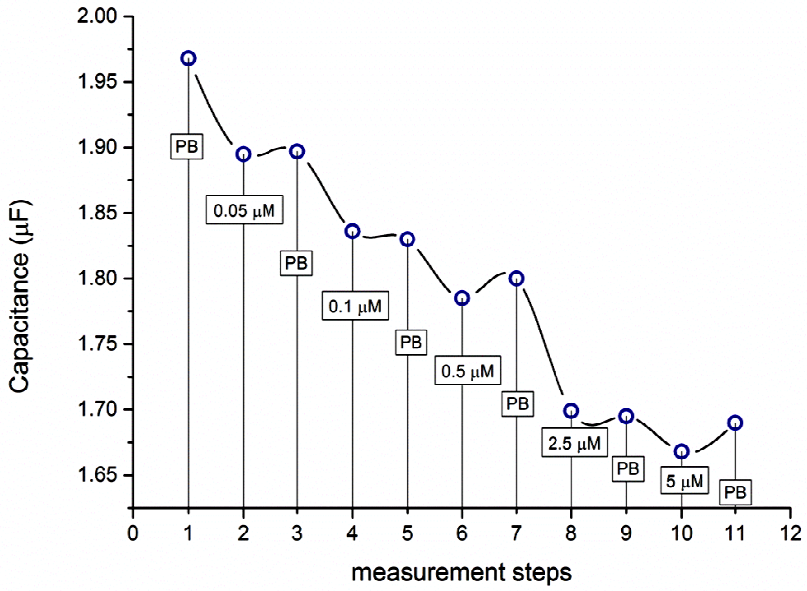

Figure 52. Dynamic of the response of pOBPF88W-biosensor at different concentrations of S-(+) carvone and after the “regeneration” step performed with PB buffer.

Reductions of the capacitance of the order of tens of nanofarads were recorded in presence of the analyte. The capacitance increased again when the buffer was injected. A full recovery of the baseline signal was not observed likely due to a slow dissociation rate between the protein and the ligand. The dissociation constant calculated for S-(+) carvone was 0.5 µM.

The observed variation in the capacitance values could be associated with several phenomena. A first hypothesis suggested that the reduction in the capacitance was caused by the increase of the distance between the EDL and

the electrode. When the analytes entered in the binding pocket of the protein, the diffuse layer was further displaced increasing the distance from the electrode surface. A second hypothesis, which was demonstrated for other capacitive biosensors (298), supported that the capacitive responses can be generated by the replacement of conducting aqueous solution present the binding pocket of the OBPs with less conductive chemical compounds. In Table 12, the dielectric constants (Ɛ) of water and the tested analytes are reported:

Substance	ε	Temperature	Reference
water	80.37	20°C	(302)
S-(+) carvone	11	22°C	(302)
2-phenylethanol	13	20°C	(302)

Table 12. List of the dielectric constants of the tested analyte and water.

The Ɛ of the ligands resulted to be almost eight times lower than the water, explaining the reduction in the capacitance value.

Before starting the measurements, the sensor was stabilised for at least 50 minutes under a constant flow of phosphate buffer in order to reach a stable baseline signal.

Figure 53 displays the drift of the sensor recorded over the time.

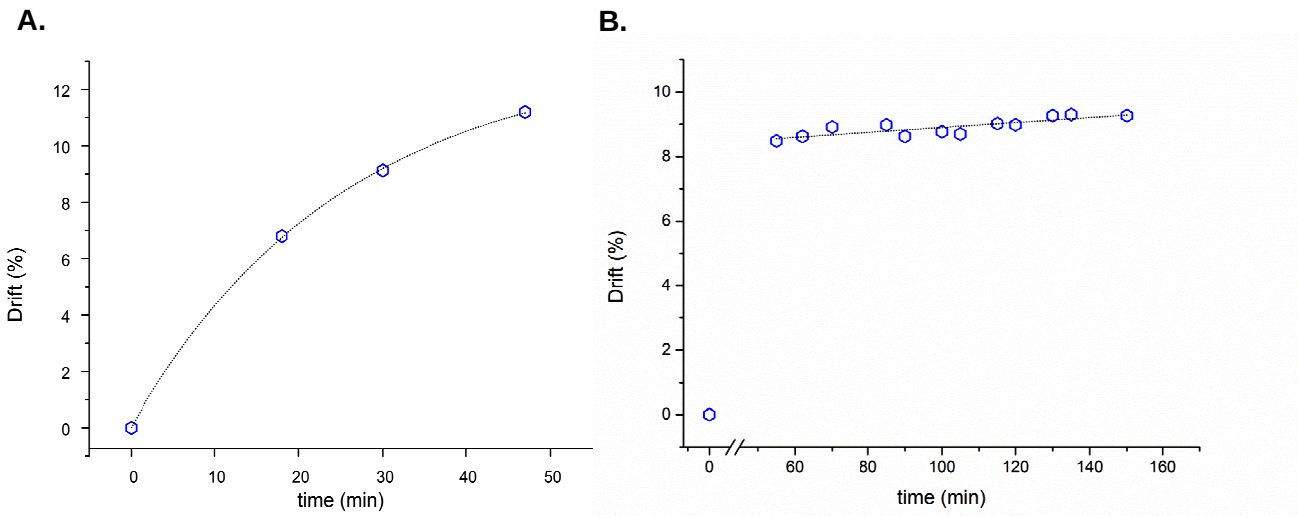

Figure 53. Evaluation of the sensor drift over the time. E_{dc} = +0.1V, Eac = 20 mV, f = 96 Hz, flow rate 0.5 ml min^{-1} of 10 mM phosphate buffer, pH 7.

The sensor was monitored at different times between 0 and 150 minutes under a constant phosphate buffer flow. In the first fifty minutes, a large drift was observed (Figure 53 A) but after this initial period, the variation of the capacitance over the time was less than 1% (Figure 53 B).This effect was likely associated to the formation of the electrical double-layer.

Several analytes were tested toward the OBPs biosensors. They were chosen on the basis of their dissociation constant estimated by means of fluorescence binding assays (see section 3.1.3.2.1).The aim was to investigate whether the interactions between OBPs and ligands could be detected as a change in the capacitance value without using auxiliary probes.

Nowadays, the fluorescence competitive binding assay is the method commonly used for determining the affinity of binding between OBPs and ligands. In the fluorescence assay, the direct interaction between the protein and the ligand cannot be detected. Sometimes, this method is not reliable due to the presence of the probe in the binding pocket of the protein, which can facilitate the entrance of other ligands.

Figure 54 shows the concentration response curve of pOBPF88W sensor to 2-phenylethanol, S-(+) and R-(-) carvone. Each point of the plot represents the variation in capacitance ($C-C_0$) normalised for the initial capacitance value

versus the ligand concentration, expressed as percentage. The measurements were repeated in triplicate. S-(+) and R-(-) carvone were chosen as target ligands for their good affinity toward the porcine OBPF88W, as previously determined. Moreover, we wanted to investigate the possibility of the capacitive sensor to discrimination between enantiomeric forms. 2-Phenylethanol was used as negative control due its low affinity for the porcine OBP (K_D >>28µM).

As a second negative control, lysozyme was also used. This protein is a glycoside hydrolase isolated form chicken egg white. Lysozyme was immobilised on the gold working electrode of screen-printed electrodes by using the same procedure employed for the OBPs. Lysozyme shares a similar size with the porcine OBP, 14 kDa against 18 kDa and it does not show any binding activity.

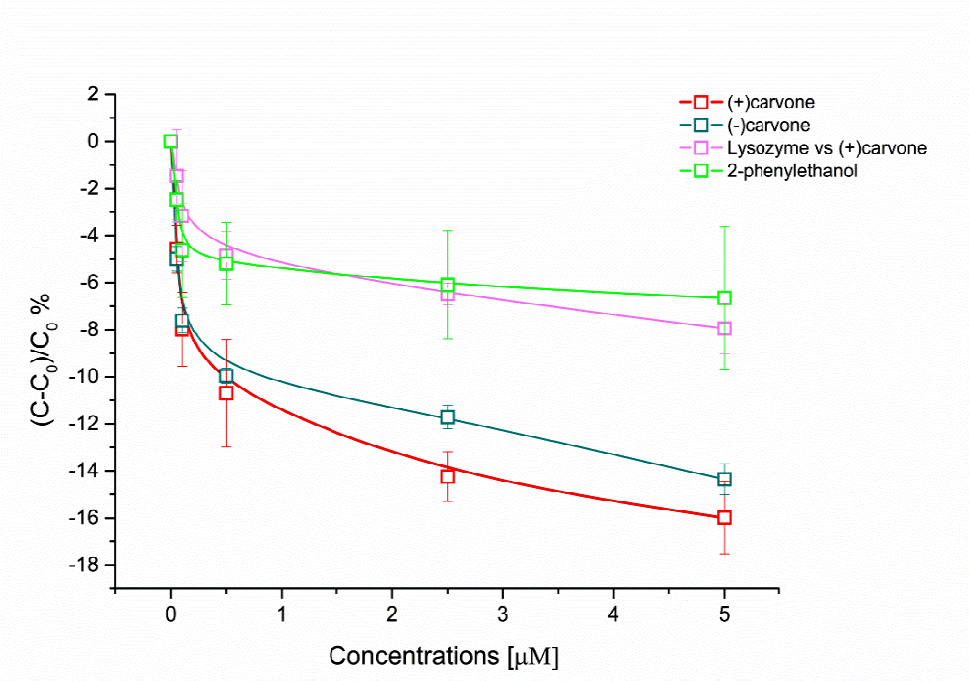

Figure 54. Responses of the OBP-biosensor to different concentrations of selected analytes. Experimental conditions required E_{dc} = +0.1V, E_{ac} = 20 mV, f = 96 Hz, flow rate 0.5 ml min^{-1} of 10 mM phosphate buffer, pH 7. n=3.

The response of the capacitive sensor against the ligands reflected the affinity of binding previously estimated in the fluorescent assays. S-(+) and R-(-) carvone showed higher variations in the capacitive response whereas the signal recorded in presence of 2-phenylethanol was more than four times lower.

The response curves of pOBPF88W to 2-phenylethanol and lysozyme against S-(+) carvone were almost superimposable, confirming the absence of binding interactions. 0.5 µM concentrations of S-(+) and R-(-) carvone seemed to saturate the sensors. The binding sites of the OBPs were all occupied by ligands and further increases in concentrations did not lead to a proportional rise of the signal.

The response of the biosensors plotted in a logarithmic scale is displayed in Figure 55.

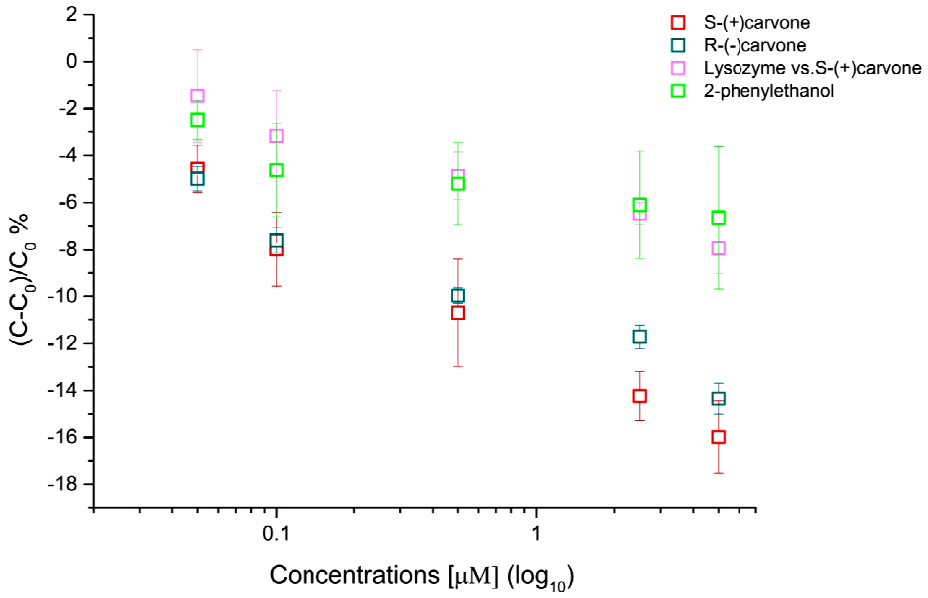

Figure 55. Responses of the OBP-biosensor to different concentrations of the selected analytes, plotted in log scale. Experimental conditions: E_{dc} = +0.1V, Eac = 20 mV, f = 96 Hz, flow rate 0.5 ml min^{-1} of 10 mM phosphate buffer, pH 7. n=3.

At the lower concentrations tested (0.05 µM), the OBPs-sensor was able to discriminate between carvone and 2-phenylethanol. Such selectivity in the response became more evident when 0.5 µM concentrations were used.

The reproducibility of the response of the sensor over the time was also investigated.

Figure 56 shows the capacitive response of three OBPs biosensors tested in different days against the ligand R-(-) carvone. All three biosensors belonged to the same batch and they were stored at the temperature of 4°C until the use.

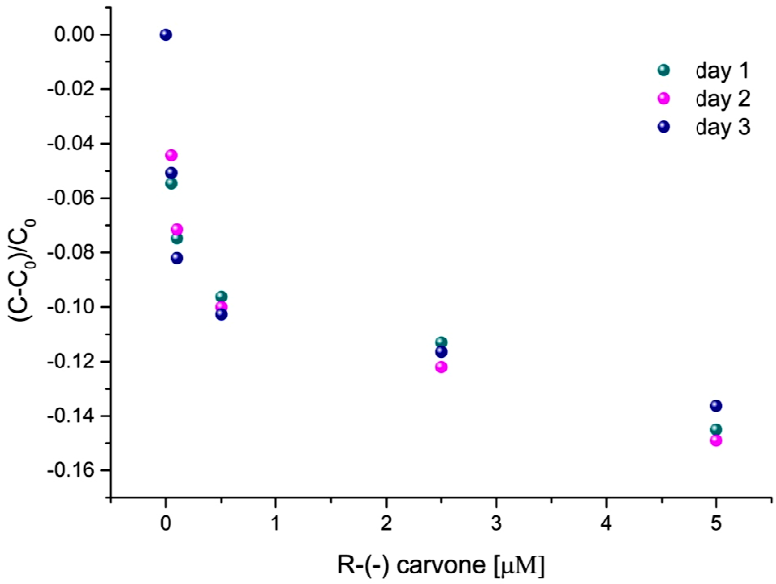

Figure 56. Reproducibility of OBPs-biosensor response determined over the time. The measurements were performed against the ligand R-(-) carvone in three different days.

The sensors were stable over a period of three days. No significant difference in the biosensor response was observed and the total standard deviation (SD) calculated among the measurements was found to be 0.005 ± 0.001.

3.6.2 Determination of the dissociation constant

The dissociation constants of the OBPs-biosensor against the ligand S-(+) and R-(-) carvone were determined by plotting the absolute value of the capacitance changes as function of the ligand concentration. The values were fitted with the non-linear regression analysis by using the Langmuir isotherm (Equation 9), assuming that the analyte is both monovalent and homogenous, the ligand is homogeneous and that all binding events are independent (303).

$$[AB] = [B]_{max} * \frac{[A]}{K_D + [A]} \qquad \textbf{Equation 9}$$

where [AB] is the degree of saturation, B_{max} is the number of maximum binding sites, and K_D is the equilibrium or dissociation constant.

Assuming a Langmuir adsorption isotherm, the change in relative capacitance was found to be directly related to the amount of ligand bound by the OBPs (304).
The dissociation constant for S-(+) and R-(-) carvone, reported in Table 13 was estimated by using Equation 9.

	K_D
S-(+) carvone	0.123µM ± 0.037
R-(-) carvone	0.084 µM ± 0.022

Table 13. Dissociation constants of pOBPF88W for R-(-) and S-(+) carvone

There was no significant difference in the affinity of binding of pOBPF88W between S-(+) and R-(-) carvone, as estimated with paired sample t-test with $p < 0.05$.

The developed capacitive OBP biosensor was not able to discriminate between the two enantiomeric forms. The values of the K_D determined by using fluorescent binding assays were different from the data obtained in the capacitive measurements. The dissociation constants in case of OBP-sensors were an order of magnitude lower than the values found in the fluorescent assays. Such differences could be related to the different methodology employed. Capacitive sensors measure the direct interaction between the protein and the ligand. The fluorescence binding assay instead uses an indirect system to calculate the K_D, and higher quantities of ligand may be required to obtain a visible signal.

However, further studies will be necessary in order to understand the reasons that form the basis of the diversity found in the dissociation constant values.

3.7 Quartz crystal microbalance-based biosensors

The Quartz Crystal Microbalance (QCM)-based biosensors are simple and label-free devices that can be used for monitoring interfacial binding reactions in real-time (178;305).

QCMs have been used for varied applications in several disciplines of science and technology. For instance, in the detection of metals, vapours, chemical analytes, environmental pollutants, biomolecules, disease biomarkers, cells and pathogens (306). In the last few years, the use of mass transducers as platforms for medical devices has been considerably increased. Extensive work have been done to develop biosensors based on biomolecules for studying the interaction between protein-protein, protein-ligands, DNA/RNA, antibodies-antigen, etc. (307).

Quartz crystal microbalances can measure any minute changes in mass due to the piezoelectric proprieties of the quartz. The adsorption of analyte molecules on the surface of the quartz crystal leads to increases of mass, resulting in a detectable decrease of the resonance frequency. The adsorption process is fully reversible and fast. The accuracy of the measurements is high, since that difference in the weight of the order of picograms can be detected (308).

The goal of our research was to investigate the possibility to use OBPs as sensitive layer of QCMs for vapour phase applications. Quartz crystal microbalances (QCMs), with a resonance frequency of 20 MHz, were functionalised with different Odorant Binding Proteins and tested against the vapour of several chemical compounds. The interaction between the OBPs and the ligands was easily recorded as variation in the resonance frequency of the QCMs, in real-time.

OBPs were immobilised on both gold electrodes of the QCMs by using a self-assembled monolayer of thioctic acid (TA) (Figure 57). The disulfide of the

thioctic acid strongly bound the gold surface via a covalent bond, while the carboxylic acid group at the other terminal end can be activated to bind covalently the free amino groups of proteins.

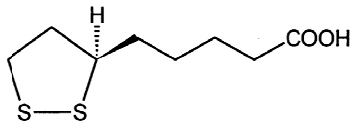

Figure 57. Thioctic acid structure

Thioctic acid was preferred to 16-mercaptohexadecanoic for its short alkyl chain, which minimises the dissipation phenomena. Monolayers made up of alkanethiols with alkyl chains shorter than 9 carbons, resulted to be less ordered and compacted when compared with molecules with a longer alkyl chain (309).The surface of the OBPs-biosensor developed using a SAM of thioctic acid was studied by several techniques as described in the section 3.4. The obtained results demonstrated that a dense and compact biofilm was formed on the gold electrode.

Two types of QCM-OBP based biosensors were developed during this research:

1. Biosensors based on Pheromone Binding Proteins and General Odorant Binding Protein (PBPs and GOBPs) for the detection of pheromones in the environment. The purpose was to realise a device for controlling of useful insects and pests with applications in agriculture.

2. Biosensors based on OBPs belonging to different species of vertebrates and invertebrates for the detection of volatile compounds released by foodstuff. The aim was to develop an array of sensors able to monitor the quality of food along the transportation and the storage, in real-time.

3.7.1 Quartz crystal microbalance biosensors based on Pheromone Binding Proteins and General Odorant Binding Proteins.

Odorant Binding Proteins can be classified in several subgroups on the base of their amino acid sequence (144). Pheromone Binding Proteins (PBPs) and General Binding Protein (GOBPs) are two classes of OBPs isolated in the antenna of insects. These proteins have been extensively studied since they seem to be involved in the recognising and transporting of pheromones in the perireceptor space (310-312).

In our research, PBP1 and GOBP2 of the silk moth *Bombyx mori* were investigated as putative active layers of QCMs for the detection of the two main components of the silk moth pheromone blend: bombykol and bombykal.

Bombykol, (E)-10,(Z)-12-hexadecadien-l-ol, was the first attractive compound discovered. It is secreted from the abdominal glands of the female of *B.mori* and serves as an attractant toward the males of the same species. Bombykal, (Z)-10,(E)-12-hexadecadienal by contrast seems to act as antagonist of bombykol in the mate behaviours (313).

PBPs and the GOBPs are both present in the antenna of *B.mori*, but their expression pattern is different between the males and females. PBP1 is expressed at high level (10mM) in the long sensilla trichodea of the antenna of males. In this kind of sensilla are present two neurones, which are highly sensitive to the female sex pheromone, bombykol and bombykal (314). The sensilla trichodea of the female of *B.mori* is instead sensitive to chemical compounds released by the host plants, such as linalool and benzoic acid (315) and always expresses GOBP2 (165).

In a study published by Zhou et al. in 2009 (310), the selectivity of PBP1 and GOBP2 of *B.mori* toward components of the pheromone blend was investigate. The affinity of binding was estimated by fluorescence binding assay, using 1-

NPN as fluorescence probe. They demonstrated that GOBP2 was able to discriminate between bombykol and bombykal, while PBP1 was not able to do this.

We repeated the same experiments and the results were shown in the section 3.1.3.2.2. Our results showed that GOBP2 could distinguish between bombykol and bombykal but the affinity was higher for bombykal than bombykol. Differing from the method published by Zhou, a delipidation step was performed before assaying the affinity of binding. Such process can increase the affinity of the recombinant proteins against the ligand, by removing any lipid residues present in the binding pocket of the OBPs. This may explain the difference in the two results.

PBP1 and GOBP2 were immobilised on the gold surface of quartz crystal microbalances as previously described and tested in vapour phase against the bombykol and bombykal.

Figure 58 shows the typical response-time curve of a VOC detection cycle. The sensor was stabilised under a constant flow of air for at least 30 minutes before the analyte injection. After that, the analyte, in this case bombykol, was introduced into the detection chamber. The frequency decreased quickly, until a saturation frequency was reached. Clean air was then introduced in the detection chamber and the frequency returned to the initial value. The response of the sensor was completely reversible.

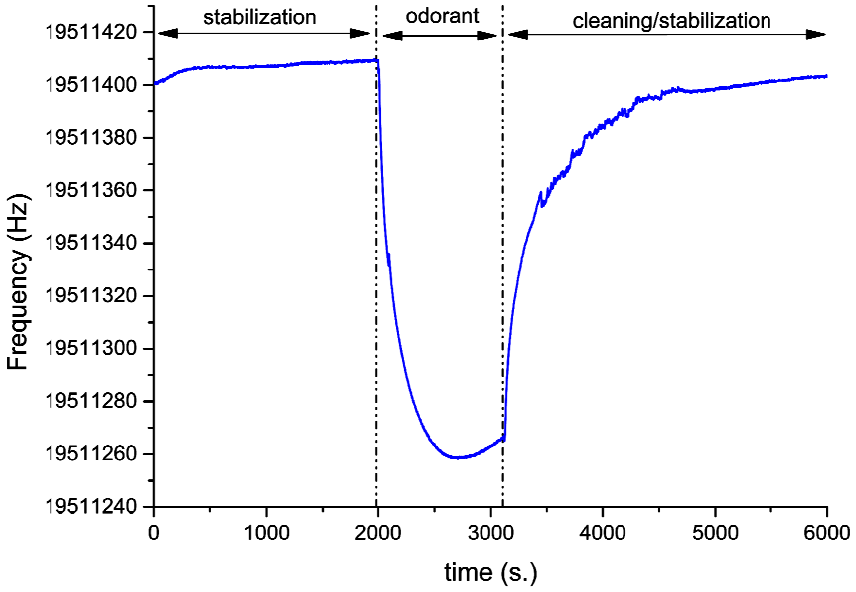

Figure 58. Typical odorant response cycle curve of the GOBP2 of QCM- based biosensor toward the analyte bombykol.

3.7.1.1 Gas Chromatography-Mass spectrometry: quantification analysis of bombykol and bombykal

Gas Chromatography-Mass spectrometry (GC-MS) was used to estimate the relative volatility of the bombykol and the bombykal. Experimental values of the saturated pressure of these two chemical compounds are not available and the only information accessible is predicted *in silico.*

Table 14 displays the values of vapour pressure predicted by using two different algorithms.

	Predicted by ACS/lab	**Predicted by EPI suite**
Bombykol (alcohol)	1.29E-4 Torr @ 25°C	5.69E-6 Torr @ 25°C
Bombykal (aldehyde)	8.89E-5 Torr @ 25°C	4.12E-4 Torr @ 25°C

Table 14. Values of saturated vapour pressure of Bombykol and Bombykal from different sources. ACD/Percepta Platform (ACS/lab) and Estimation Program Interface (EPI) Suite.

It was interesting to note the discrepancy among the different sources, and in particular ACS/lab reported a value of saturated pressure for bombykal lower that bombykol, even if it is well known that aldehydes are more volatile than alcohols.

Driven by the necessity to normalise the QCM-based biosensor data, GC-MS analysis was performed. The relative volatility of known concentrations of pure bombykol and bombykal in ethanolic solution was evaluated by this method.

Figure 59 displays the total ion chromatogram (TIC) of a 1:1 mixture of bombykol and bombykal.

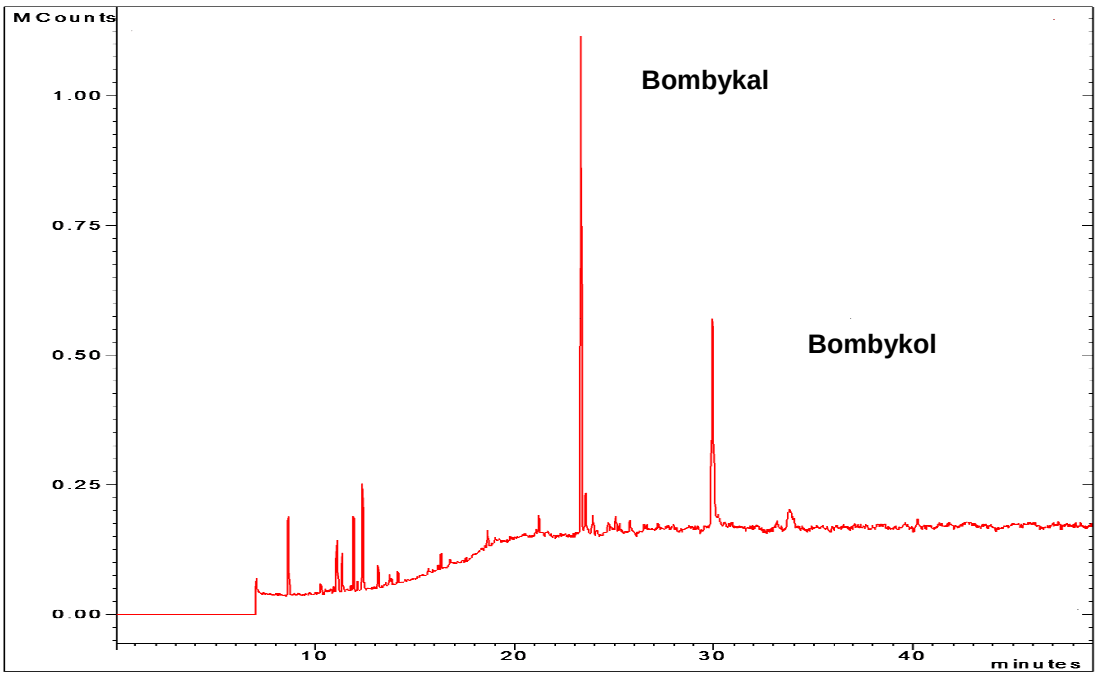

Figure 59. Total ion chromatogram, obtained by GC-MS of the mixture bombykol/bombykal.

The chromatographic peaks were identified by matching the mass spectra against mass spectra data from NIST (National Institute of Standards and Technology) and Wiley MS libraries. The mass spectra of the bombykal and bombykol are displayed in Figure 60.

A.

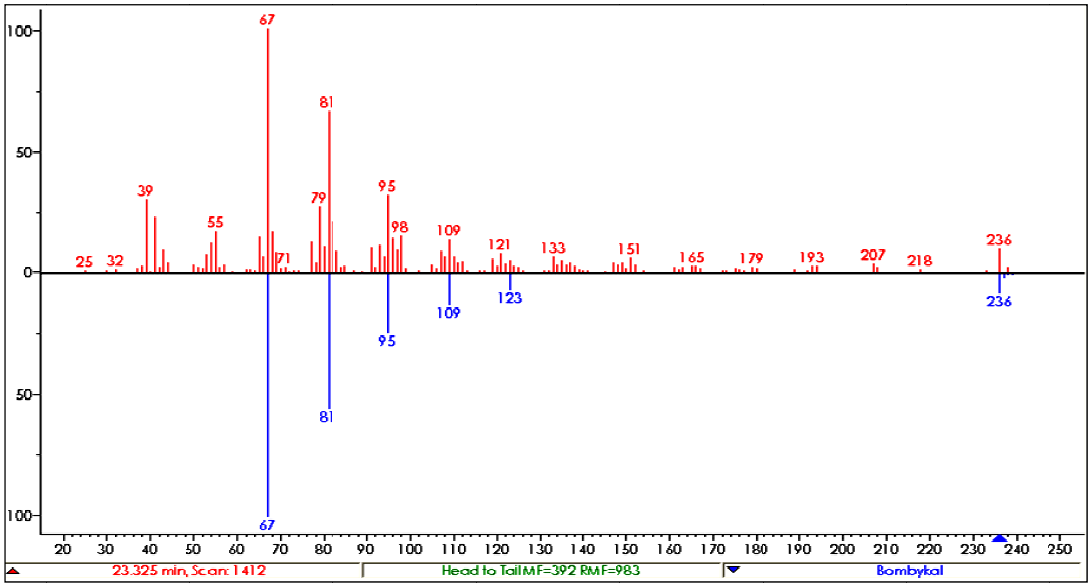

B.

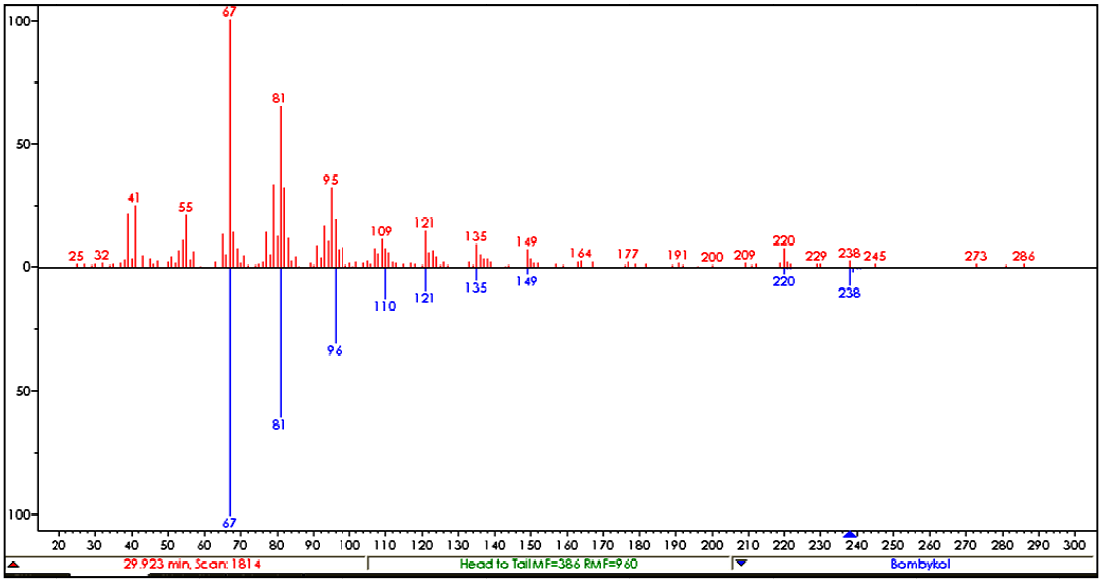

Figure 60. Mass spectra of bombykal (A) and bombykol (B).

The first peak was identified as bombykal by mass spectrometry, with a retention time (R_t) of 22.96 minutes. The bombykol was the second peak (R_t of 29.26 minutes). A high polarity column (DB-WAX) was used for our experiments. Bombykol due to its polar nature interacted strongly with the polar stationary phase of the column increasing the retention time.

The Area Normalisation method was used to estimate the relative volatility of the bombykol and the bombykal. This method is based on the calculation of area percent, which is assumed to be equal to weight percent. If X is the unknown analyte, then we obtain

$$\text{Area \% X} = \left[\frac{\text{Ax}}{\sum(\text{Ai})}\right] \text{x } 100 \qquad \textbf{Equation 10}$$

where Ax is the area of the X compound and the denominator is the sum of all the areas (316).

Since the same concentrations for both analytes were used and their molecular weights are almost identical, we assumed that the area of the peak was proportional to the concentration of the analyte in the headspace. Figure 61 displays the area of the peak normalised for the value of the total area (area bombykol plus area bombykal) of 12 replicates. The standard deviation was approximately the 5% of the calculated value.

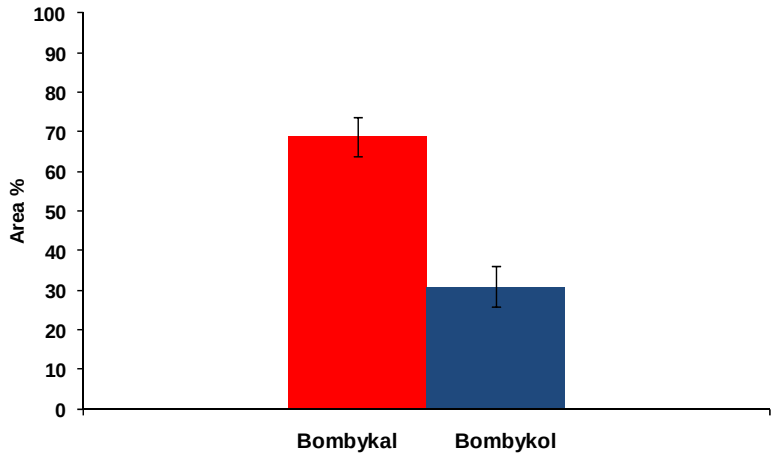

Figure 61. Area percentage of the peak of bombykol and bombykal. n=12.

The relative abundance of the two components was 68.8% bombykal and 31% bombykol.

3.7.1.2 QCM based biosensor responses

QCMs functionalised with recombinant PBP1 and GOBP2 of *B.mori* were tested, in vapour phase, by using the delivery system described in the Materials and Methods section.

The measurements were performed under constant flow of air at the rate of 20 ml min^{-1}. The biosensors were tested with different concentrations of the analyte. The pheromone flow channel was increased from 20% to 100% of the initial saturated concentration by mixing with a separate flow of air, maintaining however a total flow rate of about 20 ml min^{-1}. The amount of proteins immobilised in the gold surface of the quartz microbalance was initially estimated by using the Sauerbrey equation (Equation 2).

$$\Delta f = -\frac{2f_0^2 \Delta m}{A\sqrt{\mu_q \rho_q}} \qquad \textbf{Equation 2}$$

Where Δf is the measured frequency shift; f_0 is the fundamental resonant frequency of the crystal; Δm is the mass change; A is the piezoelectrically active area; μ_q is shear modulus of quartz; ρ_q is density of quartz.

Table 15 reports the micrograms of OBPs immobilised on each QCM tested. The final values were deducted of the contribution of the self-assembled monolayer.

QCMs	µg Protein
Q1-PBP1	1.84
Q2-PBP1	1.91
Q3-PBP1	8.38
Q4-GOBP2	4.01
Q5-GOBP2	5.80
Q6-GOBP2	5.90

Table 15. Amounts of protein immobilised of each quartz crystal microbalance estimated by using the Sauerbrey equation.

Figure 62 displays the dose-dependent responses curve of the average of three PBP1 and three GOBP2 based biosensors to bombykol and bombykal.

The data were normalised by dividing the frequency variation by the micrograms of protein immobilised on each QCM. Moreover, to compare the response of the sensors to bombykol with the response to bombykal, the normalised data were divided by the area of the GC-MS peaks. The peak area was used as index of the relative volatility. Since the vapour pressure values of bombykol and bombykal are not known, it was not possible to estimate the concentrations of the two analytes. In fact, on the x-axis of Figure 62, the flow rate of the analyte on a total flow of 20 ml min^{-1} is reported.

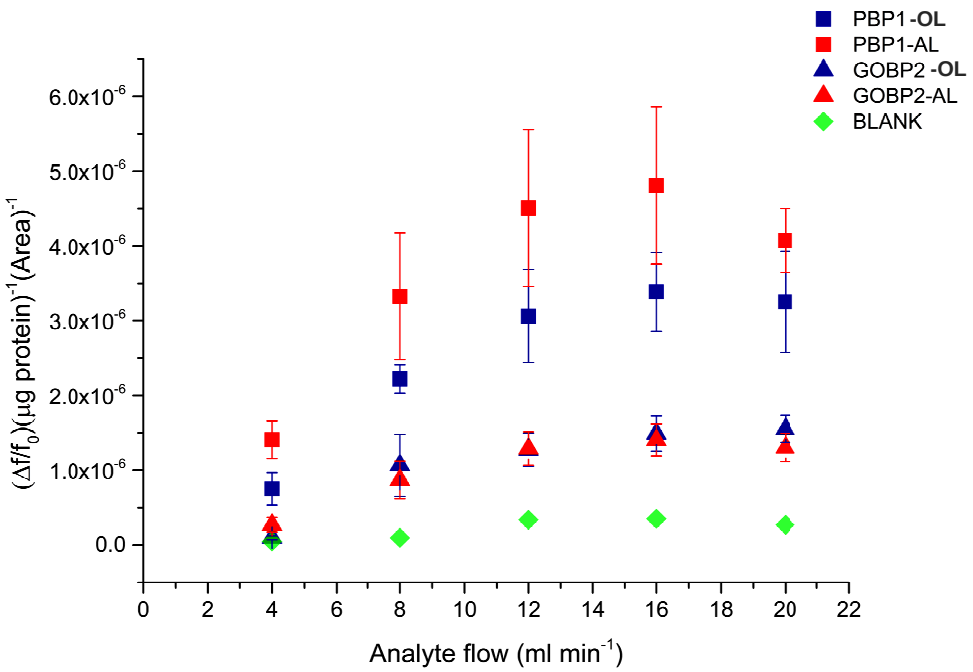

Figure 62. Dose-response curve of PBP1 and GOBP2 based biosensors. In the legend bombykol is indicated as OL and bombykal as AL. (■) Response of PBP1 to bombykol; (■) response of PBP1 to bombykal; (▲) response of GOBP2 to bombykol; (▲) response of GOBP2 to bombykal and (◆) response of an uncoated QCM (BLANK) to the analyte. n=3.

The data showed the typical dose-response behaviour. The variation in the measured frequency of the QCMs increased with the analyte concentration. All the sensors reached a plateau. At that point, even if higher concentrations of analyte were used the biosensor response was not proportionally raised, likely due to a saturation of the binding pocket of OBPs.

A second hypothesis at such response could be related to the low volatility of the analytes and to their high enthalpy of vaporization. However, when the VOCs were heated up until 90°C, the response of the sensor was not increased as well.

The results obtained from vapour phase measurements showed that neither PBP1 nor GOBP2 were able to discriminate between the two pheromone components. However, these results highlighted the high affinity of PBP1 towards both ligands compared to GBOP2.

Figure 63 A displays the response of PBP1 and GOBP2 biosensor to fixed concentrations of bombykol and bombykal. The data were analysed by using the Analysis of Variance (ANOVA)-one way (Figure 63 B). A significant difference in the response was found between PBP1 and GOBP2 to bombykol and to bombykal. There was not a significant difference between the responses of PBP1 to both pheromones. The same was observed for GOBP2.

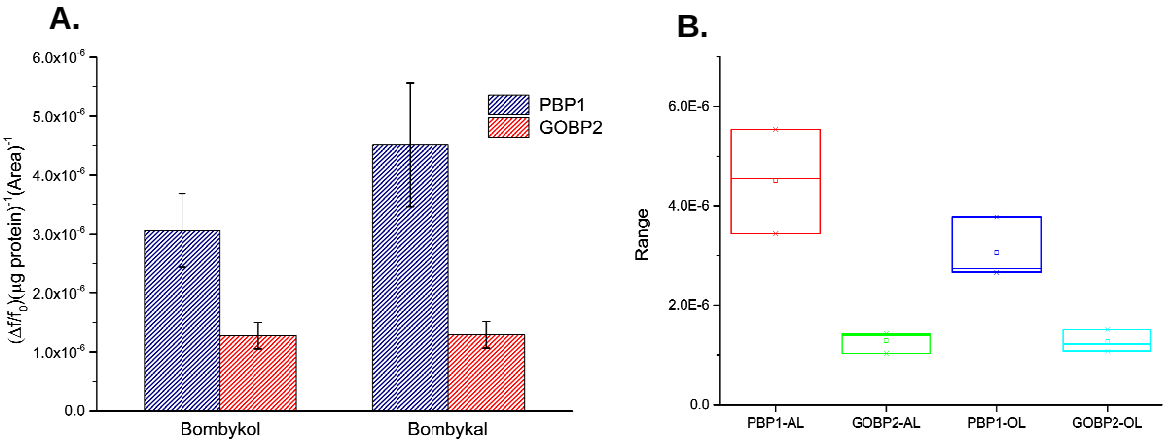

Figure 63. (A) QCM-biosensors responses at a fixed concentration of bombykol and bombykal. (B) One way Analysis of Variance (ANOVA) of the QCM-biosensors to the same concentrations of bombykol and bombykal. n=3.

The data obtained from the QCM biosensors in vapour phase differed from the fluorescence binding assay measurements. In the fluorescence assay, a lower dissociation constant was found for GOBP2 toward bombykal. The values of K_D of PBP1 against bombykol and bombykal and GOBP2 versus bombykol were not significantly different. It seemed like GOBP2 could discriminate between two pheromones.

Considering the role of the OBPs as carriers of pheromones and hydrophobic molecules through the sensillar lymph and the pattern of the expression of these two proteins in the antenna of the silk moth, the data obtained from the QCM-biosensors seemed quite reasonable. In fact, the higher response to both the female pheromones was found for PBP1. PBP1 is highly expressed in the antennae of males, where these two pheromones are perceived. However,

GOBP2 is expressed in the antenna of the females, which is sensitive to volatiles released by host plants in the environment.

Moreover, the affinity of binding of PBP1 towards three stereoisomers of the bombykol (10e-12z) was investigated. 10Z-12E hexadecadien-1-ol (10z-12e), 10Z-12Z hexadecadien-1-ol (10z-12z) and 10E-12E hexadecadien-1-ol (10e-12e) were tested. Amongst them, 10E-12E hexadecadien-1-ol is also a component of the *B.mori* pheromone blend (310).

Figure 64 shows the response of the PBP1-sensor at a flow of 8 ml min^{-1} of analyte. Each column is the average of the response of three sensors normalised by the micrograms of proteins immobilised on the QCMs. The results were analysed with one-way ANOVA test. Not significant difference ($p< 0.05$). was found among the reported values. PBP1 was not able to discriminate among different steroisomeric forms of the pheromone bombykol.

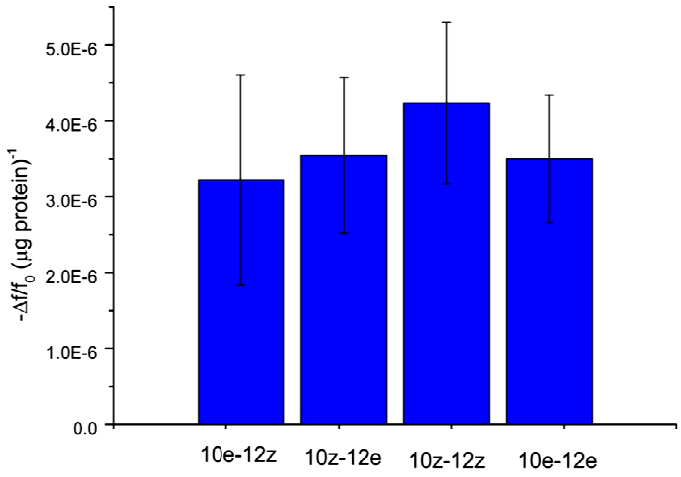

Figure 64. Response of PBP1 to bombykol and three stereisomers at a fixed concentration of analyte. Bombykol (10e-12z); 10Z-12E hexadecadien-1-ol (10z-12e); 10Z-12Z hexadecadien-1-ol (10z-12z) and 10E-12E hexadecadien-1-ol (10e-12e). n=3

The obtained data agreed with the results obtained in fluorescence competitive binding assays (data not shown).

The results obtained showed that the affinity of binding of PBP1 and GOBP2 toward the two main components of the pheromone blend, bombykol and

bombykal reflected the physiological role of these proteins in the antennae of *B.mori*.

The developed biosensor was highly sensitive, the detection limits was of the order of few *parts per billion*, even if, the exact concentration of the volatiles could not be estimated. Measurements carried out with the QCM-based biosensors were performed at the temperature of 30°C; whereas samples used for GC-MS analysis were warmed it up to 150°C, in order to obtain a detectable signal in the chromatogram.

3.7.2 Quartz crystal microbalance based on Odorant Binding Proteins (OBPs) for food monitoring

Odorant Binding Proteins belonging to different species of vertebrates and invertebrates were also investigated as sensitive layer of mass transducers for the detection of analytes related to the quality of food.

Perishable and processed foodstuffs constantly release volatile compounds in the environment, which can be used as markers for monitoring its quality. Amongst organic compounds that contribute to the food aroma, pyrazine derivatives were identified as major responsible of the roasted and cooked flavour (317). Pyrazines were mainly detected in heated foods such as beef products, toasted barley, cocoa, coffee, peanuts, popcorn, potato chips, rye crisp bread and roasted hazelnuts as result of the Maillard reaction. However, they can be also produced during the fermentation process in fermented food. Fresh foods like tomatoes, peas, green bell peppers, asparagus, kohlrabi and dairy products are also sources of pyrazines (318).

Three pyrazine derivatives were used as target analytes for testing QCMs functionalised with different OBPs, in vapour phase:

- 2-Ethylpyrazine, which is present in wheat bread (319), cocoa (320), coffee (321), black and green tea (322), roasted peanut (323), fish sauce and cooked mussels (324).

- 2,3-Dimethylpyrazine, which also existents in bread (319), coffee (321), roasted hazelnuts (325), cocoa (326), peanuts (327), dark chocolates (328) fermented soybean paste (Dienjang) (329), French fries (330) and beer (331).

- 2-Isobutyl-3-methoxypyrazine (IBMP), which is found in different species of pepper (332-334), coffee brew (335), British Cheddar cheese (336) and baked potato (337). Moreover, IBMP shows an extremely low olfactory threshold for human nose, around 2 *parts per trillion* in water (338).

Besides pyrazine derivatives, a terpene was also used as indicator of off-flavour in food. Geosmin (trans-1,10-dimethyl-trans-9-decalol) is responsible of the strong mouldy and earthy smell of fruits and water. It is a secondary metabolite produced by some *Penicillium* species (4) and by Actinomycetes (5). Human beings can detect 0.7 *parts per billion* of geosmin in fish tissues. The presence of even lower traces of geosmin in water can hamper industries that are responsible for producing drinking water, cereal, sugar, whiskey and paper tissue products (339).

In order to develop a biosensor for the detection of markers of food quality, QCMs were functionalised with six Odorant Binding Proteins belonging to different species of vertebrate and invertebrate. The aim was to identify which OBPs displayed the best performance for the tested ligands in vapour phase.

Amongst the vertebrate OBPs porcine OBP1-C (pOBP-C), porcine OBP F88W (pOBPF88W) and the major urinary protein 10 (MUP) of mouse were used.

Porcine OBP-C is a mutated form of the wild-type porcine OBP-1, bearing an additional cysteine in position 2. This protein maintained all the binding features of the wild type form and the presence of the cysteine made easier the immobilisation of the protein on the gold surface. The thiol group of the cysteine bound to the gold electrode of the quartz crystal microbalance, via a strong covalent bond.

The porcine OBP F88W is also a mutated version of the porcine OBP1. The phenylalanine in position 88 was replaced by a tryptophan. F88W mutants showed an improved affinity toward the fluorescent probe 1-aminoanthracene,

when compared to the wild type. This result was easily explained by the presence of the tryptophan indole ring that reasonably stabilised the complex through π–π interactions between the two aromatic systems (254).

The Mouse Major Urinary Proteins (MUPs) are a family of Pheromone Binding Proteins (340). MUPs act as a molecular sponge, protecting (341) and controlling the release of mouse pheromones from the urines (342). MUPs are present in nature in different isoforms. MUP 10 (formerly known as MUP II), used in our research, are proteins mainly expressed in the liver of mice. From there, they are secreted into the serum and then excreted into the urine (343). MUP 10 can bind a variety of male-derived pheromones, including 2-*sec*-butyl-4,5-dihydrothiazole, 6-hydroxy-6-methyl-3-heptanone and dehydro-*exo*-brevicomin (344), which affect the physiology and behaviour of the mouse.

Polistes dominula OBP1 (P.domOBP1), *Locusta migratoria* OBP1 (LocustOBP1) and *Bombyx mori* PBP1 (B.moriPBP1) were instead chosen from the OBPs of invertebrates.

So far, *Polistes dominula* OBP1 is the only OBP to be isolated in the European paper wasp. This protein of 15 kDa is equally expressed in antennae, wings and legs of male and female wasps but not in other parts of the body (255). Long linear alcohols and carboxylic acids result as the best ligands for the wasp OBP.

Locusta migratoria OBP1 shows a good affinity to linear aliphatic alcohols and ketones of approximately 15-carbon chain length. It is organised in a compact structure made up of six α-helices stabilised by three disulfide bridges, giving to the protein high stability. The internal binding pocket is large and accommodates relatively high molecular weight compounds (345).

The PBP1 of *Bombyx mori* was identified in the antenna of the silk moth, in the early nineties (262). It is the first Odorant Binding Protein to be characterised by X-ray diffraction spectroscopy (162) and nuclear magnetic resonance (NMR) (266;346). PBP1 has very compact structure due to the presence of three

interlocked disulphide bridges. This structure seems to require conformational changes to allow the entrance and the release of ligands from the binding pocket. However, experimental evidence of the process is not yet available. The main ligands of the PBP1 are the natural component of the pheromone blend: bombykol, bombykal and (10E,12E)-hexadecadien- 1-ol (314).

In Table 16 are summarises the OBPs used as sensing layer for QCMs for vapour phase measurements.

VERTEBRATE OBPs	INVERTEBRATE OBPs
Porcine OBP-C	*L.migratoria* OBP1
Porcine OBP F88W	*P.dominula* OBP1
MUP 10	*B.mori* PBP1

Table 16. Summary of the Odorant Binding Proteins used for functionalising quartz crystal microbalances.

3.7.2.1 Quartz crystal microbalance- Sensing experiments

The described OBPs were linked on the gold surface of QCMs by using self-assembled monolayers of thioctic acid. An ethanolic solution of thioctic acid at the concentration of 100mM was drop-casted on both gold electrode surfaces (248) and left to dry in air. Before grafting the proteins, the carboxylic groups of the TA were activated by using a water solution of EDC: NHS in ratio 1:2. Porcine OBPs-C was instead linked to the gold electrode via the thiol group of the extra cysteine, which was localised at the N-terminus of the protein.

The amount of protein linked on the QCMs was initially estimated by using the Saurbrey equation, as previously described. Table 17 reports the mass of protein immobilised on each QCM, expressed in micrograms.

OBPs	Mass of proteins (µg)
Porcine OBP F88W	2.12
***P.dominula* OBP1**	4.25
***L. migratoria* OBP1**	5.07
MUP	10.48
***B.mori* PBP1**	12.30
β- lactoglobulin	3.99
porcine OBP-C	4.50 (*)

Table 17. Amount of OBPs immobilised on the gold surface of the QCM. (*) porcine OBP-C was immobilised without using SAMs.

An array of six QCMs functionalised with different OBPs was tested simultaneously. The measurements were performed in vapour phase under a constant flow of dried air at the rate of 10 ml min^{-1}. Sensors were stabilised for at least 30 minutes, under airflow, before injecting the analyte. The analyte was introduced in the reaction chamber for about 20 minutes followed by a flow of clean air for 30 minutes, in order to regenerate the baseline frequency.

Figure 65 shows the raw response of a QCMs biosensor functionalised with *Locusta migratoria* OBP1 to different concentration of 2,3-dimethylpyrazine over the time.

The response of the biosensor, detected as reduction of the resonance frequency of the quartz microbalance (in hertz) was proportional to the concentration of the analyte tested.

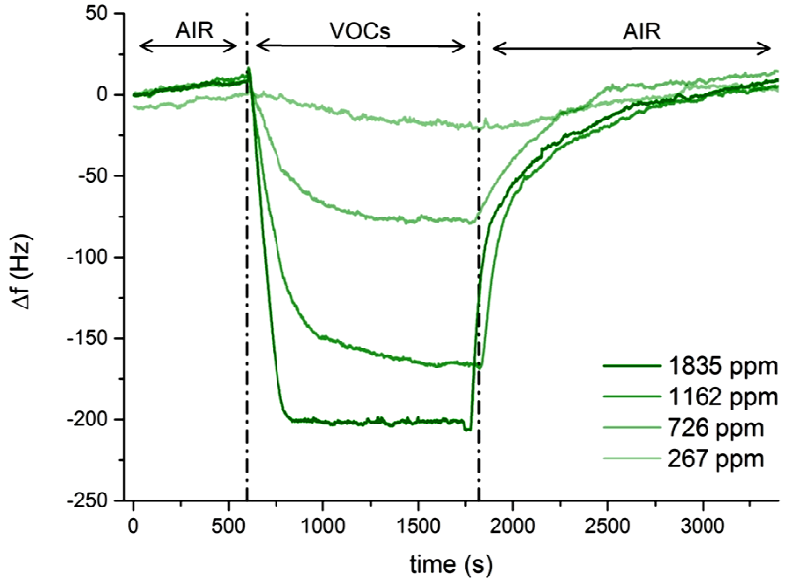

Figure 65. Typical response of a QCM-biosensor to different concentrations of analyte over time.

The developed biosensors were initially tested toward the analyte 2-isobutyl-3-methoxypyrazine. IBMP is considered to be a good ligand for all the OBPs. In 1982, Pelosi et al. identified for the first time OBPs in the olfactory mucous of cow for their ability to bind 2-isobutyl-3-methoxypyrazine, the green bell pepper smell (2). Figure 66 A shows the concentration-response curve of QCMs functionalised with six different OBPs to IBMP. Figure 66 B displays instead the reproducibility of the sensor response to the fixed concentration of 92 ppm of IBMP. Each value is the average of three measurements and the standard deviation is represented as an error bar. The plotted data represent the variation in the resonance frequency of the QCMs recorded in presence of the analyte normalised by the micrograms of protein immobilised on the sensor surface.

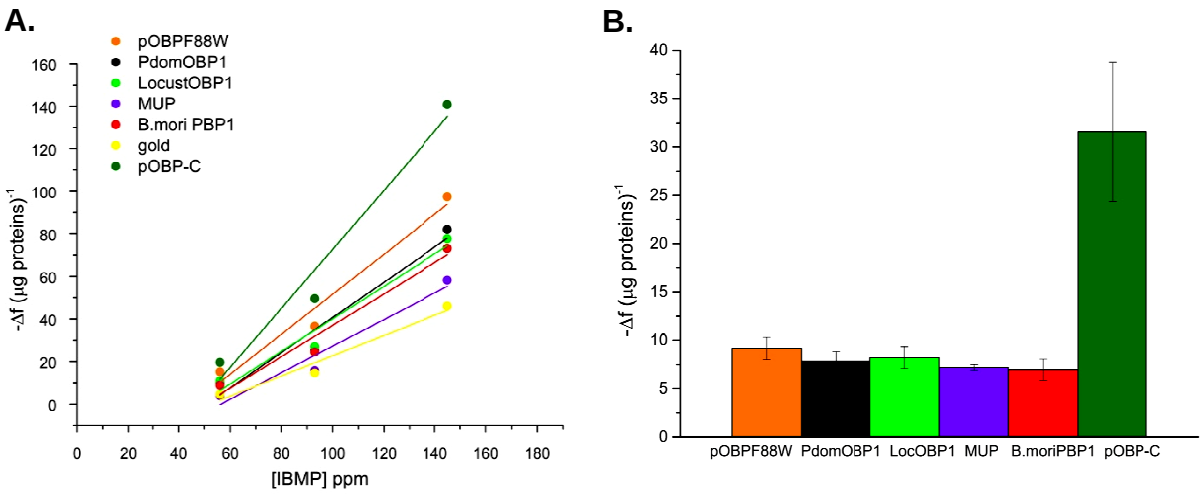

Figure 66. (A) Concentration-response curve of QCM-OBP biosensors to increased concentrations of IBMP. (B) Reproducibility of the sensors to the fixed concentration of 92 ppm of IBMP. n=3.

All the OBP-biosensors showed a good sensitivity to 2-isobutyl-3-methoxypyrazine, detecting easily concentrations below 60 ppm. However, there were no significant differences in the response to IBMP among the tested OBPs, except for the porcine OBP-C. The dissociation constant for the complex porcine OBP-IBMP determined by direct titrations was found to be very low, of the order of micromolar (0.8 µM) (154).

A bare QCM was used as control. The control displayed a response to the analyte as well, caused by nonspecific adsorptions of the pyrazine on to the gold surface via the nitrogen atom of the IBMP (347).

Figure 67 shows the response of the OBPs array to increasing concentrations of 2,3-dimethyl pyrazine. The plotted data were processed as described for the analyte IBMP.

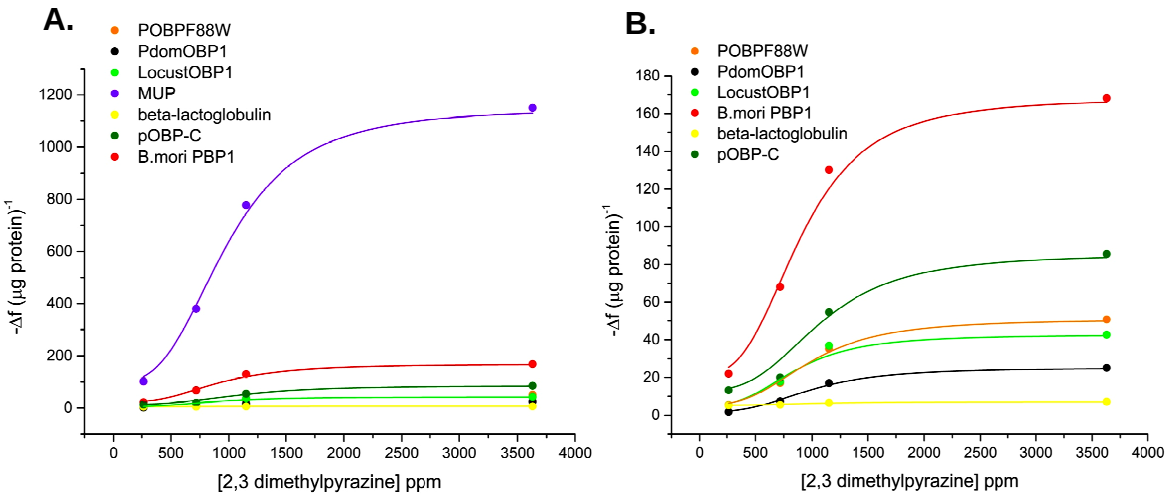

Figure 67. (A) Concentration-response curve of QCM-OBP biosensors to increasing concentrations of 2,3-dimethylpyrazine. (B) Detail of the figure (A).

The MUP-biosensor showed the higher response to 2,3-dimethylpyrazine. The high affinity of the MUP 10 toward this analyte can be explained by the similarity with mouse pheromone 2,5-dimethylpyrazine. 2,3-dimethylpyrazine is an isomer of the pheromone (Figure 68), which is released by female mice when they are kept at high population density (348).

2,5-dimethylpyrazine 2,3-dimethylpyrazine

Figure 68. Graphic representation of the two isomeric forms. On the right, 2,5-dimethylpyrazine, the mouse pheromone and on the left 2,3-dimethylpyrazine. n=3.

As control, a QCMs functionalised with the bovine β-lactoglobulin was used. β-lactoglobulin belongs to the lipocalin family as well. It is present in high concentration to the cow milk and seems to bind hydrophobic molecules, even if its physiological roles have not been clarified yet (349). As displayed in Figure 67 B, the response of the β-lactoglobulin-based biosensor was almost negligible.

Figure 69 shows the reproducibility of the response of OBP-biosensors toward 2,3-dimethylpyrazine at the fixed concentration of 730 ppm.

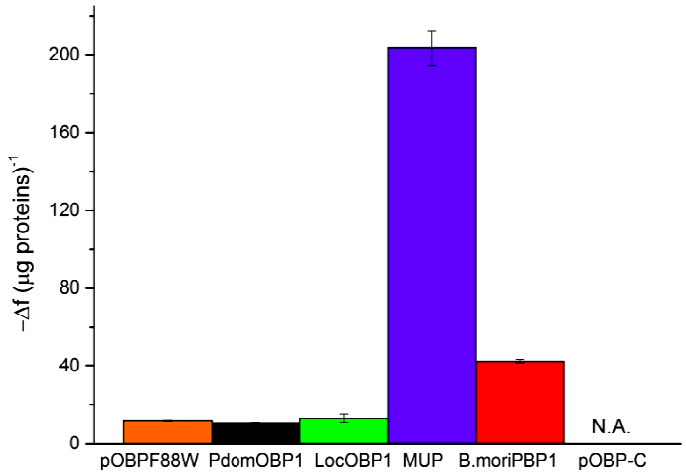

Figure 69. Reproducibility of the response of the QCM-OBP biosensors to 2,3-dimethylpyrazine at the fixed concentration of 730 ppm. n=3.

The responses of the biosensor were stable with a high degree of reproducibility with a low standard deviation.

The concentration-response curve to 2-ethylpyrazine is reported in Figure 70 A.

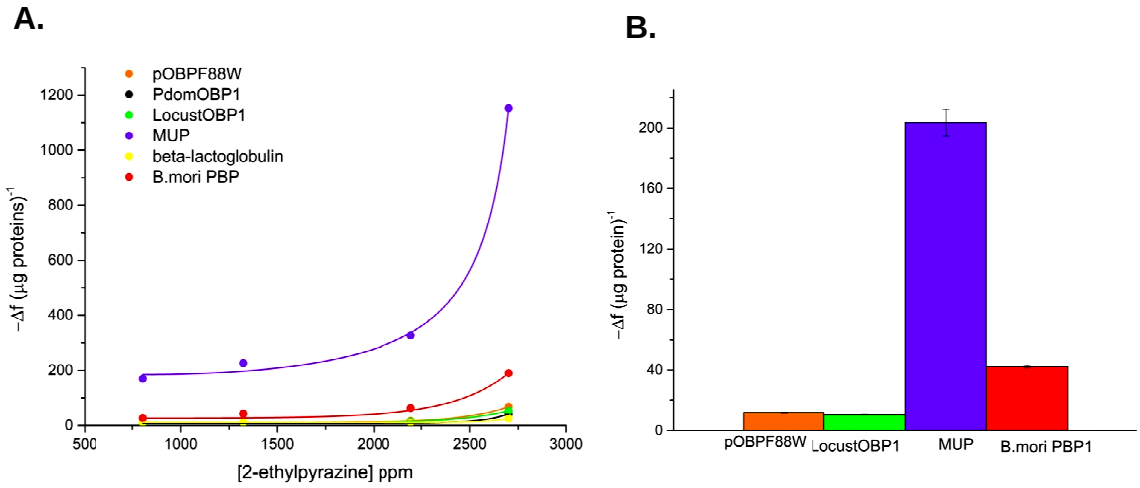

Figure 70. (A) Concentration response curve of the QCM-OBP biosensors to 2-ethylpyrazine. (B) Reproducibility of the sensors to the fixed concentration of 800 ppm of 2-ethylpyrazine. n=3.

The MUP-biosensor showed the higher response among all analytes tested. Also in this case, the chemical structure of the tested analyte was similar to a natural compound present in the urine of mature male mice, 4-(ethyl)phenol (350) .

The concentration-response curves of the biosensors against the ligand 2-ethylpyrazine seemed to follow a Brunauer-Emmett-Teller (BET) model. The BET model explains the physical adsorption of gas molecules on a solid surface, in case of formation of multilayers. Sometimes, when high concentrations of ligand are used, the analyte adsorbs on the substrate, layer upon layer, and the surface does not become saturated easily. A plausible explanation to this behaviour might be caused by the saturation of the binding site of the OBPs. After reaching the saturation point, any further increase in the analyte concentration led to nonspecific adsorption of the ligand, generating multilayers on the sensor surface.

The responses of the biosensor array to geosmin are instead reported in Figure 71.

All the tested OBPs showed a high sensitivity to the analyte with concentration detected of the order of *parts per billion* (ppb). The concentration-response curves followed a BET isotherm also in this case.

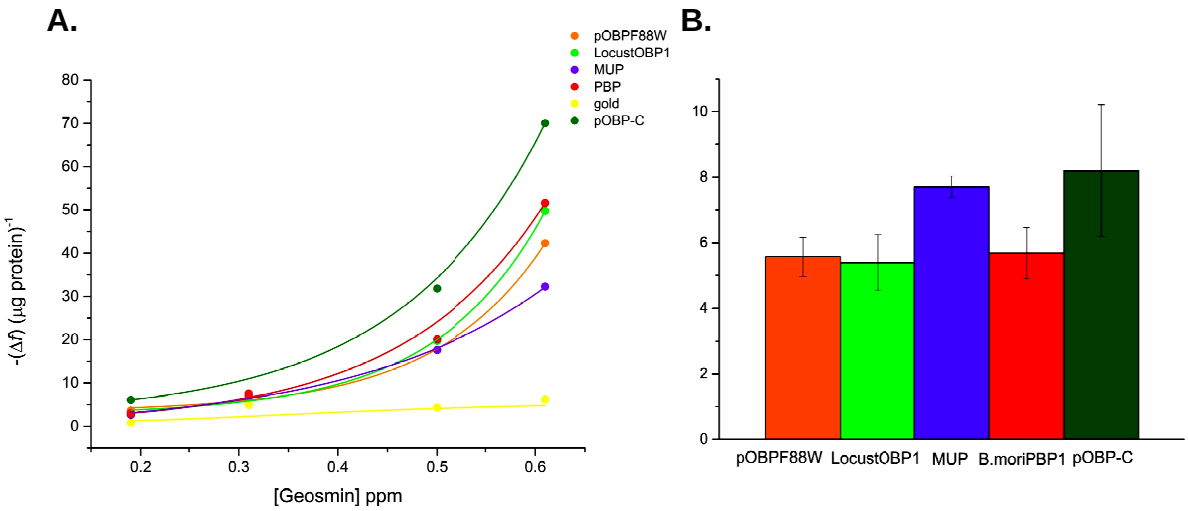

Figure 71. (A) Concentration-response curves of the QCM-OBP biosensors to gesomin. (B) Reproducibility of the OBP sensors determinates at the concentration of 320 ppb of geosmin. n=3.

Increasing the analyte concentration the response of the sensor increased as well, without reaching the saturation. The explanation hypothesized for 2-ethylpyrazine can be adopted also for the response to geosmin.

As control, a bare QCM was used. Geosmin did not show any interaction with the QCMs surface. Figure 71 B shows the reproducibility of the sensor response to the concentration of 320 ppb of geosmin. The reproducibility of the signal was good even at such low concentrations.

These results demonstrated that OBPs can be used as the sensitive layer of mass transducers for the detection of analyte related to the quality of foodstuff in real-time. OBPs can detect low concentrations of analyte of the order of *parts per billion* in vapour phase. The responses of the sensors were fast and reversible, allowing multiuse applications. Moreover, the use of an array of biosensors allows to increase the selectivity of the sensor on the basis of the specific OBPs-ligand affinities. It is remarkable, as the higher responses of the biosensor were toward compounds with a chemical structure similar to the natural ligands. Improving the features of the developed biosensor array can

lead to the realisation of a device able to discriminate and identify single volatiles released by food.

3.8 Capacitive biosensor based on interdigitated electrodes

The sensing principle of a capacitive sensor relies on changes in the dielectric properties, charge distribution and/or conductivity generated by the formation of complexes between bioreceptors and ligands, at the electrode surface. Capacitive biosensors can be constructed by immobilising a thin layer of recognition elements, such as proteins, antibodies, DNA, etc. on the electrode. Moreover, electrodes can be made into an interdigitated pattern in order to provide a larger sensor area. In this case, the capacitance between the interdigitated electrodes can be described by using Equation 5:

$$C = 2n\varepsilon_r\varepsilon_0 \frac{A}{d} \qquad \textbf{Equation 5}$$

where ε_r is the dielectric constant of the medium between the plates, ε_0 is the permittivity of free space, A is the area of the electrodes and d is the distance between the two electrodes, n being the number of electrodes and the factor 2 in this equation represent each electrode forming the two capacitors.

In this work, interdigitated electrodes realised on flexible substrates were used as transducers, for developing a biosensor based on the porcine Odorant Binding Proteins pOBPF88W. pOBPF88W were linked on the gold electrodes by using self-assembled monolayers of 16-mercaptohexadecanoic acid.

The biosensor was tested by a means of electrical impedance spectroscopy (EIS) in air, both in absence and in presence of different concentrations of odorant vapours. EIS is a powerful method for analysing the electrical impedance of a system, and in particularly to detect any binding events that happen on the transducer surface (240). In fact, EIS combines the analysis of the resistive and capacitive properties of the materials in response to the small amplitude sinusoidal excitation signal (211). Figure 72 shows the Nyquist plot of an interdigitated electrode functionalised with porcine OBPs. In black is reported the EIS spectrum of the sensor under constant flow of air (relative humidity

25%), while in red is displayed the response of the sensor to the vapour of S-(+) carvone (relative humidity 25%) at the concentration of 28.5 ppm. S-(+) carvone was chosen as target analyte in these preliminary experiments, since the porcine OBPs showed a high affinity toward it, as previously assayed. The impedance was scanned between 10^5 and 1 hertz, with a polarization potential of 1V and amplitude of 20 mV. The measurements were performed under constant flow of humid air at the rate of 180 ml min^{-1}. The analyte was injected in the flow cell, where the biosensor was contained, for a time of 10 minutes. After that, fresh air was introduced for 10 minutes in the flow cell to remove any residues of the VOC. The impedance was recorded at the end of each incubation time.

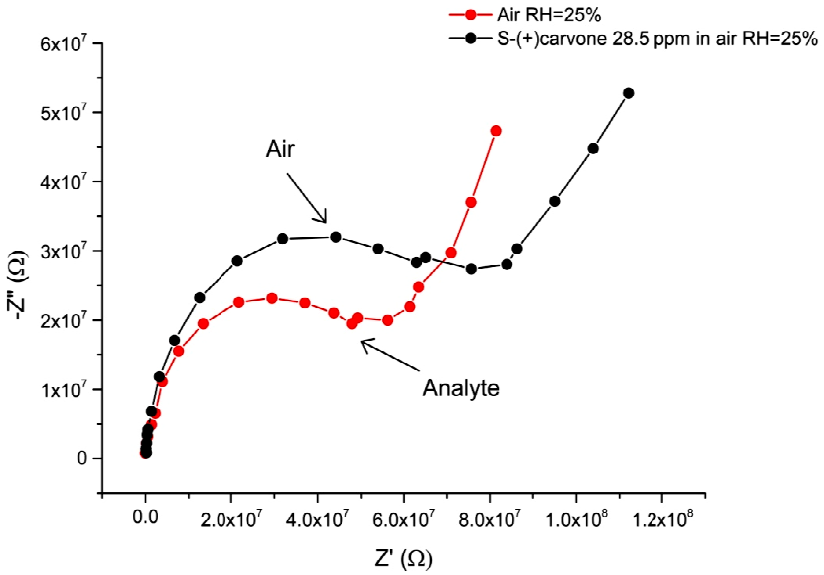

Figure 72. Nyquist plots of pOBPF88W- IDE biosensor under exposure at humid air at RH=25% (black line) and under 28.5 ppm of S-(+) carvone in humid air at RH=25% (red line).

The impedimetric semicircle obtained under exposure to S-(+) carvone was smaller than the curve in humid air.

This effect can be attributed to occur of binding events between porcine OBPs and the analyte, that may cause conformational changes and/or molecular rearrangement of the proteins (240).

The developed biosensor showed a good degree of reversibility. In Figure 73, Nyquist plots of two consecutive measurements carried out at a fixed analyte concentration are displayed. The EIS spectrum of the chemical sensor in presence of the analyte is reported in red. As described before, a reduction in the impedimetric curve was observed when the EIS was recorded in presence of the analyte. The impedimetric curve increased again under cleaned air. In the second analyte exposure, the sensor showed repeatable behaviour, with only slight differences in the response when compared with the first measurement cycle.

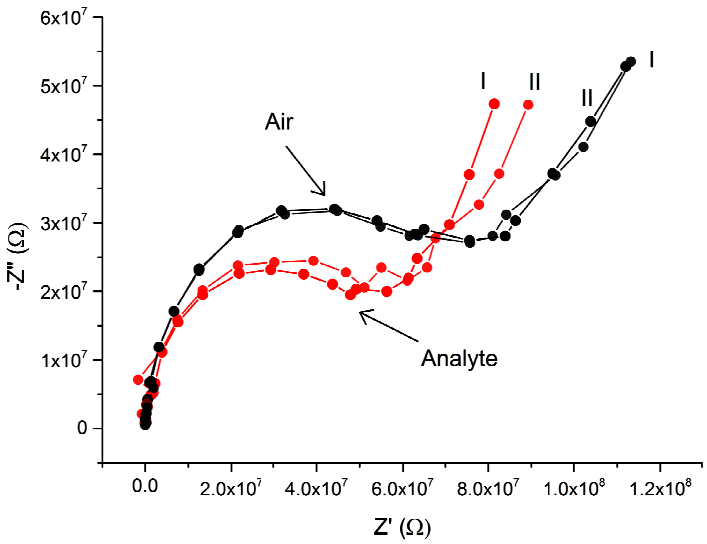

Figure 73. Reversibility. Nyquist plots of pOBPF88W- IDE biosensor of a two cycles of exposure to the volatile. In red under exposure to 28.5 ppm of S-(+) carvone vapour in humid air at RH=25% (red line) and in black under humid air at RH=25% (black line).

The concentration response curve of the pOBPF88W biosensor upon exposure to different concentrations of S-(+) carvone is displayed in Figure 74.
The analyte was tested in a range of concentrations between 14 and 120 ppm.

On the y-axis of the plot was reported the relative capacitance variation recorded at the frequency of 100 Hz. The capacitance variation was calculated by using the Equation 11.

$$\frac{C-C_0}{C_0} \times 100\ (\%)$$ **Equation 11**

Where C_0 is the initial value of capacitance of the biosensors and C is the capacitance measured at different concentrations of analyte. On the x-axis was instead reported the concentration of the S-(+) carvone expressed as *parts per million* (ppm). Each point of the plot is the average value of three independent measurements. The standard deviations are shown as error bars.

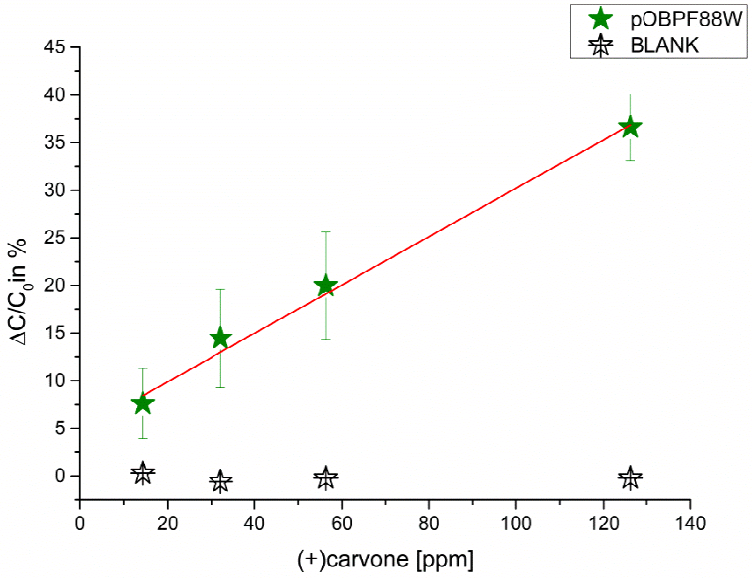

Figure 74. Concentration response curve for pOBPF88W based biosensor upon exposure to different concentrations of S-(+) carvone (filled stars). The empty stars are the control, an uncoated gold IDE. Error bars indicate the reproducibility. n=3.

Higher concentrations of analyte led to a higher response of the sensor, with a linear relationship. The concentration calibration curve was fitted with a straight line. The response of the control, an uncoated IDE, was negligible. The biosensor did not reach a saturation point, a sign of a nonspecific binding interaction. A hypothetical explanation of such behaviour can be due to the high concentrations of volatile used, hiding the saturation point.

Figure 75 shows the reproducibility of the signal of the pOBPF88W-IDE biosensor. In the plot was reported the response of the sensor to random

concentrations of analyte. At the concentration of 28.5 ppm the variation in capacitance of the sensor was almost 28%. When the concentration was raised to 31.5 ppm the response of the sensor was around 66%. When the analyte concentration was decreased again to 28.5 ppm the variation in capacitance measured was 25%, which was only 3% less compared to the former measurement.

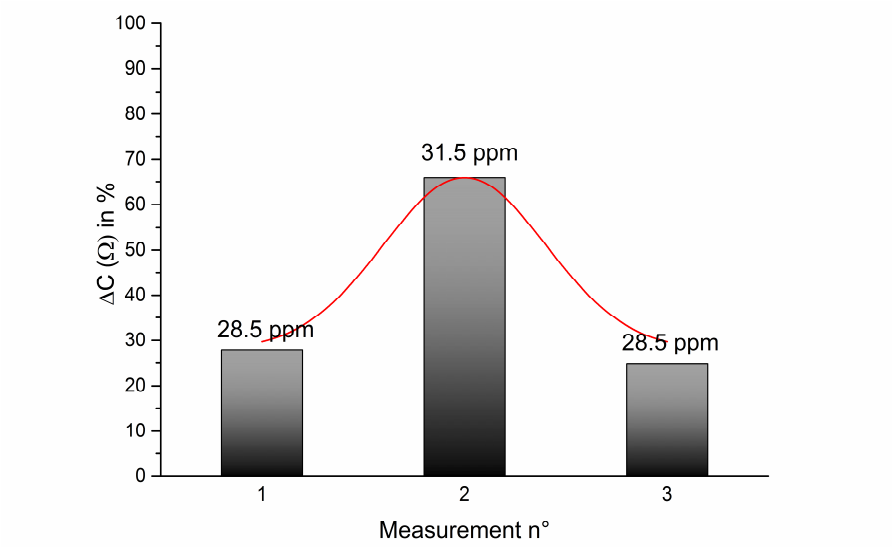

Figure 75. Reproducibility of the pOBPF88W-IDE biosensor. The sensor was tested at different concentrations of S-(+) carvone in humid air (RH 25%).

In each measurement of Figure 75, the analyte was in contact with the sensor for a period of 10 minutes, followed by a cleaning step with air.

We demonstrated that it was possible to use OBPs as the sensitive layer of ID electrodes in vapour phase. The interaction between proteins and ligands can be detected with electrochemical transducers in both liquid and vapour phase.

The biosensor response was reversible and repeatable, with a detection limit of 14 ppm. Further studies are required in order to understand better all the mechanisms that led to the signal generation. These results can be considered as a preliminary step for investigating the possibility of using OBPs as sensing layers of electrochemical sensors for vapour phase applications.

3.9 Conclusions

Odorant Binding Proteins belonging to different species of mammals and insects were successfully expressed in bacterial system, with good yields. The recombinant proteins were selected on the basis of their natural ligand affinity, by using fluorescence binding assays, and used for developing different types of biosensors.

The proteins were immobilised on the gold surface of chosen transducers by means of self-assembled monolayers. The covalent immobilisation did not affect the structure and the activity of the protein, producing a compact insulator layer on the electrode surface, as demonstrated in electrochemical experiments.

The developed OBP-based biosensors showed a rapid and reversible response towards the tested analytes, in both vapour and liquid phases. The biosensors were label-free, hence they can detect the interaction between proteins and ligands directly, in absence of auxiliary species.

Impedimetric OBP-biosensors developed on disposable SPEs discriminated between organic compounds with sensitivity of the order of *nanomolar* concentrations. The low voltage supplied to the device and the use of disposable electrodes, allow the realisation of portable devices for in real-time monitoring.

IDEs were also employed for developing impedimetric biosensors. The devices were tested in vapour phase against the ligand S-(+) carvone. OBPs preserved their binding activity in air and the interaction with the analyte was directly detected as capacitance variations.

The use of an array of QCMs allowed instead the simultaneous testing of up to six different OBPs, in vapour phase. The results showed the higher response of the sensor was against compounds with chemical structure similar to natural ligands, as in the case of MUPs and 2,3-dimethylpyrazine. The experiments performed with two Odorant Binding Proteins of the silkmoth *Bombyx mori* also

demonstrated the high sensitivity of the system. The OBP-biosensor can detect few *parts per billion* of both pheromones, displaying sensing capabilities comparable to traditional analytical equipment i.e. GC-MS.

Concluding, we successfully combined biological components of the olfactory system together with simple signal transducers. The developed OBP-biosensors showed a high sensitivity and selectivity, together with other important features such as label-free measurements, reusability and real-time detection. These characteristics are considered essential for developing merchandisable devices that can find applications in several fields, including health care, industrial process monitoring and environmental control.

4 Conclusions and future work

The research findings achieved during the PhD project supported the possibility of utilising Odorant Binding Proteins for the development of biosensors for both liquid and vapour applications.

The ability of the OBPs to bind organic compounds with different affinities and in a reversible way has allowed development of sensitive and reusable devices. Moreover, the possibility of synthesised OBPs in bacterial systems and in high quantity reduced the biosensor costs.

Three OBP-based biosensors that rely on different transduction mechanisms were developed. (I) Quartz crystal microbalances, (II) screen-printed electrodes and (III) interdigitated electrodes were used for detecting the interaction between proteins and ligands. The transducers converted the binding events directly into electric signals, with a label-free approach.

Recombinant Pheromone Binding Proteins (PBP1) and General Odorant Binding Proteins (GOBP2) of *B.mori* were used as bio-recognition elements of quartz crystal microbalances. The developed biosensors were tested against the vapour of the two main pheromones of the silkmoth, bombykol and bombykal. In air, the two proteins showed different affinity against the ligands. PBP1-based biosensors displayed a higher affinity against both bombykol and bombykal, whereas the responses of GOBP2 were less defined. When both proteins were tested in fluorescence assays, towards the same ligands, not substantial difference was found, expect for a slightly preference of the GOBP2 towards the bombykal. PBP1 and GOBP2 bound both bombykol and bombykal with an extraordinary high affinity, with dissociation constants of the order of 10^{-8}M. The high affinity of the proteins was preserved also in the biosensor configuration, considering the low vapour pressure of the two pheromones. The results obtained with the QCM-based biosensors did not agree with data collected from fluorescence experiments. However, these findings can be supported by two important physiological features of *B.mori*. In fact, both pheromones, bombykol and bombykal, are released by the females of *B.mori*

and they act on the mate behaviour of males. Moreover, the expression pattern of PBP1 and GOBP2 is different between males and females of *B.mori.* GOBP2 is present in the female antennae, while PBP1 is mainly expressed in the sensilla of males that respond to the female pheromones. The results obtained from the PBP1 and GOBP2 biosensors seem to comply with the physiological role that these two proteins can have in semiochemical communication, paving the way to a new technology for studying the affinity of binding.

An impedimetric biosensor was also developed by using porcine OBPs as sensitive substrates. The developed sensor was tested in liquid phase against several organic compounds. The ligands were selected on the basis of the binding affinity determined in fluorescence binding assays. They included 2-phenylethanol and the two enantiomeric forms of carvone. Porcine OBPF88W showed a good affinity of binding against both carvones, with a K_D of 0.500 µM for the S-(+) carvone and 1.219 µM for the R-(-) form. The 2-phenylethanol was instead used as a negative control, since the porcine OBPs did not bind it. The developed impedimetric biosensor detected the direct interaction between protein and ligand as variation of the capacitance value, without the use of auxiliary probes. Capacitance changes can be induced by several factors such as (a) modification of the protein conformation due to the binding of the ligand, (b) replacement of aqueous solution with less conductive compounds from inside the binding pocket of the protein, and/or (c) increase of the distance between the electrical-double layer and the electrode surface in presence of the analyte. The results obtained from the porcine OBP-biosensor reflected the affinity of binding of the protein, with a detection limit in the *nanomolar* range. A large variation of capacitance was observed when both carvones were tested, while in presence of the ligand 2-phenylethanol the sensor showed less substantial response. The calculated K_D for the S-(+) and R-(-) carvone were 0.123 µM and 0.084 µM, respectively (not statistical significant difference). These values differed from the K_D estimated in the fluorescence experiments. However, it is import to consider a fundamental difference in these two methods. The biosensor detected the direct interaction between the protein and the ligand. In the fluorescence measurements instead, the interaction was visualised as reduction in the fluorescence intensity emits by a probe, in

presence of the target analyte. This might explain the lower K_D values found for the porcine OBP-biosensor compared to the traditional competitive fluorescence binding assays, being the sensor more sensitive and able to detect lower concentrations of analyte. However, further investigations are considered necessary to better understand the mechanisms at the base of the signal generation.

The impedimetric response of the porcine OBP-biosensor was also investigated in vapour phase. Interdigitated electrodes (IDEs), developed on flexible substrates, were used as biosensor transducers. This preliminary study was carried out for demonstrating the interaction between OBPs and ligands can be detected also in vapour phase, in a label-free mode. When OBPs bound the ligand, variations in the capacitive value of the sensor were observed. These changes were proportional to the analyte concentration and they were probably caused by rearrangement of the protein conformation to accommodate the ligand. The response of the sensor was fast, reversible and with a detection limit of 14 ppm.

Concluding, we demonstrated the possibility to employ OBPs as bio-recognition elements of different types of transducers. OBPs kept their binding activity in both liquid and vapour phases and the use of transducers increased the sensitivity of the system. The developed biosensors can detect the interaction between protein and ligand directly, without the use of secondary species that could interfere with the sensor signal. The responses of the sensors were fast and reversible, allowing to the same device to be reused several times.

The next steps in this research can be addressed to the improvement of the OBP selectivity and to the development of a reproducible and oriented immobilisation method. In fact, the affinity of OBPs against target ligand can be modified by replacing few amino acid residues in the binding pocket of the protein, in order to suite the sensor requirements. The use of orientated immobilisation techniques, i.e. histidine tags, can instead contribute to improve the performance of the sensor, reducing any unspecific interactions that can affect the protein activity.

This work is an initial contribution to the research performed on the use of OBPs as sensing layers of biosensors. At present, the findings in this area are still sparse. However, the obtained results support and prove possible future applications of OBP-biosensors in several fields ranging from food industry, agriculture, environment and national safety. The realisation of low-cost and portable systems can pave the way to a new generation of devices able to replace expensive analytical equipment.

Publications

Pelosi, P., Mastrogiacomo, R., Iovinella, I., Tuccori, E., & Persaud, K. C. (2014). Structure and biotechnological applications of Odorant Binding Proteins. *Applied microbiology and biotechnology*, *98*(1), 61-70.

Persaud, K. C., & Tuccori, E. (2014). Biosensors Based on Odorant Binding Proteins. In *Bioelectronic Nose* (pp. 171-190).Ed. T-H Park Springer Netherlands.

Manai, R., Scorsone. E., Rousseau, L., Ghassemi, F., Possas Abreu, M., Lissorgues, G., Tremillon, N., Ginisty, H., Arnault, J-C., Tuccori, E., Bernabei, M., Cali, K., Persaud, K.C., Bergonzo, P. (2014) Grafting Odorant Binding Proteins on diamond bio-MEMS. Biosensors and Bioelectronics15;60(0):311-317.

Conference publications

Tuccori, E. & Persaud K.C. A piezoelectric biosensor based on Odorant Binding Proteins. *The European chemoreception organisation* (ECRO). Manchester, UK; Sep. 2011.

Tuccori, E. & Persaud K.C. Odorant binding proteins as active layer of biosensors for detecting volatile organic compounds (VOCs) in vapour phase. *The International Symposium on Olfaction and Taste* (ISOT), Stockholm, Sweden; Jun. 2012.

Tuccori, E. & Persaud K.C. Self-assembled odorant binding proteins as biosensors for the detection of odorants and pheromones. The Nanosensor Technologies for Monitoring- materials and methods. *The Royal Society of Chemistry (*RSC), London, UK; Nov. 2012

Tuccori, E., Danash E. and Persaud K.C. The study of Odorant binding proteins as sensitive layer of label-free biosensors with vapor and liquid applications. *The European chemoreception organisation* (ECRO). Leuven, Belgium; Aug. 2013.

Tuccori, E., Danash, E., Gaspar, C., Persaud K.C. Odorant binding proteins as active layer of biosensors for detection of organic compounds in vapor and liquid phase*. The 15th International Symposium on olfaction and Electronic Nose* (ISOEN). Daegu, South Korea; Jul. 2013.

5 Reference List

(1) Bond M, Meacham T, Bhunnoo R, Benton TG. Food waste within global food systems. www.foodsecurity.ac.uk: A Global Food Security report; 2013.

(2) Pelosi P, Baldaccini NE, Pisanelli AM. Identification of A Specific Olfactory Receptor for 2-Isobutyl-3-Methoxypyrazine. Biochem J 1982;201(1):245-8.

(3) Hamilton-Kemp T, Newman M, Collins R, Elgaali H, Yu K, Archbold D. Production of the Long-Chain Alcohols Octanol, Decanol, and Dodecanol by Escherichia coli. Current Microbiology 2005 Aug 31;51(2):82-6.

(4) Mattheis JP, Roberts RG. Identification of geosmin as a volatile metabolite of Penicillium expansum. Applied and Environmental Microbiology 1992;58(9):3170-2.

(5) Gerber NN. Geosmin An Earthy-Smelling Substance Isolated from Actinomycetes. Biotechnology and Bioengineering 1967;9(3):321-7.

(6) Altintas Z, Tothill I. Biomarkers and biosensors for the early diagnosis of lung cancer. Sensors and Actuators B: Chemical 2013 Nov;188(0):988-98.

(7) Bansi DM, Turner AP. Adavence in biosensors. 1 ed. Amsterdam: 2003.

(8) Evtugyn G. Biosensor Signal Transducers. Biosensors: Essentials. 84 ed. Springer Berlin Heidelberg; 2014. p. 99-205.

(9) Fracchiolla NS, Artuso S, Cortelezzi A. Biosensors in Clinical Practice: Focus on Oncohematology. Sensors 2013;13(5):6423-47.

(10) Sadana A, Sadana N. Chapter 1 - Introduction. In: Sadana A, Sadana N, editors. Handbook of Biosensors and Biosensor Kinetics.Amsterdam: Elsevier; 2011. p. 1-14.

(11) Global Industry Analysts, Inc.
www.prweb com/releases/chemical/sensors, 2010 February

(12) Clark LC. Monitor and Control of Blood and Tissue Oxygen Tensions. Transactions American Society for Artificial Internal Organs 1956;2:41-8.

(13) Thakur MS, Ragavan KV. Biosensors in food processing. J Food Sci Technol 2013;50(4):625-41.

(14) Guilbault GG, Lubrano GJ. An enzyme electrode for the amperometric determination of glucose. Analytica Chimica Acta 1973 May;64(3):439-55.

(15) Wang J. Electrochemical Glucose Biosensors. Chemical Reviews 2007 Dec 23;108(2):814-25.

(16) Wang J. Glucose Biosensors: 40 Years of Advances and Challenges. Electroanalysis 2001 Aug 1;13(12):983-8.

(17) Janata J. Immunoelectrode. Journal of the American Chemical Society 1975 May 1;97(10):2914-6.

(18) Luppa PB, Sokoll LJ, Chan DW. Immunosensors-principles and applications to clinical chemistry. Clinica Chimica Acta 2001 Dec;314(1-2):1-26.

(19) Ricci F, Adornetto G, Palleschi G. A review of experimental aspects of electrochemical immunosensors. Electrochimica Acta 2012 Dec 1;84(0):74-83.

(20) Ricci F, Volpe G, Micheli L, Palleschi G. A review on novel developments and applications of immunosensors in food analysis. Analytica Chimica Acta 2007;605(2):111-29.

(21) Park M, Cella LN, Chen W, Myung NV, Mulchandani A. Carbon nanotubes-based chemiresistive immunosensor for small molecules: Detection of nitroaromatic explosives. Biosensors & Bioelectronics 2010;26(4):1297-301.

(22) Cass AEG, Davis G, Francis GD, Hill HA, Aston WJ, Higgins IJ, et al. Ferrocene-mediated enzyme electrode for amperometric determination of glucose. Anal Chem 1984 Apr 1;56(4):667-71.

(23) ZHANG W, LI G. Third-Generation Biosensors Based on the Direct Electron Transfer of Proteins. Analytical Sciences 2004;20(4):603-9.

(24) Yoo EH, Lee SY. Glucose Biosensors: An Overview of Use in Clinical Practice. Sensors 2010;10(5):4558-76.

(25) Turner APF. Biosensors: sense and sensibility. Chem Soc Rev 2013;42(8):3184-96.

(26) Liedberg B, Nylander C, Lunström I. Surface plasmon resonance for gas detection and biosensing. Sensors and Actuators 1983;4(0):299-304.

(27) Freire RS, Pessoa CA, Mello LD, Kubota LT. Direct electron transfer: an approach for electrochemical biosensors with higher selectivity and sensitivity. Journal of the Brazilian Chemical Society 2003;14:230-43.

(28) Tarasevich MR, Yaropolov AI, Bogdanovskaya VA, Varfolomeev SD. 293 - Electrocatalysis of a cathodic oxygen reduction by laccase. Bioelectrochemistry and Bioenergetics 1979 Sep;6(3):393-403.

(29) Putzbach W, Ronkainen NJ. Immobilization Techniques in the Fabrication of Nanomaterial-Based Electrochemical Biosensors: A Review. Sensors 2013;13(4):4811-40.

(30) Ohara TJ, Rajagopalan R, Heller A. Glucose electrodes based on cross-linked bis(2,2'-bipyridine)chloroosmium(+/2+) complexed poly(1-vinylimidazole) films. Anal Chem 1993 Dec 1;65(23):3512-7.

(31) Soloducho J, Cabaj J. Electrochemical Nanosized Biosensors: Perspectives and Future of Biocatalysts. Journal of Analytical & Bioanalytical Techniques 2013 Apr;S7(005).

(32) Rasooly A. ANALYSIS | Biosensors. In: Editor-in-Chief:- Hubert Roginski, editor. Encyclopedia of Dairy Sciences.Oxford: Elsevier; 2002. p. 85-93.

(33) Chambers JP, Arulanandam BP, Matta LL, Weis A, Valdes JJ. Biosensor recognition elements. Curr Issues Mol Biol 2008;10(1-2):1-12.

(34) Monošík R, Stredanský M, Šturdík E. Biosensors - classification, characterization and new trends. Acta Chimica Slovaca 2012 May;5(1):109-20.

(35) Evtugyn G. Biochemical Components Used in Biosensor Assemblies. Biosensors: Essentials. 84 ed. Springer Berlin Heidelberg; 2014. p. 21-97.

(36) Xu X, Ying Y. Microbial Biosensors for Environmental Monitoring and Food Analysis. Food Reviews International 2011 May 23;27(3):300-29.

(37) Oungpipat W, Alexander PW, Southwell-Keely P. A reagentless amperometric biosensor for hydrogen peroxide determination based on asparagus tissue and ferrocene mediation. Analytica Chimica Acta 1995 Jun 20;309(1-3):35-45.

(38) Ozcan HM, Sagiroglu A. Fresh broad (Vicia faba) tissue homogenate-based biosensor for determination of phenolic compounds. Artificial Cells, Nanomedicine, and Biotechnology 2013 Jan 30;1-6.

(39) Wu FQ, Huang YM, Huang CZ. Chemiluminescence biosensor system for lactic acid using natural animal tissue as recognition element. Biosensors & Bioelectronics 2005;21(3):518-22.

(40) Vo-Dinh T. Biosensors and Biochips BioMEMS and Biomedical Nanotechnology. In: Ferrari M, Bashir R, Wereley S, editors. Springer US; 2007. p. 1-20.

(41) Conroy PJ, Hearty S, Leonard P, O'Kennedy RJ. Antibody production, design and use for biosensor-based applications. Seminars in Cell & Developmental Biology 2009 Feb;20(1):10-26.

(42) Mosiello L, Laconi C, Del Gallo M, Ercole C, Lepidi A. Development of a monoclonal antibody based potentiometric biosensor for terbuthylazine detection. Sensors and Actuators B: Chemical 2003 Oct 15;95(1-3):315-20.

(43) Kim N, Kim DK, Kim WY. Sulfamethazine detection with direct-binding optical waveguide lightmode spectroscopy-based immunosensor. Food Chemistry 2008 May 15;108(2):768-73.

(44) Tully E, Higson SP, O'Kennedy R. The development of a 'labeless' immunosensor for the detection of Listeria monocytogenes cell surface protein, Internalin B. Biosensors and Bioelectronics 2008 Jan 18;23(6):906-12.

(45) Halámek J, Makower A, Knösche K, Skládal P, Scheller FW. Piezoelectric affinity sensors for cocaine and cholinesterase inhibitors. Talanta 2005 Jan 30;65(2):337-42.

(46) Vo-Dinh T, Cullum B. Biosensors and biochips: advances in biological and medical diagnostics. Fresenius Journal of Analytical Chemistry 2000;366(6-7):540-51.

(47) Uygun ZO, Sezgintürk MK. A novel, ultra sensible biosensor built by layer-by-layer covalent attachment of a receptor for diagnosis of tumor growth. Analytica Chimica Acta 2011 Nov 14;706(2):343-8.

(48) Kim BK, Li J, Im JE, Ahn KS, Park TS, Cho SI, et al. Impedometric estrogen biosensor based on estrogen receptor alpha-immobilized gold electrode. Journal of Electroanalytical Chemistry 2012 Apr 15;671(0):106-11.

(49) Wu C, Du L, Wang D, Wang L, Zhao L, Wang P. A novel surface acoustic wave-based biosensor for highly sensitive functional assays of olfactory receptors. Biochemical and Biophysical Research Communications 2011;407(1):18-22.

(50) Tothill I. Biosensors and nanomaterials and their application for mycotoxin determination. World Mycotoxin Journal 2011;4(4):361-74.

(51) Tothill I. Peptides as Molecular Receptors. In: Zourob M, editor. Recognition Receptors in Biosensors. Springer New York; 2010. p. 249-74.

(52) Mascini M, Macagnano A, Scortichini G, Del Carlo M, Diletti G, D'Amico A, et al. Biomimetic sensors for dioxins detection in food samples. Sensors and Actuators B-Chemical 2005;111:376-84.

(53) Pournaghi-Azar MH, Ahour F, Hejazi MS. Direct detection and discrimination of double-stranded oligonucleotide corresponding to hepatitis C virus genotype 3a using an electrochemical DNA biosensor

based on peptide nucleic acid and double-stranded DNA hybridization. Anal Bioanal Chem 2010;397(8):3581-7.

(54) Mohan R, Mach KE, Bercovici M, Pan Y, Dhulipala L, Wong PK, et al. Clinical Validation of Integrated Nucleic Acid and Protein Detection on an Electrochemical Biosensor Array for Urinary Tract Infection Diagnosis. Plos One 2011;6(10).

(55) Glynn B, O'Connor L. Nucleic Acid Diagnostic Biosensors. In: Zourob M, editor. Recognition Receptors in Biosensors. Springer New York; 2010. p. 343-63.

(56) Grieshaber D, MacKenzie R, Voeroes J, Reimhult E. Electrochemical biosensors - Sensor principles and architectures. Sensors 2008;8(3):1400-58.

(57) Pohanka M, Skladai P. Electrochemical biosensors - principles and applications. Journal of Applied Biomedicine 2008;6(2):57-64.

(58) Mehrvar M, Abdi M. Recent developments, characteristics, and potential applications of electrochemical biosensors. Analytical Sciences 2004;20(8):1113-26.

(59) Soledad Belluzo M, Elida Ribone M, Marina Lagier C. Assembling amperometric biosensors for clinical diagnostics. Sensors 2008;8(3):1366-99.

(60) Viswanathan S, Radecka H, Radecki J. Electrochemical biosensors for food analysis. Monatshefte fur Chemie 2009;140(8):891-9.

(61) Trojanowicz M. Determination of Pesticides Using Electrochemical Enzymatic Biosensors. Electroanalysis 2002 Nov 1;14(19-20):1311-28.

(62) Yemini M, Levi Y, Yagil E, Rishpon J. Specific electrochemical phage sensing for Bacillus cereus and Mycobacterium smegmatis. Bioelectrochemistry 2007 Jan;70(1):180-4.

(63) Pohanka M, Skládal P. Serological Diagnosis of Tularemia in Mice Using the Amperometric Immunosensor. Electroanalysis 2007 Dec 1;19(24):2507-12.

(64) Sharma H, Mutharasan R. Review of biosensors for foodborne pathogens and toxins. Sensors and Actuators B: Chemical 2013 Jul 5;183(0):535-49.

(65) Lee CS, Kim SK, Kim M. Ion-Sensitive Field-Effect Transistor for Biological Sensing. Sensors 2009;9(9):7111-31.

(66) Wang Y, Ye Z, Ying Y. New Trends in Impedimetric Biosensors for the Detection of Foodborne Pathogenic Bacteria. Sensors 2012;12(3):3449-71.

(67) Davis F, Hughes MA, Cossins AR, Higson SaPJ. Single Gene Differentiation by DNA-Modified Carbon Electrodes Using an AC Impedimetric Approach. Anal Chem 2007 Jan 3;79(3):1153-7.

(68) Ouerghi O, Touhami A, Jaffrezic-Renault N, Martelet C, Ouada HB, Cosnier S. Impedimetric immunosensor using avidin-biotin for antibody immobilization. Bioelectrochemistry 2002 May 15;56(1-2):131-3.

(69) Vidal JC, Bonel L, Ezquerra A, Hernández S, Bertolín JR, Cubel C, et al. Electrochemical affinity biosensors for detection of mycotoxins: A review. Biosensors and Bioelectronics 2013 Nov 15;49(0):146-58.

(70) Choi MMF. Progress in Enzyme-Based Biosensors Using Optical Transducers. Microchim Acta 2004;148(3-4):107-32.

(71) Gauglitz G. Direct optical detection in bioanalysis: an update. Anal Bioanal Chem 2010;398(6):2363-72.

(72) Ralf W.Glaser. Surface Plasmo Resonanace Biosensor. In: Yang VC, Ngo TT, editors. Biosensors and their applications. 2000. p. 195-214.

(73) Ralph PC, Josè IRDC. Biosensors. Encyclopedia of Agricultural, Food, and Biological Engineering. Taylor & Francis; 2007. p. 119-23.

(74) Hasanzadeh M, Shadjou N, Soleymani J, Omidinia E, de la Guardia M. Optical immunosensing of effective cardiac biomarkers on acute myocardial infarction. TrAC Trends in Analytical Chemistry 2013 Nov;51(0):158-68.

(75) Arora P, Sindhu A, Dilbaghi N, Chaudhury A. Biosensors as innovative tools for the detection of food borne pathogens. Biosensors and Bioelectronics 2011 Oct 15;28(1):1-12.

(76) Long F, Zhu A, Shi H. Recent Advances in Optical Biosensors for Environmental Monitoring and Early Warning. Sensors 2013;13(10):13928-48.

(77) Nirschl M, Reuter F, Vörös J. Review of Transducer Principles for Label-Free Biomolecular Interaction Analysis. Biosensors 2011;1(3):70-92.

(78) Bizet K, Gabrielli C, Perrot H. Biosensors based on piezolectric transducers. Analusis 1999 Sep;27(7):609-16.

(79) Rocha-Gaso MI, March-Iborra C, Montoya-Baides A, rnau-Vives A. Surface Generated Acoustic Wave Biosensors for the Detection of Pathogens: A Review. Sensors 2009;9(7):5740-69.

(80) Gruhl FJ, Laenge K. Surface Acoustic Wave (SAW) Biosensor for Rapid and Label-Free Detection of Penicillin G in Milk. Food Analytical Methods 2014;7(2):430-7.

(81) Chen D, Wang J, Xu Y, Li D, Zhang L, Li Z. Highly sensitive detection of organophosphorus pesticides by acetylcholinesterase-coated thin film bulk acoustic resonator mass-loading sensor. Biosensors & Bioelectronics 2013;41:163-7.

(82) Wu C, Du L, Wang D, Zhao L, Wang P. A biomimetic olfactory-based biosensor with high efficiency immobilization of molecular detectors. Biosensors & Bioelectronics 2012;31(1):44-8.

(83) Onen O, Sisman A, Gallant ND, Kruk P, Guldiken R. A Urinary Bcl-2 Surface Acoustic Wave Biosensor for Early Ovarian Cancer Detection. Sensors 2012;12(6):7423-37.

(84) Wu TZ, Su CC, Chen LK, Yang HH, Tai DF, Peng KC. Piezoelectric immunochip for the detection of dengue fever in viremia phase. Biosensors and Bioelectronics 2005 Nov 15;21(5):689-95.

(85) Papadakis G, Gizeli E. Screening for mutations in BRCA1 and BRCA2 genes by measuring the acoustic ratio with QCM. Analytical Methods 2014;6(2):363-71.

(86) Ding P, Liu R, Liu S, Mao X, Hu R, Li G. Reusable gold nanoparticle enhanced QCM immunosensor for detecting C-reactive protein. Sensors and Actuators B-Chemical 2013;188:1277-83.

(87) Wei XL, Zhang J, Zhao N. Acoustic sensing of the initial adhesion of chemokine-stimulated cancer cells. Colloids and Surfaces B-Biointerfaces 2013;111:688-92.

(88) Lee YH, Mutharasan R. Chapter 6 - Biosensors. In: Jon S.Wilson, editor. Sensor Technology Handbook.Burlington: Newnes; 2005. p. 161-80.

(89) Mello LD, Kubota LT. Review of the use of biosensors as analytical tools in the food and drink industries. Food Chemistry 2002 May;77(2):237-56.

(90) Park SC, Cho EJ, Moon SY, Yoon SI, Kim YJ, Kim DH, et al. A calorimetric biosensor and its application for detecting a cancer cell with optical imaging. 2007.

(91) Harborn U, Xie B, Venkatesh R, Danielsson B. Evaluation of a miniaturized thermal biosensor for the determination of glucose in whole blood. Clinica Chimica Acta 1997;267(2):225-37.

(92) Vermeir S, Nicolai B, Verboven P, Van Gerwen P, Baeten B, Hoflack L, et al. Microplate differential calorimetric biosensor for ascorbic acid analysis in food and pharmaceuticals. Anal Chem 2007;79(16):6119-27.

(93) Ramanathan K, Danielsson B. Principles and applications of thermal biosensors. Biosensors and Bioelectronics 2001 Aug;16(6):417-23.

(94) Sassolas A, Blum LJ, Leca-Bouvier BD. Immobilization strategies to develop enzymatic biosensors. Biotechnology Advances 2012 May;30(3):489-511.

(95) Dugas V, Elaissari A, Chevalier Y. Surface Sensitization Techniques and Recognition Receptors Immobilization on Biosensors and Microarrays. In: Zourob M, editor. Recognition Receptors in Biosensors. Springer New York; 2010. p. 47-134.

(96) Lin JN, Drake B, Lea AS, Hansma PK, Andrade JD. Direct observation of immunoglobulin adsorption dynamics using the atomic force microscope. Langmuir 1990 Feb 1;6(2):509-11.

(97) Caruso F, Rinia HA, Furlong DN. Gravimetric Monitoring of Nonionic Surfactant Adsorption from Nonaqueous Media onto Quartz Crystal Microbalance Electrodes and Colloidal Silica. Langmuir 1996 Jan 1;12(9):2145-52.

(98) Collings and Frank Caruso AF. Biosensors: recent advances. Reports on Progress in Physics 1997;60(11):1397.

(99) Lin JN, Herron J, Andrade JD, Brizgys M. Characterization of immobilized antibodies on silica surfaces. IEEE Transactions on Biomedical Engineering 1988;35(6):466-71.

(100) Peterman JH, Tarcha PJ, Chu VP, Butler JE. The immunocytochemistry of sandwich-ELISA. IV. The antigen capture capacity of antibody covalently attached to bromoacetyl surface-functionalized polystyrene. Journal of Immunological Methods 1988;111(2):271-5.

(101) Leggett GJ, Roberts CJ, Williams PM, Davies MC, Jackson DE, Tendler SJB. Approaches to the immobilization of proteins at surfaces for analysis by scanning tunneling microscopy. Langmuir 1993 Sep 1;9(9):2356-62.

(102) Geddes NJ, Paschinger EM, Furlong DN, Caruso F, Hoffmann CL, Rabolt JF. Surface chemical activation of quartz crystal microbalance gold electrodes -analysis by frequency changes, contact angle measurements and grazing angle FTIR. Thin Solid Films 1995 May 15;260(2):192-9.

(103) Ulman A. Formation and Structure of Self-Assembled Monolayers. Chemical Reviews 1996 Jan 1;96(4):1533-54.

(104) Gorton L. Biosensors and Modern Biospecific Analytical Techniques. 1-20. Elsevier.

(105) Wink T, Zuilen Jv, Bult A, Bennekom Pv. Self-assembled Monolayers for Biosensors. Analyst 1997;122(4):43R-50R.

(106) Rusmini F, Zhong Z, Feijen J. Protein Immobilization Strategies for Protein Biochips. Biomacromolecules 2007 Apr 20;8(6):1775-89.

(107) Castangia R. Microarray on gold. New applications for biocatalysis and proteomics 2012.

(108) Burnham MR, Turner JN, Szarowski D, Martin DL. Biological functionalization and surface micropatterning of polyacrylamide hydrogels. Biomaterials 2006 Dec;27(35):5883-91.

(109) Su L, Jia W, Hou C, Lei Y. Microbial biosensors: A review. Biosensors and Bioelectronics 2011 Jan 15;26(5):1788-99.

(110) Miao Y, Chia LS, Goh NK, Tan SN. Amperometric Glucose Biosensor Based on Immobilization of Glucose Oxidase in Chitosan Matrix Cross-Linked with Glutaraldehyde. Electroanalysis 2001;13(4):347-9.

(111) Andreescu S, Bucur B, Marty JL. Affinity Immobilization of Tagged Enzymes. Immobilization of Enzymes and Cells. 22 ed. 2006. p. 97-106.

(112) Brattoli M, de Gennaro G, de Pinto V, Loiotile AD, Lovascio S, Penza M. Odour Detection Methods: Olfactometry and Chemical Sensors. Sensors 2011;11(5):5290-322.

(113) Wilson AD, Baietto M. Applications and Advances in Electronic-Nose Technologies. Sensor 2009;9(7):5099-148.

(114) Stitzel SE, Aernecke MJ, Walt DR. Artificial Noses. Annu Rev Biomed Eng 2011 Jul 14;13(1):1-25.

(115) Arshak K, Moore E, Lyons GM, Harris J, Clifford S. A review of gas sensors employed in electronic nose applications. Sensor Review 2004;24(2):181-98.

(116) Mgode GF, Weetjens BJ, Nawrath T, Lazar D, Cox C, Jubitana M, et al. *Mycobacterium tuberculosis* volatiles for diagnosis of tuberculosis by Cricetomys rats. Tuberculosis 2012;92(6):535-42.

(117) Poling A, Weetjens B, Cox C, Beyene N, Durgin A, Mahoney A. Tuberculosis detection by giant african pouched rats. Behavior Analyst 2011;34(1):47-54.

(118) Poling A, Weetjens B, Cox C, Beyene NW, Bach H, Sully A. Using trained pouched rats to detect land mines: another victory for operant conditioning. Journal of Applied Behavior Analysis 2011;44(2):351-5.

(119) Rodacy PJ, Bender SFA, Bromenshenk JJ, Henderson CB, Bender G. The training and deployment of honeybees to detect explosives and other agents of harm. 2002.

(120) Frederickx C, Verheggen FJ, Haubruge E. Biosensors in forensic sciences. Biotechnologie Agronomie Societe et Environnement 2011;15(3):449-58.

(121) Wu TZ. A piezoelectric biosensor as an olfactory receptor for odour detection: electronic nose. Biosensors and Bioelectronics 1999 Jan;14(1):9-18.

(122) Bushdid C, Magnasco MO, Vosshall LB, Keller A. Humans Can Discriminate More than 1 Trillion Olfactory Stimuli. Science 2014 Mar 21;343(6177):1370-2.

(123) Firestein S. How the olfactory system makes sense of scents. Nature 2001 Sep 13;413(6852):211-8.

(124) Shepherd GM. Neurobiology (2nd ed.). New York, NY, US: Oxford University Press; 1988.

(125) Harkema JR, Carey SA, Wagner JG. The Nose Revisited: A Brief Review of the Comparative Structure, Function, and Toxicologic Pathology of the Nasal Epithelium. Toxicologic Pathology 2006 Apr 1;34(3):252-69.

(126) Touhara K, Vosshall LB. Sensing Odorants and Pheromones with Chemosensory Receptors. Annu Rev Physiol 2009 Feb 12;71(1):307-32.

(127) Buck L, Axel R. A novel multigene family may encode odorant receptors: A molecular basis for odor recognition. Cell 1991 Apr 5;65(1):175-87.

(128) Mori K, Nagao H, Yoshihara Y. The Olfactory Bulb: Coding and Processing of Odor Molecule Information. Science 1999 Oct 22;286(5440):711-5.

(129) Breer H. Olfactory receptors: molecular basis for recognition and discrimination of odors. Anal Bioanal Chem 2003;377(3):427-33.

(130) Rinaldi A. The scent of life. EMBO reports 2007;8(7).

(131) Pellegrino M, Nakagawa T, Vosshall LB. Single Sensillum Recordings in the Insects *Drosophila melanogaster* and *Anopheles gambiae*. 2010;(36):e1725.

(132) Steinbrecht RA. Pore structures in insect olfactory sensilla: A review of data and concepts. International Journal of Insect Morphology & Embryology 1997;26(3-4):229-45.

(133) Ernst KD. Die Feinstruktor bon Reichsensillen auf der Antenne des Aakafers *Necrophorus* (Coleptera). Z Zellforsch 1969;92:72-102.

(134) Galizia CG, Rössler W. Parallel Olfactory Systems in Insects: Anatomy and Function. Annu Rev Entomol 2009 Dec 4;55(1):399-420.

(135) Nakagawa T, Pellegrino M, Sato K, Vosshall LB, Touhara K. Amino acid residues contributing to function of the heteromeric insect olfactory receptor complex. Plos One 2012;7(3).

(136) Sato K, Pellegrino M, Nakagawa T, Nakagawa T, Vosshall LB, Touhara K. Insect olfactory receptors are heteromeric ligand-gated ion channels. Nature 2008;452(7190):1002-U9.

(137) Wicher D, Schafer R, Bauernfeind R, Stensmyr MC, Heller R, Heinemann SH, et al. Drosophila odorant receptors are both ligand-gated and cyclic-nucleotide-activated cation channels. Nature 2008 Apr 24;452(7190):1007-11.

(138) Hildebrand JG. Olfactory control of behavior in moths: central processing of odor information and the functional significance of olfactory glomeruli. Journal of Comparative Physiology A: Neuroethology, Sensory, Neural, and Behavioral Physiology 1996 Jan 1;178(1):5-19.

(139) Hansson BS, Carlsson MA, Kalinová B. Olfactory activation patterns in the antennal lobe of the sphinx moth, *Manduca sexta*. Journal of Comparative Physiology A: Neuroethology, Sensory, Neural, and Behavioral Physiology 2003 Apr 1;189(4):301-8.

(140) Lee SG, Baker TC. Incomplete electrical isolation of sex-pheromone responsive olfactory receptor neurons from neighboring sensilla. Journal of Insect Physiology 2008 Apr;54(4):663-71.

(141) Pelosi P. Perireceptor events in olfaction. J Neurobiol 1996;30(1):3-19.

(142) Pelosi P, Pisanelli AM, Baldaccini NE, Gagliardo A. Binding of [3H]-2-isobutyl-3-methoxypyrazine to cow olfactory mucosa. Chemical Senses 1981 Jan 1;6(2):77-85.

(143) Vogt RG, Riddiford LM. Pheromone binding and inactivation by moth antennae. Nature 1981 Sep 10;293(5828):161-3.

(144) Pelosi P, Zhou JJ, Ban LP, Calvello M. Soluble proteins in insect chemical communication. Cellular and Molecular Life Sciences 2006;63(14):1658-76.

(145) Bignetti E, Cavaggioni A, Pelosi P, Persaud KC, Sorbi RT, Tirindelli R. Purification and characterisation of an odorant-binding protein from cow nasal tissue. European Journal of Biochemistry 1985 Jun 1;149(2):227-31.

(146) Garibotti M, Navarrini A, Pisanelli AM, Pelosi P. Three odorant-binding proteins from rabbit nasal mucosa. Chemical Senses 1997 Aug 1;22(4):383-90.

(147) Paolini S, Tanfani F, Fini C, Bertoli E, Paolo P. Porcine odorant-binding protein: structural stability and ligand affinities measured by Fourier-

transform infrared spectroscopy and fluorescence spectroscopy. Biochimica et Biophysica Acta (BBA) - Protein Structure and Molecular Enzymology 1999 Apr 12;1431(1):179-88.

(148) Felicioli A, Ganni M, Garibotti M, Pelosi P. Multiple types and forms of odorant-binding proteins in the Old-World porcupine *Hystrix cristata*. Comp Biochem Physiol B 1993 Jul;105(3-4):775-84.

(149) Pes D, Pelosi P. Odorant-binding proteins of the mouse. Comparative Biochemistry and Physiology Part B: Biochemistry and Molecular Biology 1995 Nov;112(3):471-9.

(150) Briand L, Eloit C, Nespoulous C, Bézirard V, Huet JC, Henry C, et al. evidence of an odorant-binding protein in the human olfactory mucus: location, structural characterization, and odorant-binding properties. Biochemistry 2002 May 15;41(23):7241-52.

(151) Zhao H, Ivic L, Otaki JM, Hashimoto M, Mikoshiba K, Firestein S. Functional expression of a mammalian odorant receptor. Science 1998 Jan 9;279(5348):237-42.

(152) Breer H, Krieger J, Meinken C, Kiefer H, Strotmann J. expression and functional analysis of olfactory receptors. Annals of the New York Academy of Sciences 1998;855(1):175-81.

(153) Vogt RG, Prestwich GD, Lerner MR. Odorant-Binding-Protein subfamilies associate with distinct classes of olfactory receptor neurons in insects. J Neurobiol 1991;22(1):74-84.

(154) Vincent F, Spinelli S, Ramoni R, Grolli S, Pelosi P, Cambillau C, et al. Complexes of porcine odorant binding protein with odorant molecules belonging to different chemical classes. Journal of Molecular Biology 2000 Jun 30;300(1):127-39.

(155) Xu P, Atkinson R, Jones DNM, Smith DP. Drosophila OBP LUSH Is required for activity of pheromone-sensitive neurons. Neuron 2005 Jan 20;45(2):193-200.

(156) Swarup S, Williams TI, Anholt RRH. Functional dissection of Odorant binding protein genes in *Drosophila melanogaster*. Genes, Brain and Behavior 2011 Aug 1;10(6):648-57.

(157) Qiao H, Tuccori E, He X, Gazzano A, Field L, Zhou JJ, et al. Discrimination of alarm pheromone (E)-b-farnesene by aphid odorant-binding proteins. Insect Biochemistry and Molecular Biology 2009 May;39(5-6):414-9.

(158) Matsuo T, Sugaya S, Yasukawa J, Aigaki T, Fuyama Y. Odorant-binding proteins OBP57d and OBP57e affect taste perception and host-plant preference in *Drosophila sechellia*. Plos Biology 2007;5(5):985-96.

(159) Laughlin JD, Ha TS, Jones DN, Smith DP. Activation of pheromone-sensitive neurons is mediated by conformational activation of pheromone-binding protein. Cell 2008;133(7):1255-65.

(160) Flower DR, North ACT, Sansom CE. The lipocalin protein family: structural and sequence overview. Biochimica et Biophysica Acta (BBA) - Protein Structure and Molecular Enzymology 2000 Oct 18;1482(1-2):9-24.

(161) Tegoni M, Pelosi P, Vincent F, Spinelli S, Campanacci V, Grolli S, et al. Mammalian odorant binding proteins. Biochimica et Biophysica Acta (BBA) - Protein Structure and Molecular Enzymology 2000 Oct 18;1482(1-2):229-40.

(162) Sandler BH, Nikonova L, Leal WS, Clardy J. Sexual attraction in the silkworm moth: structure of the pheromone-binding-protein-bombykol complex. Chemistry & Biology 2000 Feb 1;7(2):143-51.

(163) Leal WS, Nikonova L, Peng G. Disulfide structure of the pheromone binding protein from the silkworm moth, *Bombyx mori*. FEBS Letters 1999 Dec 24;464(1-2):85-90.

(164) Tegoni M, Campanacci V, Cambillau C. Structural aspects of sexual attraction and chemical communication in insects. Trends in biochemical sciences 29[5], 257-264. 1-5-2004.

(165) Maida R, Mameli M, Müller B, Krieger J, Steinbrecht R. The expression pattern of four odorant-binding proteins in male and female silk moths, *Bombyx mori*. Journal of Neurocytology 2005 Mar 1;34(1):149-63.

(166) Zhang Sg, Maida R, Steinbrecht RA. Immunolocalization of Odorant-binding Proteins in *Noctuid Moths* (Insecta, Lepidoptera). Chemical Senses 2001 Sep 1;26(7):885-96.

(167) Zhou JJ. Odorant-Binding Proteins in Insects. In: Vitamins and Hormones, editor. Academic Press; 2010. p. 241-72.

(168) Riviere S, Lartigue A, Quennedey B, Campanacci V, Farine JP, Tegoni M, et al. A pheromone-binding protein from the cockroach *Leucophaea maderae*: cloning, expression and pheromone binding. Biochem J 2003 Apr 15;371(Pt 2):573-9.

(169) Vieira FG, Rozas J. Comparative Genomics of the Odorant-Binding and Chemosensory Protein Gene Families across the Arthropoda: Origin and evolutionary history of the chemosensory system. Genome Biology and Evolution 2011 Apr 28.

(170) Xu PX, Zwiebel LJ, Smith DP. Identification of a distinct family of genes encoding atypical odorant-binding proteins in the malaria vector mosquito, *Anopheles gambiae.* Insect Molecular Biology 2003;12(6):549-60.

(171) Zhou JJ, Huang W, Zhang GA, Pickett JA, Field LM. "Plus-C" odorant-binding protein genes in two Drosophila species and the malaria mosquito *Anopheles gambiae*. Gene 2004 Feb 18;327(1):117-29.

(172) Zhou JJ, Zhang GA, Huang W, Birkett MA, Field LM, Pickett JA, et al. Revisiting the odorant-binding protein LUSH of *Drosophila melanogaster*: evidence for odour recognition and discrimination. FEBS Letters 2004 Jan 30;558(1-3):23-6.

(173) Marchese S, Pes D, Scaloni A, Carbone V, Pelosi P. Lipocalins of boar salivary glands binding odours and pheromones. European Journal of Biochemistry 1998;252(3):563-8.

(174) Shaw PH, Held WA, Hastie ND. The gene family for Major Urinary Proteins - expression in several secretory-tissues of the mouse. Cell 1983;32(3):755-61.

(175) Henzel WJ, Rodriguez H, Singer AG, Stults JT, Macrides F, Agosta WC, et al. The Primary Structure of Aphrodisin. Journal of Biological Chemistry 1988;263(32):16682-7.

(176) Pelosi P. The role of perireceptor events in vertebrate olfaction. Cellular and Molecular Life Sciences 2001 Apr 19;58(4):503-9.

(177) Miyawaki A, Matsushita F, Ryo Y, Mikoshiba K. Possible pheromone-carrier function of 2 lipocalin proteins in the vomeronasal organ. Embo Journal 1994;13(24):5835-42.

(178) Sandeep Kumar Vashist, Priya Vashist. Recent Advances in quartz crystal microbalance-based sensors. Journal of Sensors 2011;2011.

(179) Lietai Yang. Techniques for corrosion monitoring. First ed. Woodhead Pubblishing Limited and CRC Press LLC; 2008.

(180) Sullivan CK, Guilbault GG. Commercial quartz crystal microbalances-theory and applications. Biosensors and Bioelectronics 1999 Dec;14(8-9):663-70.

(181) Allan L. Chapter 5. The quartz crystal microbalance. In: Michael E.Brown and Patrick, editor. Handbook of Thermal Analysis and Calorimetry Recent Advances, Techniques and Applications. Volume 5 ed. Elsevier Science B.V.; 2008. p. 133-69.

(182) Alder JF, McCallum JJ. Piezoelectric crystals for mass and chemical measurements. A review. Analyst 1983;108(1291):1169-89.

(183) Deakin MR, Buttry DA. Electrochemical applications of the quartz crystal microbalance. Analytical Chemistry 1989 Oct 1;61(20):1147A-54A.

(184) Lu F, Lee HP, Lim SP. Quartz crystal microbalance with rigid mass partially attached on electrode surfaces. Sensors and Actuators A: Physical 2004 May 1;112(2-3):203-10.

(185) Bunde RL, Jarvi EJ, Rosentreter JJ. Piezoelectric quartz crystal biosensors. Talanta 1998 Aug;46(6):1223-36.

(186) Wegener J, Janshoff A, Steinem C. The quartz crystal microbalance as a novel means to study cell-substrate interactions In situ. Cell Biochem Biophys 2001;34(1):121-51.

(187) Marx KA. Quartz Crystal Microbalance: A Useful Tool for Studying Thin Polymer Films and Complex Biomolecular Systems at the Solution-Surface Interface. Biomacromolecules 2003 Aug 13;4(5):1099-120.

(188) Casero E, Vazquez L, Parra-Alfambra AM, Lorenzo E. AFM, SECM and QCM as useful analytical tools in the characterization of enzyme-based bioanalytical platforms. Analyst 2010;135(8):1878-903.

(189) Zhang Y, Islam N, Carbonell RG, Rojas OJ. Specificity and Regenerability of Short Peptide Ligands Supported on Polymer Layers for Immunoglobulin G Binding and Detection. Acs Applied Materials & Interfaces 2013;5(16):8030-7.

(190) Tan L, Lin P, Chisti MM, Rehman A, Zeng X. Real Time Analysis of Binding between Rituximab (Anti-CD20 Antibody) and B Lymphoma Cells. Analytical Chemistry 2013;85(18):8543-51.

(191) Liu S, Zhou D, Guo T. Construction of a novel macroporous imprinted biosensor based on quartz crystal microbalance for ribonuclease A detection. Biosensors & Bioelectronics 2013;42:80-6.

(192) Liu N, Li X, Ma X, Ou G, Gao Z. Rapid and multiple detections of staphylococcal enterotoxins by two-dimensional molecularly imprinted film-coated QCM sensor. Sensors and Actuators B-Chemical 2014;191:326-31.

(193) Davila J, Toulemon D, Garnier T, Garnier A, Senger B, Voegel JC, et al. Bioaffinity Sensor Based on Nanoarchitectonic Films: Control of the Specific Adsorption of Proteins through the Dual Role of an Ethylene Oxide Spacer. Langmuir 2013;29(24):7488-98.

(194) Bouchet-Spinelli A, Reuillard B, Coche-Guerente L, Armand S, Labbe P, Fort S. Oligosaccharide biosensor for direct monitoring of enzymatic activities using QCM-D. Biosensors & Bioelectronics 2013;49:290-6.

(195) Salam F, Uludag Y, Tothill IE. Real-time and sensitive detection of *Salmonella Typhimurium* using an automated quartz crystal microbalance (QCM) instrument with nanoparticles amplification. Talanta 2013;115:761-7.

(196) Ittarat W, Chomean S, Sanchomphu C, Wangmaung N, Promptmas C, Ngrenngarmlert W. Biosensor as a molecular malaria differential diagnosis. Clinica Chimica Acta 2013;419:47-51.

(197) Farka Z, Kovar D, Pribyl J, Skladal P. Piezoelectric and surface plasmon resonance biosensors for Bacillus atrophaeus spores. International Journal of Electrochemical Science 2013;8(1):100-12.

(198) Funari R, la Ventura B, Schiavo L, Esposito R, Altucci C, Velotta R. Detection of Parathion Pesticide by Quartz Crystal Microbalance Functionalized with UV-Activated Antibodies. Analytical Chemistry 2013;85(13):6392-7.

(199) Jia K, Toury T, Ionescu RE. Fabrication of an atrazine acoustic immunosensor based on a drop-deposition procedure. Ieee Transactions on Ultrasonics Ferroelectrics and Frequency Control 2012;59(9):2015-21.

(200) Berggren C, Bjarnason B, Johansson G. Capacitive Biosensors. Electroanalysis 2001 Mar 1;13(3):173-80.

(201) Berggren C, Johansson G. Capacitance measurements of antibody-antigen interactions in a flow system. Anal Chem 1997 Sep 1;69(18):3651-7.

(202) Terzic E, Terzic J, Nagarajah R, Alamgir M. Capacitive sensing technology. a neural network approach to fluid quantity measurement in dynamic environments. Springer London; 2012. p. 11-37.

(203) Regtien Paul P.L. Capacitive Sensors. In: Elsevier Insights, editor. Sensors for Mechatronics. 2012.

(204) Tsouti V, Boutopoulos C, Zergioti I, Chatzandroulis S. Capacitive microsystems for biological sensing. Biosensors and Bioelectronics 2011 Sep 15;27(1):1-11.

(205) Bontidean I, Berggren C, Johansson G, Csöregi, Elisabeth, Mattiasson B, et al. Detection of heavy metal ions at femtomolar levels using protein-based biosensors. Anal Chem 1998 Sep 4;70(19):4162-9.

(206) Berggren C, Bjarnason B, Johansson G. An immunological Interleukine-6 capacitive biosensor using perturbation with a potentiostatic step. Biosensors and Bioelectronics 1998 Nov;13(10):1061-8.

(207) Janek RP, Fawcett WR, Ulman A. Impedance spectroscopy of self-assembled monolayers on Au(111): evidence for complex double-layer structure in aqueous $NaClO_4$ at the potential of zero charge. J Phys Chem B 1997 Oct 1;101(42):8550-8.

(208) Mamishev AV, Sundara-Rajan K, Fumin Y, Yanqing D, Zahn M. Interdigital sensors and transducers. Proceedings of the IEEE 2004 May;92(5):808-45.

(209) A.S.Abu-Abed, R.G.Lindquist. Capacitive interdigital sensor with inhomogeneous nematic liquid crystal film. Progress In Electromagnetics Research B 2008;7:75-87.

(210) Arya SK, Chornokur G, Venugopal M, Bhansali S. Antibody functionalized interdigitated m-electrode (IDmE) based impedimetric cortisol biosensor. Analyst 2010;135(8):1941-6.

(211) Varshney M, Li Y. Interdigitated array microelectrodes based impedance biosensors for detection of bacterial cells. Biosensors and Bioelectronics 2009 Jun 15;24(10):2951-60.

(212) Altintas Z, Kallempudi SS, Gurbuz Y. Gold nanoparticle modified capacitive sensor platform for multiple marker detection. Talanta 2014 Jan 15;118(0):270-6.

(213) Tekaya N, Saiapina O, Ben Ouada H, Lagarde F, Ben Ouada H, Jaffrezic-Renault N. Ultra-sensitive conductometric detection of pesticides based on inhibition of esterase activity in *Arthrospira platensis*. Environmental Pollution 2013 Jul;178(0):182-8.

(214) Varshney M, Li Y. Double interdigitated array microelectrode-based impedance biosensor for detection of viable *Escherichia coli* O157:H7 in growth medium. Talanta 2008 Jan 15;74(4):518-25.

(215) Labib M, Hedström M, Amn M, Mattiasson. A capacitive biosensor for detection of staphylococcal enterotoxin B. Analytical and Bioanalytical Chemistry 2009 Mar 1;393(5):1539-44.

(216) Numnuam A, Kanatharana P, Mattiasson B, Asawatreratanakul P, Wongkittisuksa B, Limsakul C, et al. Capacitive biosensor for quantification of trace amounts of DNA. Biosensors and Bioelectronics 2009 Apr 15;24(8):2559-65.

(217) Sankaran S, Khot LR, Panigrahi S. Biology and applications of olfactory sensing system: A review. Sensors and Actuators B: Chemical 2012 Aug;171-172(0):1-17.

(218) Chen Q, Xiao L, Liu Q, Ling S, Yin Y, Dong Q, et al. An olfactory bulb slice-based biosensor for multi-site extracellular recording of neural networks. Biosensors and Bioelectronics 2011 Mar 15;26(7):3313-9.

(219) Liu Q, Hu N, Zhang F, Zhang D, Hsia KJ, Wang P. Olfactory epithelium biosensor: odor discrimination of receptor neurons from a bio-hybrid sensing system. Biomed Microdevices 2012;14(6):1055-61.

(220) Liu Q, Ye W, Xiao L, Du L, Hu N, Wang P. Extracellular potentials recording in intact olfactory epithelium by microelectrode array for a bioelectronic nose. Biosensors and Bioelectronics 2010 Jun 15;25(10):2212-7.

(221) Liu Q, Ye W, Yu H, Hu N, Du L, Wang P, et al. Olfactory mucosa tissue-based biosensor: A bioelectronic nose with receptor cells in intact olfactory epithelium. Sensors and Actuators B: Chemical 2010 Apr 29;146(2):527-33.

(222) Schütz S, Schöning MJ, Schroth P, Malkoc B, Weißbecker B, Kordos P, et al. An insect-based BioFET as a bioelectronic nose. Sensors and Actuators B: Chemical 2000 Jun 30;65(1-3):291-5.

(223) Myrick AJ, Park K-C, Hetlinh JR, Baker TC. Real-time odor discrimination using a bioelectronic sensor array based on the insect electroantennogram. Bioinspiration & Biomimetics 2008;3(4):046006.

(224) Ling S, Gao T, Liu J, Li Y, Zhou J, Li J, et al. The fabrication of an olfactory receptor neuron chip based on planar multi-electrode array and its odor-response analysis. Biosensors and Bioelectronics 2010 Nov 15;26(3):1124-8.

(225) Wu C, Chen P, Yu H, Liu Q, Zong X, Cai H, et al. A novel biomimetic olfactory-based biosensor for single olfactory sensory neuron monitoring. Biosensors and Bioelectronics 2009 Jan 1;24(5):1498-502.

(226) Du L, Wu C, Peng H, Zhao L, Huang L, Wang P. Bioengineered olfactory sensory neuron-based biosensor for specific odorant detection. Biosensors & Bioelectronics 2013;40(1):401-6.

(227) Misawa N, Mitsuno H, Kanzaki R, Takeuchi S. Highly sensitive and selective odorant sensor using living cells expressing insect olfactory receptors. Proceedings of the National Academy of Sciences 2010 Aug 31;107(35):15340-4.

(228) Miller AJ, Zhou JJ. Xenopus oocytes as an expression system for plant transporters. Biochimica et Biophysica Acta (BBA) - Biomembranes 2000 May 1;1465(1-2):343-58.

(229) Lee SH, Jun SB, Ko HJ, Kim SJ, Park TH. Cell-based olfactory biosensor using microfabricated planar electrode. Biosensors and Bioelectronics 2009 Apr 15;24(8):2659-64.

(230) Marrakchi M, Vidic J, Jaffrezic-Renault N, Martelet C, Pajot-Augy E. A new concept of olfactory biosensor based on interdigitated microelectrodes and immobilized yeasts expressing the human receptor OR17-40. Eur Biophys J 2007;36(8):1015-8.

(231) Benilova IV, Minic Vidic J, Pajot-Augy E, Soldatkin AP, Martelet C, Jaffrezic-Renault N. Electrochemical study of human olfactory receptor

OR 17-40 stimulation by odorants in solution. Materials Science and Engineering C 2008;28(5-6):633-9.

(232) Kim TH, Lee SH, Lee J, Song HS, Oh EH, Park TH, et al. Single-carbon-atomic-resolution detection of odorant molecules using a human olfactory receptor-based bioelectronic nose. Adv Mater 2009 Jan 5;21(1):91-4.

(233) Du L, Wu C, Peng H, Zou L, Zhao L, Huang L, et al. Piezoelectric olfactory receptor biosensor prepared by aptamer-assisted immobilization. Sensors and Actuators B: Chemical 2013 Oct;187(0):481-7.

(234) Vidic JM, Grosclaude J, Persuy MA, Aioun J, Salesse R, Pajot-Augy E. Quantitative assessment of olfactory receptors activity in immobilized nanosomes: a novel concept for bioelectronic nose. Lab Chip 2006;6(8):1026-32.

(235) Vidic J, Grosclaude J, Monnerie R, Persuy MA, Badonnel K, Baly C, et al. On a chip demonstration of a functional role for odorant binding protein in the preservation of olfactory receptor activity at high odorant concentration. Lab Chip 2008;8(5):678-88.

(236) Ko HJ, Park TH. Piezoelectric olfactory biosensor: ligand specificity and dose-dependence of an olfactory receptor expressed in a heterologous cell system. Biosensors and Bioelectronics 2005 Jan 15;20(7):1327-32.

(237) Sankaran S, Panigrahi S, Mallik S. Odorant binding protein based biomimetic sensors for detection of alcohols associated with Salmonella contamination in packaged beef. Biosensors and Bioelectronics 2011 Mar 15;26(7):3103-9.

(238) Di Pietrantonio F, Cannatá D, Benetti M, Verona E, Varriale A, Staiano M, et al. Detection of odorant molecules via surface acoustic wave biosensor array based on odorant-binding proteins. Biosensors and Bioelectronics 2013 Mar 15;41(0):328-34.

(239) Lu Y, Li H, Zhuang S, Zhang D, Zhang Q, Zhou J, et al. Olfactory biosensor using odorant-binding proteins from honeybee: Ligands of floral odors and pheromones detection by electrochemical impedance. Sensors and Actuators B: Chemical 2014 Mar 31;193(0):420-7.

(240) Capone S, Pascali C, Francioso L, Siciliano P, Persaud KC, Pisanelli AM. Odorant Binding Proteins as sensing layers for novel gas biosensors: an impedance spectroscopy characterization. In: Neri G, Donato N, d'Amico A, Di Natale C, editors. Sensors and Microsystems. 91 ed. Springer Netherlands; 2011. p. 317-24.

(241) Hou Y, Jaffrezic-Renault N, Martelet C, Tlili C, Zhang A, Pernollet JC, et al. Study of Langmuir and Langmuir-Blodgett films of odorant-binding protein/amphiphile for odorant biosensors. Langmuir 2005 Mar 29;21(9):4058-65.

(242) Hengen PN. Purification of His-Tag fusion proteins from *Escherichia coli*. Trends in Biochemical Sciences 1995 Jul;20(7):285-6.

(243) Arnau J, Lauritzen C, Petersen GE, Pedersen J. Current strategies for the use of affinity tags and tag removal for the purification of recombinant proteins. Protein Expression and Purification 2006 Jul;48(1):1-13.

(244) Sun YF, De Biasio F, Qiao HL, Iovinella I, Yang SX, Ling Y, et al. Two odorant-binding proteins mediate the behavioural response of aphids to the alarm pheromone (E)-beta-farnesene and structural analogues. Plos One 2012;7(3).

(245) Lautenschlager C, Leal WS, Clardy J. Coil-to-helix transition and ligand release of *Bombyx mori* pheromone-binding protein. Biochemical and Biophysical Research Communications 2005 Oct 7;335(4):1044-50.

(246) Meillour PN, Lagant P, Cornard JP, Brimau F, Le Danvic C, Vergoten G, et al. Phenylalanine 35 and tyrosine 82 are involved in the uptake and release of ligand by porcine odorant-binding protein. Biochimica et Biophysica Acta (BBA) - Proteins and Proteomics 2009 Aug;1794(8):1142-50.

(247) Maly J, Krejci J, Ilie M, Jakubka L, Masojìdek J, Pilloton R, et al. Monolayers of photosystem II on gold electrodes with enhanced sensor response-effect of porosity and protein layer arrangement. Analytical and Bioanalytical Chemistry 2005 Apr 1;381(8):1558-67.

(248) Akram M, Stuart MC, Wong DKY. Direct application strategy to immobilise a thioctic acid self-assembled monolayer on a gold electrode. Analytica Chimica Acta 2004;504(2):243-51.

(249) Zhang J, Wu X, Chen P, Lin N, Chen J, Chen G, et al. Electrochemical genotyping and detection of single-nucleotide polymorphisms based on junction-probe containing 2'-deoxyinosine. Chem Commun 2010;46(37):6986-8.

(250) Daimon T, Fujii T, Yago M, Hsu YF, Nakajima Y, Fujii T, et al. Female sex pheromone and male behavioral responses of the bombycid moth *Trilocha varians*: comparison with those of the domesticated silkmoth *Bombyx mori*. Naturwissenschaften 2012;99(3):207-15.

(251) Burova TV, Choiset Y, Jankowski CK, Haertle T. Conformational stability and binding properties of porcine odorant binding protein. Biochemistry 1999 Nov 9;38(45):15043-51.

(252) Herent MF, Collin S, Pelosi P. Affinities of nutty and green-smelling pyrazines and thiazoles to odorant-binding proteins, in relation with their lipophilicity. Chemical Senses 1995 Dec 1;20(6):601-8.

(253) Dalmonte M, Centini M, Anselmi C, Pelosi P. Binding of selected odorants to bovine and porcine odorant-binding proteins. Chemical Senses 1993;18(6):713-21.

(254) Wei Y, Brandazza A, Pelosi P. Binding of polycyclic aromatic hydrocarbons to mutants of odorant-binding protein: A first step towards biosensors for environmental monitoring. Biochimica et Biophysica Acta (BBA) - Proteins & Proteomics 2008 Apr;1784(4):666-71.

(255) Calvello M, Guerra N, Brandazza A, D'Ambrosio C, Scaloni A, Dani FR, et al. Soluble proteins of chemical communication in the social wasp *Polistes dominulus*. Cellular and Molecular Life Sciences 2003 Sep 1;60(9):1933-43.

(256) Elgaali H, Hamilton-Kemp TR, Newman MC, Collins RW, Yu K, Archbold DD. Comparison of long-chain alcohols and other volatile compounds emitted from food-borne and related Gram positive and Gram negative bacteria. J Basic Microbiol 2002 Dec 1;42(6):373-80.

(257) Spinelli S, Lagarde A, Iovinella I, Legrand P, Tegoni M, Pelosi P, et al. Crystal structure of *Apis mellifera* OBP14, a C-minus odorant-binding protein, and its complexes with odorant molecules. Insect Biochemistry and Molecular Biology 2012 Jan;42(1):41-50.

(258) Moio L, Piombino P, Addeo F. Odour-impact compounds of Gorgonzola cheese. Journal of Dairy Research 2000;67(2):273-85.

(259) Moller AR. Chemical Senses: Olfaction and Gustation. Sensory Systems.San Diego: Academic Press; 2003. p. 425-50.

(260) Kruse SW, Zhao R, Smith DP, Jones DNM. Structure of a specific alcohol-binding site defined by the odorant binding protein LUSH from *Drosophila melanogaster*. Nat Struct Mol Biol 2003 Sep;10(9):694-700.

(261) Ban L, Scaloni A, D'Ambrosio C, Zhang L, Yan Y, Pelosi P. Biochemical characterization and bacterial expression of an odorant-binding protein from *Locusta migratoria*. Cellular and Molecular Life Sciences 2003 Feb 19;60(2):390-400.

(262) Maida R, Steinbrecht A, Ziegelberger G, Pelosi P. The pheromone binding protein of *Bombyx mori*: Purification, characterization and immunocytochemical localization. Insect Biochemistry and Molecular Biology 1993 Mar;23(2):243-53.

(263) Maida R, Proebstl T, Laue M. Heterogeneity of Odorant-binding proteins in the antennae of *Bombyx mori*. Chemical Senses 1997 Oct 1;22(5):503-15.

(264) Forét S, Maleszka R. Function and evolution of a gene family encoding odorant binding-like proteins in a social insect, the honey bee (*Apis mellifera*). Genome Research 2006 Nov 1;16(11):1404-13.

(265) Iovinella I, Bozza F, Caputo B, la Torre A, Pelosi P. Ligand-binding study of *Anopheles gambiae* chemosensory proteins. Chemical Senses 2013 Apr 18.

(266) Horst R, Damberger F, Luginbuhl P, Guntert P, Peng G, Nikonova L, et al. NMR structure reveals intramolecular regulation mechanism for pheromone binding and release. Proceedings of the National Academy of Sciences 2001 Dec 4;98(25):14374-9.

(267) Smyrl TG, LeMaguer M. Solubilities of terpenic essential oil components in aqueous solutions. J Chem Eng Data 1980 Apr 1;25(2):150-2.

(268) Stephenson R, Stuart J. Mutual binary solubilities: water-alcohols and water-esters. J Chem Eng Data 1986 Jan 1;31(1):56-70.

(269) D'Souza SF. Immobilization and stabilization of biomaterials for biosensor applications. Appl Biochem Biotechnol 2001;96(1-3):225-38.

(270) Gupta R, Chaudhury NK. Entrapment of biomolecules in sol-gel matrix for applications in biosensors: Problems and future prospects. Biosensors and Bioelectronics 2007 May 15;22(11):2387-99.

(271) Nogala W, Szot K, Burchardt M, Jönsson-Niedziolka M, Rogalski J, Wittstock G, et al. Scanning electrochemical microscopy activity mapping of electrodes modified with laccase encapsulated in sol-gel processed matrix. Bioelectrochemistry 2010 Aug;79(1):101-7.

(272) Lovino M, Cardinal MF, Zubiri DBV, Bernik DL. Electronic nose screening of ethanol release during sol-gel encapsulation: A novel non-invasive method to test silica polymerisation. Biosensors and Bioelectronics 2005 Dec 15;21(6):857-62.

(273) Urban GA, Weiss T. Hydrogels for Biosensors Hydrogel Sensors and Actuators. In: Gerlach G, Arndt KF, editors. 6 ed. Springer Berlin Heidelberg; 2010. p. 197-220.

(274) Aymard P, Martin DR, Plucknett K, Foster TJ, Clark AH, Norton IT. Influence of thermal history on the structural and mechanical properties of agarose gels. Biopolymers 2001;59(3):131-44.

(275) Liu HH, Tian ZQ, Lu ZX, Zhang ZL, Zhang M, Pang DW. Direct electrochemistry and electrocatalysis of heme-proteins entrapped in agarose hydrogel films. Biosensors and Bioelectronics 2004 Sep 15;20(2):294-304.

(276) Hara M, Iazvovskaia S, Ohkawa H, Asada Y, Miyake J. Immobilization of P450 monooxygenase and chloroplast for use in light-driven bioreactors. Journal of Bioscience and Bioengineering 1999 Jun;87(6):793-7.

(277) Wang S, Guo Z, Zhang H. Direct electrochemistry of cytochrome c entrapped in agarose hydrogel in room temperature ionic liquids. Bioelectrochemistry 2011 Aug;82(1):55-62.

(278) Migneault I, Dartiguenave C, Bertrand MJ, Waldron KC. Glutaraldehyde: behavior in aqueous solution, reaction with proteins, and application to enzyme crosslinking. Biotechniques 2004;37(5):790-6.

(279) McArdle FA, Persaud KC. Development of an enzyme-based biosensor for atrazine detection. Analyst 1993;118(4):419-23.

(280) Freedman KJ, Haq SR, Edel JB, Jemth P, Kim MJ. Single molecule unfolding and stretching of protein domains inside a solid-state nanopore by electric field. Sci Rep 2013 Apr 10;3.

(281) Mandke R, Layek B, Sharma G, Singh J. Fabrication and Evaluation of Nanoparticle-Based Biosensors. Biosensor Nanomaterials. Wiley-VCH Verlag GmbH & Co. KGaA; 2011. p. 73-93.

(282) Lu X, Zhang Y, Zhang M, Chen Y, Kang J. Electrochemical and microscopic studies of surface-confined DNA. J Solid State Electrochem 2007;11(4):496-504.

(283) Zhang S, Wang N, Yu H, Niu Y, Sun C. Covalent attachment of glucose oxidase to an Au electrode modified with gold nanoparticles for use as glucose biosensor. Bioelectrochemistry 2005 Sep;67(1):15-22.

(284) Ding SJ, Chang BW, Wu CC, Lai MF, Chang HC. Impedance spectral studies of self-assembly of alkanethiols with different chain lengths using different immobilization strategies on Au electrodes. Analytica Chimica Acta 2005 Dec 4;554(1-2):43-51.

(285) Li Z, Niu T, Zhang Z, Feng G, Bi S. Studies on the effect of solvents on self-assembly of thioctic acid and Mercaptohexanol on gold. Thin Solid Films 2011 Apr 29;519(13):4225-33.

(286) Douglass J, Driscoll PF, Liu D, Burnham NA, Lambert CR, McGimpsey WG. Effect of electrode roughness on the capacitive behavior of Self-Assembled Monolayers. Anal Chem 2008 Sep 24;80(20):7670-7.

(287) Mashazi PN, Ozoemena KI, Nyokong T. Tetracarboxylic acid cobalt phthalocyanine SAM on gold: Potential applications as amperometric sensor for H_2O_2 and fabrication of glucose biosensor. Electrochimica Acta 2006 Oct 5;52(1):177-86.

(288) Aljabali AAA, Barclay JE, Butt JN, Lomonossoff GP, Evans DJ. Redox-active ferrocene-modified *Cowpea mosaic* virus nanoparticles. Dalton Trans 2010;39(32):7569-74.

(289) Wang ZX, Nygard AM, Cook MJ, Russell DA. An evanescent-field-driven self-assembled molecular photoswitch for macrocycle coordination and release. Langmuir 2004;20(14):5850-7.

(290) Weisser M, Nelles G, Wohlfart P, Wenz G, Mittler-Neher S. Immobilization kinetics of cyclodextrins at gold surfaces. J Phys Chem 1996 Jan 1;100(45):17893-900.

(291) Zhu Z, Li C, Li NQ. Electrochemical studies of quercetin interacting with DNA. Microchemical Journal 2002 Jan;71(1):57-63.

(292) Vacca A, Mascia M, Rizzardini S, Palmas S, Mais L. Coating of gold substrates with polyaniline through electrografting of aryl diazonium salts. Electrochimica Acta(0).

(293) Janek RP, Fawcett WR, Ulman A. Impedance Spectroscopy of Self-Assembled Monolayers on Au(111): Sodium Ferrocyanide charge transfer at modified electrodes. Langmuir 1998 May 1;14(11):3011-8.

(294) Le TT, Wilde CP, Grossman N, Cass AEG. A simple method for controlled immobilization of proteins on modified SAMs. Phys Chem Chem Phys 2011;13(12):5271-8.

(295) Melnik BS, Povarnitsyna TV, Melnik TN. Can the fluorescence of green fluorescent protein chromophore be related directly to the nativity of protein structure? Biochemical and Biophysical Research Communications 2009 Dec 25;390(4):1167-70.

(296) Kirchhofer A, Helma J, Schmidthals K, Frauer C, Cui S, Karcher A, et al. Modulation of protein properties in living cells using nanobodies. Nat Struct Mol Biol 2010 Jan;17(1):133-8.

(297) Chalfie M, Tu Y, Euskirchen G, Ward WW, Prasher DC. Green Fluorescent Protein As A Marker for Gene-Expression. Science 1994;263(5148):802-5.

(298) Berggren C, Stalhandske P, Brundell J, Johansson G. A feasibility study of a capacitive biosensor for direct detection of DNA hybridization. Electroanalysis 1999;11(3):156-60.

(299) Mattiasson B, Teeparuksapun K, Hedström M. Immunochemical binding assays for detection and quantification of trace impurities in biotechnological production. Trends in Biotechnology 2010 Jan;28(1):20-7.

(300) Ghafar-Zadeh E, Sawan M. Capacitive Bio-interfaces. CMOS Capacitive Sensors for Lab-on-Chip Applications. Springer Netherlands; 2010. p. 35-50.

(301) Mortari A, Brown NL, Geczy C, Coster HGL, Valenzuela SM, Martin D, et al. Applications of Protein-Based Capacitive Biosensors for the Detection of Heavy-Metal Ions. 2006.

(302) Maryott AA, Smith ER. Table of dielectric constants of pure liquids. Washington: U.S. Govt. Print. Off.; 1951.

(303) Duan X, Li Y, Rajan NK, Routenberg DA, Modis Y, Reed MA. Quantification of the affinities and kinetics of protein interactions using silicon nanowire biosensors. Nat Nano 2012 Jun.

(304) Qureshi A, Gurbuz Y, Kallempudi S, Niazi JH. Label-free RNA aptamer-based capacitive biosensor for the detection of C-reactive protein. Phys Chem Chem Phys 2010;12(32):9176-82.

(305) Song W, Zhu Z, Mao Y, Zhang S. A sensitive quartz crystal microbalance assay of adenosine triphosphate via DNAzyme-activated and aptamer-based target-triggering circular amplification. Biosensors and Bioelectronics 2014 Mar 15;53(0):288-94.

(306) Becker B, Cooper MA. A survey of the 2006 -2009 quartz crystal microbalance biosensor literature. J Mol Recognit 2011 Sep 1;24(5):754-87.

(307) Speight RE, Cooper MA. A Survey of the 2010 Quartz Crystal Microbalance Literature. J Mol Recognit 2012 Sep 1;25(9):451-73.

(308) Pelosi P, Mastrogiacomo R, Iovinella I, Tuccori E, Persaud K. Structure and biotechnological applications of odorant-binding proteins. Appl Microbiol Biotechnol 2013;1-10.

(309) Ulman A. Formation and Structure of Self-Assembled Monolayers. Chem Rev 1996 Jan 1;96(4):1533-54.

(310) Zhou JJ, Robertson G, He X, Dufour S, Hooper AM, Pickett JA, et al. Characterisation of *Bombyx mori* odorant-binding proteins reveals that a general odorant-binding protein discriminates between sex pheromone components. Journal of Molecular Biology 2009 Jun 12;389(3):529-45.

(311) Pophof B. Pheromone-binding proteins contribute to the activation of olfactory receptor neurons in the Silkmoths *Antheraea polyphemus* and *Bombyx mori*. Chemical Senses 2004 Feb 1;29(2):117-25.

(312) Grosse-Wilde E, Svatos A, Krieger J. A Pheromone-Binding protein mediates the bombykol-induced activation of a pheromone receptor in vitro. Chemical Senses 2006 Jul 1;31(6):547-55.

(313) Kasang G, Kaissling KE, Vostrowsky O, Bestmann HJ. Bombykal, a Second Pheromone Component of the Silkworm Moth *Bombyx mori* L. Angew Chem Int Ed Engl 1978;17(1):60.

(314) Kaissling KE, Kasang G, Bestmann HJ, Stransky W, Vostrowsky O. A new pheromone of the silkworm moth *Bombyx mori*. Naturwissenschaften 1978 Jul 1;65(7):382-4.

(315) Heinbockel T, Kaissling KE. Variability of olfactory receptor neuron responses of female silkmoths (*Bombyx mori* L.) to benzoic acid and (±)-linalool. Journal of Insect Physiology 1996 Jun;42(6):565-78.

(316) Mcnair HM, Miller JM. Basic Gas Chromatography. second ed. New York, NY, USA, John Wiley & Sons,Inc.; 2009.

(317) Maga JA, Sizer CE. Pyrazines in foods. Review. J Agric Food Chem 1973 Jan 1;21(1):22-30.

(318) Mueller R, Rappert S. Pyrazines: occurrence, formation and biodegradation. Applied Microbiology and Biotechnology 2010;85(5):1315-20.

(319) Poinot P, Arvisenet Gl, Grua-Priol Jl, Fillonneau C, Prost C. Use of an artificial mouth to study bread aroma. Food Research International 2009 Jun;42(5-6):717-26.

(320) Serra Bonvehì J, Ventura Coll F. Factors affecting the formation of alkylpyrazines during roasting treatment in natural and alkalinized cocoa powder. J Agric Food Chem 2002 May 15;50(13):3743-50.

(321) Pickard S, Becker I, Merz KH, Richling E. Determination of the alkylpyrazine composition of coffee using Stable Isotope Dilution-Gas Chromatography-Mass Spectrometry (SIDA-GC-MS). J Agric Food Chem 2013;61(26):6274-81.

(322) Pripdeevech P, Machan T. Fingerprint of volatile flavour constituents and antioxidant activities of teas from Thailand. Food Chemistry 2011 Mar 15;125(2):797-802.

(323) Didzbalis J, Ritter KA, Trail AC, Plog FJ. Identification of fruity/fermented odorants in high-temperature-cured roasted peanuts. J Agric Food Chem 2004 Jun 25;52(15):4828-33.

(324) Le Guen S, Prost C, Demaimay M. Critical comparison of three olfactometric methods for the identification of the most potent odorants in cooked mussels (*Mytilus edulis*). J Agric Food Chem 2000 Apr 1;48(4):1307-14.

(325) Nicolotti L, Cordero C, Bicchi C, Rubiolo P, Sgorbini B, Liberto E. Volatile profiling of high quality hazelnuts (*Corylus avellana* L.): Chemical indices of roasting. Food Chemistry 2013;138(2-3):1723-33.

(326) Ducki S, Miralles-Garcia J, Zumbé A, Tornero A, Storey DM. Evaluation of solid-phase micro-extraction coupled to gas chromatography-mass

spectrometry for the headspace analysis of volatile compounds in cocoa products. Talanta 2008 Feb 15;74(5):1166-74.

(327) Williams JE, Duncan SE, Williams RC, Mallikarjunan K, Eigel WN, O'Keefe SF. Flavor Fade in Peanuts During Short-term Storage. Journal of Food Science 2006 Apr 1;71(3):S265-S269.

(328) Counet C, Callemien D, Ouwerx C, Collin S. Use of Gas Chromatography- Olfactometry to identify key odorant compounds in dark chocolate. Comparison of Samples before and after Conching. J Agric Food Chem 2002 Mar 15;50(8):2385-91.

(329) Jo YJ, Cho IH, Song CK, Shin HW, Kim YS. Comparison of fermented soybean paste (doenjang) prepared by different methods based on profiling of volatile compounds. Journal of Food Science 2011 Apr 1;76(3):C368-C379.

(330) van Loon WAM, Linssen JPH, Legger A, Posthumus A, Voragen AGJ. Identification and olfactometry of French fries flavour extracted at mouth conditions. Food Chemistry 2005 May;90(3):417-25.

(331) Harding RJ, Nursten HE, Wren JJ. Basic compounds contributing to beer flavour. J Sci Food Agric 1977 Feb 1;28(2):225-32.

(332) Mazida MM, Salleh MM, Osman H. Analysis of volatile aroma compounds of fresh chilli (*Capsicum annuum)* during stages of maturity using solid phase microextraction (SPME). Journal of Food Composition and Analysis 2005 Aug;18(5):427-37.

(333) Pino J, Sauri-Duch E, Marbot R. Changes in volatile compounds of Habanero chile pepper (*Capsicum chinense* Jack. cv. Habanero) at two ripening stages. Food Chemistry 2006 Feb;94(3):394-8.

(334) Huffman VL, Schadle ER, Villalon B, Burns EE. Volatile components and pungency in fresh and processed jalapeno peppers. Journal of Food Science 1978 Nov 1;43(6):1809-11.

(335) Semmelroch P, Grosch W. Studies on character impact odorants of coffee brews. J Agric Food Chem 1996 Jan 1;44(2):537-43.

(336) Suriyaphan O, Drake M, Chen XQ, Cadwallader KR. characteristic aroma components of British farmhouse Cheddar cheese. J Agric Food Chem 2001 Feb 7;49(3):1382-7.

(337) Duckham SC, Dodson AT, Bakker J, Ames JM. Volatile flavour components of baked potato flesh. A comparison of eleven potato cultivars. Nahrung 2001 Oct 1;45(5):317-23.

(338) Seifert RM, Buttery RG, Guadagni DG, Black DR, Harris JG. Synthesis and odor properties of some additional compounds related to 2-isobutyl-3-methoxypyrazine. J Agric Food Chem 1972 Jan 1;20(1):135-7.

(339) Hurlburt B, Lloyd SW, Grimm CC. Comparison of analytical techniques for detection of geosmin and 2-methylisoborneol in aqueous samples. Journal of Chromatographic Science 2009;47(8):670-3.

(340) Cavaggioni A, Mucignat-Caretta C. Major urinary proteins, α_{2U}-globulins and aphrodisin. Biochimica et Biophysica Acta (BBA) - Protein Structure and Molecular Enzymology 2000 Oct 18;1482(1-2):218-28.

(341) Timm DE, Baker LJ, Mueller H, Zidek L, Novotny MV. Structural basis of pheromone binding to mouse major urinary protein (MUP-I). Protein Science 2001;10(5):997-1004.

(342) Roy J, Laughton CA. Long-timescale molecular-dynamics simulations of the major urinary protein provide atomistic interpretations of the unusual thermodynamic of ligand binding. Biophysical Journal 2010 Jul 7;99(1):218-26.

(343) Shahan K, Gilmartin M, Derman E. Nucleotide sequences of liver, lachrymal, and submaxillary gland mouse major urinary protein mRNAs: mosaic structure and construction of panels of gene-specific synthetic oligonucleotide probes. Molecular and Cellular Biology 1987 May 1;7(5):1938-46.

(344) Sharrow SD, Vaughn JL, Lukáš Ž, Novotny MV, Stone MJ. Pheromone binding by polymorphic mouse major urinary proteins. Protein Science 2002 Sep 1;11(9):2247-56.

(345) Jiang QY, Wang WX, Zhang Z, Zhang L. Binding specificity of locust odorant binding protein and its key binding site for initial recognition of alcohols. Insect Biochemistry and Molecular Biology 2009 Jul;39(7):440-7.

(346) Damberger F, Horst R, Wuthrich K, Peng G, Nikonova L, Leal WS. NMR characterization of a pH-dependent equilibrium between two folded solution conformations of the pheromone-binding protein from Bombyx mori. Protein Science 2000;9(5):1038-41.

(347) Cai WB, Amano T, Osawa M. A comparison of surface-enhanced infrared and surface-enhanced Raman spectra of pyrazine adsorbed on polycrystalline gold electrodes. Journal of Electroanalytical Chemistry 2001 Mar 16;500(1-2):147-55.

(348) Daev EV, Dukelskaya AV. The Female Pheromone 2,5-Dimethylpyrazine Induces Sperm-Head Abnormalities in Male CBA Mice. Russian Journal of Genetics 2003 Jul 1;39(7):811-5.

(349) Dominguez-Ramirez L, Del Moral-Ramirez E, Cortes-Hernandez P, Garcia-Garibay M, Jimenez-Guzman J. beta-Lactoglobulin's conformational requirements for ligand binding at the calyx and the dimer interphase: a flexible docking study. Plos One 2013;8(11).

(350) Achiraman S, Archunan G. Characterization of urinary volatiles in Swiss male mice (*Mus musculus*): bioassay of identified compounds. Journal of Biosciences 2002;27(7):679-86.